SCUOLA INTERNAZIONALE SUPERIORE DI STUDI AVANZATI

NEURONAL CORRELATES OF TACTILE WORKING MEMORY IN RAT BARREL CORTEX AND PREFRONTAL CORTEX

Thesis submitted for the degree of
"*Doctor Philosophiæ*"

CANDIDATE:

Vahid Esmaeili

SUPERVISOR:

Prof. Mathew E. Diamond

December 2014

Cognitive Neuroscience sector
SISSA, Via Bonomea 265, TRIESTE, ITALY

ACKNOWLEDGMENTS

I would like to thank Mathew. E. Diamond
without his constant support and great ideas this work would have never been done.

I would like to express my special thanks to Arash Fassihi and Athena Akrami
without their collaboration and ideas it was impossible to accomplish this work.

I am grateful to Romain Brasselet, Houman Safaai, Hernan Rey, Vinzenz Schoenfelder and Natalia Grion
for their substantial contribution to the data analysis.

Marco Gigante, Fabrizio Manzino, Rudy Boz, Erik Zorzin and Stefano Parusso
provided outstanding technical help and thus made the work much easier.

I am thankful to Francesca Pulecchi for training the rats, helping during surgeries and performing the
histologies.

I would like to specially acknowledge Rodrigo Quian Quiroga
for his valuable comments and suggestions in decoding algorithms.

I would like to thank Sina Tafazoli for his help in electrophysiological setup and Yousef, Thérèse and Kiana
for their help in training animals.

I am also thankful to TPLL lab members Nader, Shima, Adina, Maris and Sergey and my special friends
Akbar, Ladan and Houman for making these 4 years an unforgettable experience.

I owe my loving thanks to my family whose care and support enabled me to complete this work.

At the end I would like to thank "the love" of my life, Sadaf, for her infinite patience, support and
understanding.

Index

ABSTRACT **1**

INTRODUCTION **3**

WORKING MEMORY IN RODENTS 4
TACTILE WORKING MEMORY 5
THE WHISKER SENSORY SYSTEM 6
ACTIVE SENSING AND MODES OF OPERATION 7
Generative mode. *8*
Receptive mode. *8*
DISTRIBUTED NETWORKS OF WORKING MEMORY 9
MEDIAL PREFRONTAL CORTEX ORGANIZATION IN RATS 11
NEURONAL COMMUNICATION THROUGH COHERENT OSCILLATIONS 13

MATERIALS AND METHODS **16**

SUBJECTS 16
APPARATUS 17
STIMULI 19
STIMULUS GENERALIZATION MATRIX 21
EXCLUSION OF NON-TACTILE SIGNALS 21
SURGERY 22
ELECTROPHYSIOLOGICAL RECORDINGS 23
DATA ANALYSIS 24
Spike density functions. *24*
Generalized Linear Model. *24*
Test of significance for the slope of the fit. *24*
Information theoretic analysis. *25*
Test of significance of information. *27*
Linear Discriminant Analysis. *27*
Local Field Potentials. *29*
LFP power spectrum. *29*
LFP-LFP phase coherence. *29*
Statistical test of WPLI and FDR control for multiple comparisons. *29*
LFP-LFP phase shifts. *30*

RESULTS - BEHAVIORAL PERFORMANCE **31**

APPENDIX 1. WORKING MEMORY PERFORMANCE OF INDIVIDUAL RATS **35**

RESULTS – NEURONAL ANALYSIS **37**

ENCODING OF TASK PARAMETERS BY NEURONAL FIRING 39
Representation of the ongoing stimulus. *40*
Memory of the first stimulus. *42*
Response modulation in different neurons. *42*
Representation of action. *45*

Proportion of informative neurons. *48*
DECODING OF TASK PARAMETERS FROM POPULATIONS OF NEURONS 50
RESULTS - LOCAL FIELD POTENTIAL ANALYSIS **54**
DISCUSSION **58**
GENERAL OBSERVATIONS 58
WHAT ARE HOMOLOGOUS NEOCORTICAL REGIONS ACROSS PRIMATES AND RATS? 58
WORKING MEMORY IN RODENTS 59
NEURONAL REPRESENTATION OF THE DELAYED COMPARISON TASK 60
NOVEL INFORMATION MEASURES 63
DECODING 64
LONG-DISTANCE NETWORK COMMUNICATION 64
CONCLUSIONS 65
BIBLIOGRAPHY **66**
APPENDIX 2. BEHAVIORAL PAPER (PNAS) **81**

Abstract

The neuronal mechanisms of parametric working memory – the short-term storage of graded stimuli to guide behavior – are not fully elucidated. We have designed a working memory task where rats compare two sequential vibrations, S1 and S2, delivered to their whiskers (Fassihi et al, 2014). Vibrations are a series of velocities sampled from a zero-mean normal distribution. Rats must judge which stimulus had greater velocity standard deviation, σ (e.g. $\sigma_1 > \sigma_2$ turn left, $\sigma_1 < \sigma_2$ turn right). A critical operation in this task is to hold S1 information in working memory for subsequent comparison. In an earlier work we uncovered this cognitive capacity in rats (Fassihi et al, 2014), an ability previously ascribed only to primates. Where in the brain is such a memory kept and what is the nature of its representation?

To address these questions, we performed simultaneous multi-electrode recordings from barrel cortex – the entryway of whisker sensory information into neocortex – and prelimbic area of medial prefrontal cortex (mPFC) which is involved in higher order cognitive functioning in rodents. During the presentation of S1 and S2, a majority of neurons in barrel cortex encoded the ongoing stimulus by monotonically modulating their firing rate as a function of σ; i.e. 42% increased and 11% decreased their firing rate for progressively larger σ values. During the 2 second delay interval between the two stimuli, neuronal populations in barrel

cortex kept a graded representation of S1 in their firing rate; 30% at early delay and 15% at the end. In mPFC, neurons expressed divers coding characteristics yet more than one-fourth of them varied their discharge rate according to the ongoing stimulus. Interestingly, a similar proportion carried the stimulus signal up to early parts of delay period. A smaller but considerable proportion (10%) kept the memory until the end of delay interval.

We implemented novel information theoretic measures to quantify the stimulus and decision signals in neuronal responses in different stages of the task. By these measures, a decision signal was present in barrel cortex neurons during the S2 period and during the post stimulus delay, when the animal needed to postpone its action. Medial PFC units also represented animal choice, but later in the trial in comparison to barrel cortex. Decision signals started to build up in this area after the termination of S2.

We implemented a regularized linear discriminant algorithm (RDA) to decode stimulus and decision signals in the population activity of barrel cortex and mPFC neurons. The RDA outperformed individual clusters and the standard linear discriminant analysis (LDA). The stimulus and animal's decision could be extracted from population activity simply by linearly weighting the responses of neuronal clusters. The population signal was present even in epochs of trial where no single cluster was informative.

We predicted that coherent oscillations between brain areas might optimize the flow of information within the networks engaged by this task. Therefore, we quantified the phase synchronization of local field potentials in barrel cortex and mPFC. The two signals were coherent at theta range during S1 and S2 and, interestingly, prior to S1. We interpret the pre-stimulus coherence as reflecting top-down preparatory and expectation mechanisms.

We showed, for the first time to our knowledge, the neuronal correlates of parametric working memory in rodents. The existence of both positive and negative codes in barrel cortex, besides the representation of stimulus memory and decision signals suggests that multiple functions might be folded into single modules. The mPFC also appears to be part of parametric working memory and decision making network in rats.

Introduction

Working memory is the active storage of information across a limited time interval, to manipulate behavior or guide decision. We use our working memory for performing everyday life tasks; one example is remembering a phone number for the time necessary to punch it into the keypad; another example is looking for keys and remembering the places that have been already checked.

To correctly perform a behavioral task, different types of memories are required. Reference memory is a memory for information, invariant across time and context, upon which the "rules" of a given task must be applied. For example, a specific sound cue if followed by a specific action will always be followed by reward. Working memory, in contrast to reference memory, is typically a delay-dependent representation of information that is used to guide behavior within a trial (Of course, action must to be taken according to the information in the memory buffer by use of reference memory for the task rule). Initial studies of working memory described it as a representation of a cue over a delay period in which the cue is not present, to make a subsequent response (Honig, 1978). However, recent definitions emphasized the "working" aspect of this type of memory; Eichenbaum and Cohen define working memory as a type of short-term memory that involves active storage and manipulation (Eichenbaum & Cohen, 2001).

Working memory in rodents

In rats, working memory (WM) has been examined in a variety of tasks that can be categorized into two distinct frameworks: spatial navigation tasks, and delayed match- or nonmatch-to-sample. Spatial WM has been mostly studied in the form of maze tasks (e.g. T-maze, radial arm maze, Morris water maze, etc.) (Figure 1A). They usually require rats to remember a location or a set of locations visited recently (Morris, 1984; Jadhav et al., 2012) for a short period of time. Spatial WM tasks rely on rats' spontaneous alternation tendency which is the consequence of exploratory behavior in rats. However, navigation tasks do not constrain the modality or entity of stored information and multimodal sensory inputs might be combined for successful execution of these tasks (e.g., combined visual cues and path integration). Thus, it is difficult to specify what is being stored in navigational WM.

WM has also been examined in the context of delayed non-matching to sample tasks (DNMS) in the framework of operant chambers (Figure 1B). The animal is required to remember a stimulus over a delay in which that stimulus is no longer present (Grobe & Spector, 2006; Peña et al., 2006; Otto & Eichenbaum, 1992) and then compare it to the same or an alternative stimulus. DNMS tasks have the advantage that the experimenter specifies the to-be-remembered stimuli. However, they involve storage of information about *quality* or *identity* of the stimulus (e.g. an object or an odor). As will be seen below, our interest was in memory for things that can be defined in parameter space rather than by perceptual qualia.

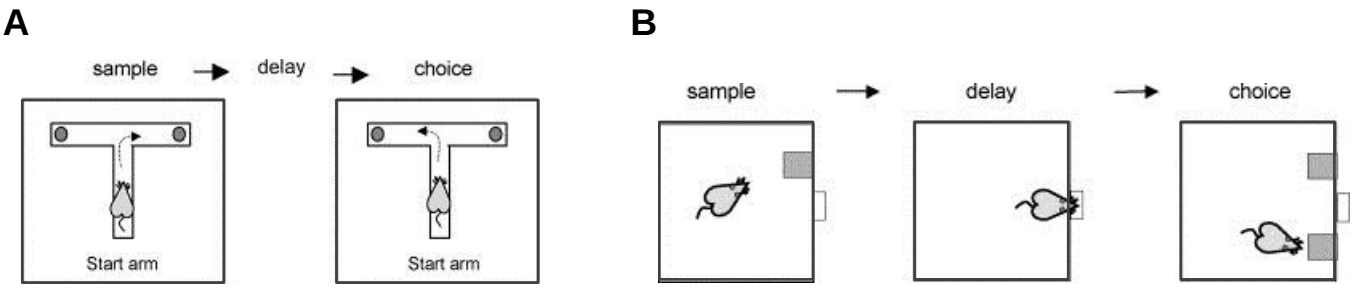

Figure 1. WM tasks in rodents (A) Delayed alternation on a T-maze. On the first or sample run, the rat is placed on the stem of the T-maze and permitted to enter one of the arms. The rat may then be removed from the maze for a delay period. After the delay, the rat is returned to the stem of the maze, and, will typically choose the alternate arm of the T. (B) Delayed non-matching to sample task in an operant chamber. The sample phase of the task consists of the presentation of a lever. During the ensuing delay, the lever is retracted and the rat must make a nose poke to a central food tray. Following the delay, the rat is presented with both levers, and reinforcement is obtained by a response to the lever that had not been presented during the sample phase of the trial. (The figure is adapted from Dudchenko 2004, Neuroscience & Biobehavioral Reviews.)

The main challenge associated with the paradigms mentioned above is that the precise content of the memory used to solve the task is not clear (in the case of spatial WM) or not quantifiable (DNMS). As a consequence, the mechanism of information coding during memory maintenance remains unknown. Moreover, many of the tasks used to study WM are categorized as "delayed response" tasks; where the animal can predict the correct response prior to the delay onset (Pontecorvo et al., 1996). It has been argued that postural mediation of the to-be-remembered response can occur in this case, which makes the interpretation of memory-dependent performance challenging.

Our interest in this dissertation was to study sensory working memory – the short term storage of quantifiable stimulus parameters. To our knowledge, in the literature, there is no systematic study of parametric working memory, with graded stimuli in rodents.

One recent study showed that rats could compare two sequential odorant mixtures in a "delayed comparison" task (Perry & Felsen, 2012). However, because shifts in the proportion of odorants in a mixture lead to qualitatively different odor percepts (Barkat et al., 2012), it is not clear whether the odor mixtures are sensed as steps in a single parameter or else as discrete percepts.

Tactile working memory

Various tasks have been used to investigate sensory working memory in primates. Many of the early studies involved delayed discrimination of basic attributes of visual stimuli such as size, orientation, contrast or direction of motion (Regan, 1985; Vogels & Orban, 1986; Miyashita & Chang, 1988; Magnussen & Greenlee, 1992; Magnussen et al., 1996; Lee & Harris, 1996; Blake et al., 1997; Chelazzi et al., 1998; Magnussen et al. 1998; McIntosh et al., 1999; Bisley & Pasternak, 2000; Magnussen, 2000; Zaksas et al., 2001; Bisley et al., 2001; Lalonde & Chaudhuri, 2002; Kahana & Sekuler, 2002 and Bisley et al. 2004).

Although much of the information about sensory working memory comes from studies of the visual system, there is a growing body of literature that deals with the storage of information in other sensory modalities, especially tactile (Sullivan & Turvey, 1972; Sinclair & Burton, 1996; Hernandez et al., 1997; Hernandezet al., 2000; Romo & Salinas, 2001; Romo & Salinas, 2003; Romo et al., 2002; Koch & Fuster, 1989; Burton, H. & Sinclair, 2000) and auditory (Deutsch, 1972; Deutsch, 1973; Gottlieb et al, 1989; Lu et al., 1992; Samms et al., 1993; Zatorre et al., 1994; Clarke et al., 1998; Clement et al., 1999; Anourova et al.,1999; Romanski et al., 1999).

In particular Romo and colleagues in a series of studies investigated the neuronal circuits underlying working memory in a flutter discrimination task. The monkey received two vibrations separated by a variable delay on the fingertip; it then made a choice according to the difference between the vibrations (Figure 2). Combining psychophysical and neurophysiological experiments in behaving monkeys, these investigators provided new insights into how several cortical areas integrate efforts to solve the vibrotactile discrimination task. In this project we adapted Romo's vibrotactile discrimination task and put it into the realm of rats for investigating the neuronal correlates of WM. Instead of the fingertip, we applied stimuli to the whiskers.

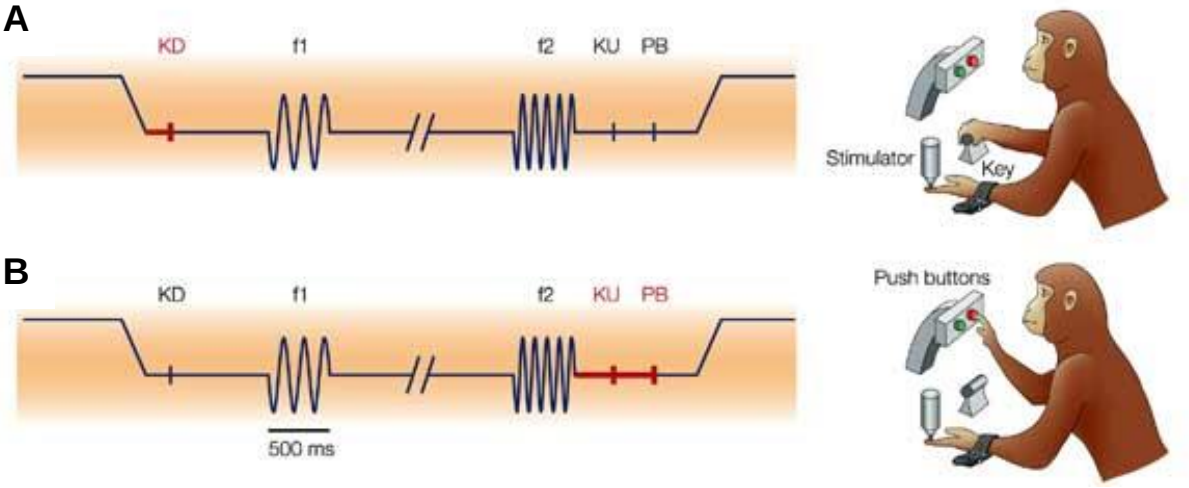

Figure 2. Vibration Discrimination Task and Performance. (A, B) Sequence of events. The mechanical stimulator is lowered, indenting the fingertip of one digit of the restrained hand. The monkey places its free hand on an immovable key (A, red line; KD). The probe oscillates vertically at the base stimulus frequency (f1). After a delay, a second mechanical vibration is delivered at the comparison frequency (f2). The monkey releases the key (B, red line; KU), and presses either a medial or a lateral push button (B, red line; PB) to indicate whether the comparison frequency was lower or higher than the base frequency. (The figure is adapted from Romo & Salinas 2003, Nature Reviews.)

The whisker sensory system

Rats are nocturnal animals in nature; they are active in dark environments and have poor vision. The classic study by Vincent illustrated that a rat's ability to navigate through a raised labyrinth depends on the use of its whiskers (Vincent, 1912). They use their whiskers — also called facial vibrissae — to recognize the positions of floors, walls and object. Recent research has shown that whisker touch represents a major channel (along

with olfaction) through which rodents collect information from the nearby environment (Diamond et al., 2008).

The rat somatosensory system is well suited for examining how neuronal activity encodes stimuli, not only because of its excellent functional capacities but also because of its unique anatomic and physiological organization. This region contains anatomically and functionally distinguishable clusters of neurons called "barrels" (Woolsey & Van der Loos, 1970; Welker, 1974; Jensen & Killackey, 1987) (Figure 3). In rats, each barrel contains an average of 2,500 neurons (Jones & Diamond, 1995) that respond primarily to their corresponding whisker (Simons, 1978; Armstrong-James & Fox, 1987; Diamond et al., 1993). The detailed knowledge of this processing circuitry, combined with the animals' high-level sensory capacities, makes the rat whisker sensory system a good platform for studying the neuronal bases of perception and memory.

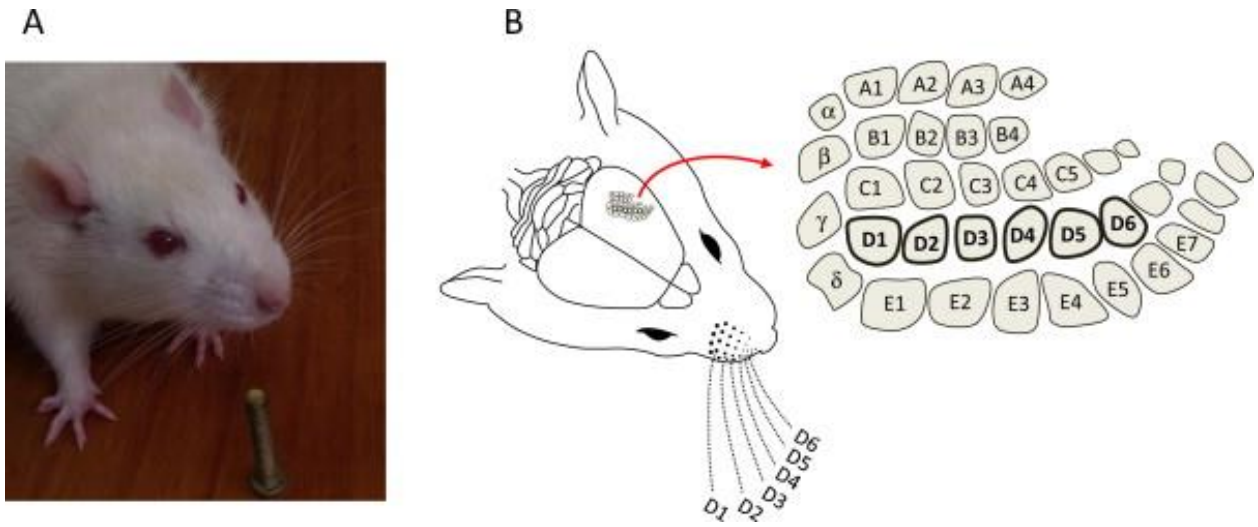

Figure 3. Rat whisker sensory system (A) Close-up of a Wistar rat as it explores objects using its whiskers. Photograph courtesy of Mehdi Adibi. (B) Arrangement of the barrels in the left somatosensory cortex of a rat, with each barrel labeled by its corresponding whisker. Whiskers of the D row are shown full length with their corresponding barrels highlighted in the cortical map. (The figure is adapted from Diamond & Arabzadeh 2013, Progress in Neurobiology.)

Active sensing and modes of operation

Active sensing usually entails sensor movement, but more generally involves control of the sensor apparatus, in whatever manner best suits the task, so as to maximize information gain (Prescott et al., 2011).

It is purposive and information-seeking. Although the concept of sensor apparatus control applies to all modalities, it is perhaps most evident in the modality of touch.

The rat whisker-mediated sensory system is a prominent case of active sensing inasmuch as the rat precisely controls its whiskers. The active sensing in rats arises through two modes of operation: (1) generative mode, and (2) receptive mode (Diamond & Arabzadeh, 2013).

Generative mode. In the generative mode, the rat moves its whiskers forward and backward to actively seek contact with objects and to palpate the object after initial contact. The animal causes the percept by its own motion. Self-generated whisker motion is critical for wall following (Jenk et al., 2010), distance estimation (Harris et al., 1999), and identifying properties such as shape and size (Brecht et al., 1997; Harvey et al., 2001). As a rat or mouse feels its way through the world, it senses its own whisking (Ganguly & Kleinfeld, 2004). From the relationship between the whisking cycle and the contact signal (Curtis & Kleinfeld, 2009) the animal localizes objects with millimeter-precision (Knutsen et al., 2006). The discrimination of texture is one condition in which rats generate neuronal sensory representations through their own whisker motion (Maravall et al., 2007; von Heimendahl et al., 2007; Diamond et al., 2008; Khoshnoodi et al., 2008; Lak et al., 2008; Mitchinson et al., 2008; Arabzadeh et al., 2009; Montani et al., 2009; Diamond, 2010; Prescott et al., 2011; Diamond, 2012).

Receptive mode. It is difficult to quantify rodents' use of their whiskers in natural, out-of-laboratory settings. But even in the absence of objective data it seems reasonable to assume that some forms of perception rely on blocking motor output to keep the whiskers immobile. For example, how do rats perceive the passage of a large predator above their burrow? We speculate that they place their whiskers in contact with the walls and floor, with negligible whisking output, to "listen" for vibrations (see Figure 4).

We can further develop the illustration of the rat feeling for ground vibrations in the receptive mode. If the burrow's walls tremble, is the predator approaching (increasing vibration intensity) or moving away (decreasing vibration intensity)? Changes and differences in vibration intensity seem ecologically relevant, and it is exactly this form of perception that we have tried to bring from nature to the laboratory in this project.

It is tempting to name the state of the sensory system characterized by exploratory whisking as "active" and the state of quiet immobility as "passive" (Kleinfeld et al., 2006), but this nomenclature is misleading in its

implication that the nervous system itself becomes passive in the immobile state, waiting to be subjected to unknown events. Observations collected in the present experiments suggest that the animal is highly "active" even when it places and holds its whiskers in contact with a moving stimulus. For this reason we refer to the "quiet" whisker state as the "receptive mode" rather than the passive mode.

To summarize, in the receptive mode, rats immobilize their whiskers to optimize the collection of signals from an object that is moving by its own power (Diamond & Arabzadeh, 2013). The receptive mode – specifically, the perception of vibrations applied to the whiskers by external devices – will be the focus of this thesis.

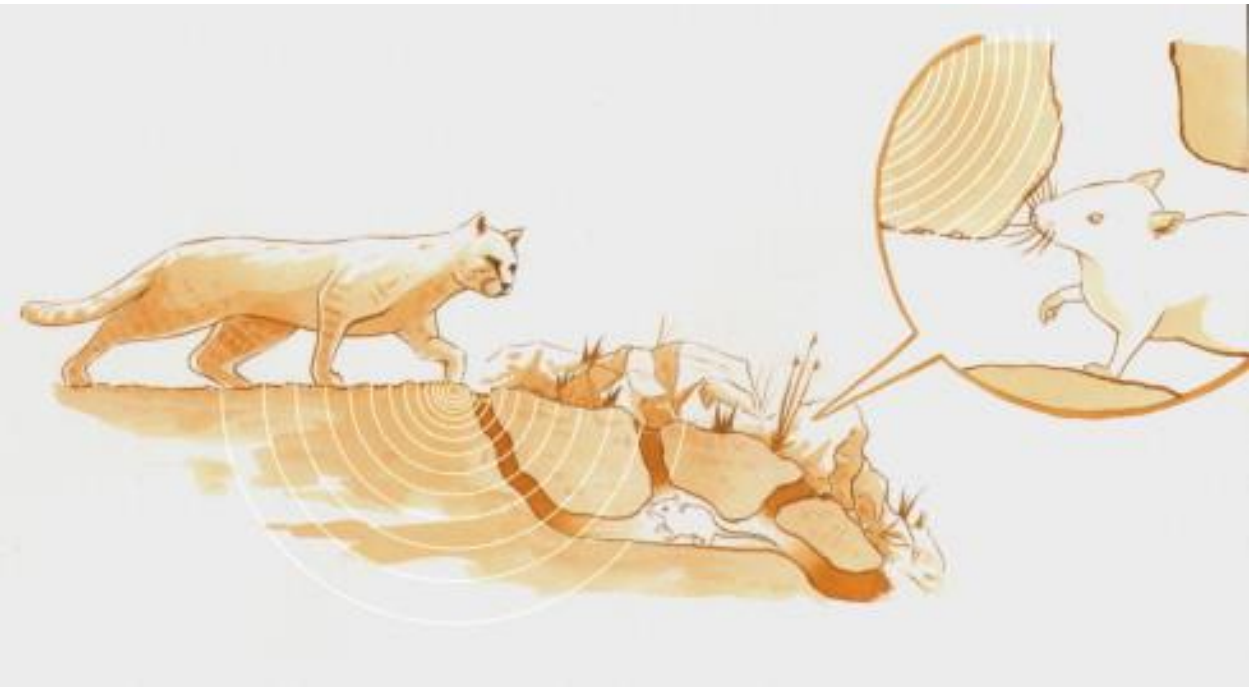

Figure 4. The receptive mode. As a predator approaches the rat's hiding place, the vibration signal might be transferred to the whiskers through their contact with the walls and floor of the burrow. Changes in vibration intensity over short time intervals would provide important information about the speed and direction of the predator. Drawing by Marco Gigante, SISSA Tactile and Perception Lab.

Distributed networks of working memory

Microelectrode recordings of cortical activity in primates performing working memory tasks reveal some cortical neurons exhibiting sustained or graded persistent elevations in firing rate during the period in which sensory information is actively maintained in short-term memory. These neurons are called "memory cells". Imaging and transcranial magnetic stimulation studies indicate that memory cells may arise from distributed

cortical networks. Depending on the sensory modality of the memorandum in working memory tasks, neurons exhibiting memory-correlated patterns of firing have been detected in different association cortices including prefrontal cortex, and primary sensory cortices as well (Wang et al., 2013).

Over the last decade, great progress has been achieved in understanding the organization of working memory networks and the functional specialization of brain areas that constitute the networks. Neurons with memory-related responses have been reported in multiple brain regions, such as the prefrontal cortex (D'Esposito et al., 1995; D'Esposito et al., 1999; D'Esposito et al., 2000; Fuster, 1973; Fuster & Alexander, 1971; Hernandez et al., 2002; Miller et al., 1996; Petrides et al., 1995 and Romo et al., 1999), the inferior temporal cortex (Fiebach et al., 2006; Fuster & Jervey, 1982; Miller et al., 1993 and Miyashita & Chang, 1988) and the posterior parietal cortex (PPC) (Champod & Petrides, 2007; Constantinidis & Steinmetz, 1996; Curtis et al., 2004; Joelving et al., 2007; Koch & Fuster, 1989; Pierrot-Deseilligny et al., 2005 and Zhou et al., 2007). These distributed cortical areas play a critical role in working memory networks. Especially, neuronal synchronization between PFC and PPC has been proposed to be the representation of task-specific information in visual working memory (Salazar et al., 2012), and other cognitive processes (Buschman & Miller, 2007 and Pesaran et al., 2008). Recently, there is increasing evidence that elemental sensory dimensions, such as tactile information in the somatosensory system (Hernandez et al., 2000 and Zhou & Fuster, 1996), are stored by segregated feature-selective systems that include not only the associative cortex, but also the sensory cortex that carries out early-stage processing (Gottlieb et al., 1989 and Super et al., 2001). Neuronal circuits in these cortical areas seem to have a dual function: the precise sensory encoding and the short-term storage of the encoded information.

Romo and colleagues, during the tactile discrimination task (explained above), demonstrated that the neurons in SI are only involved in on-line processing of stimulus. They encoded the base or comparison stimulus separately, showing no memory trace or comparison mechanism. SII neurons show a brief trace of the concluded stimulus, while neurons in PFC and VPC show a much more pronounced working memory, and a more prominent representation of the stimulus difference during the comparison period (Figure 5A).

Recent findings suggest that primary sensory cortex may also be part of this network when the task requires retention of information of a sensory rather than semantic or categorical quality. Specifically, several studies with monkeys have observed neuronal activity in primary somatosensory (SI) or visual (VI) cortex that is correlated with working memory for tactile or visual information (Zhou and Fuster, 1996, 2000 and Super et

al., 2001). Human psychophysical and brain stimulation experiments provide additional evidence consistent with a role for SI in tactile working memory in humans (Harris et al., 2001a; Harris et al., 2002).

In primates, working memory appears to engage widely distributed cortical areas which include not only association areas, such as prefrontal cortex and posterior parietal cortex, but also sensory areas, such as SI and SII – the modality-specific cortical stage of the system. Here we investigated how rat's brain manages to perform a similar task with a much smaller brain and less number of neurons and connections. We argue that prefrontal cortex in rats should be re-evaluated (Figure 5B).

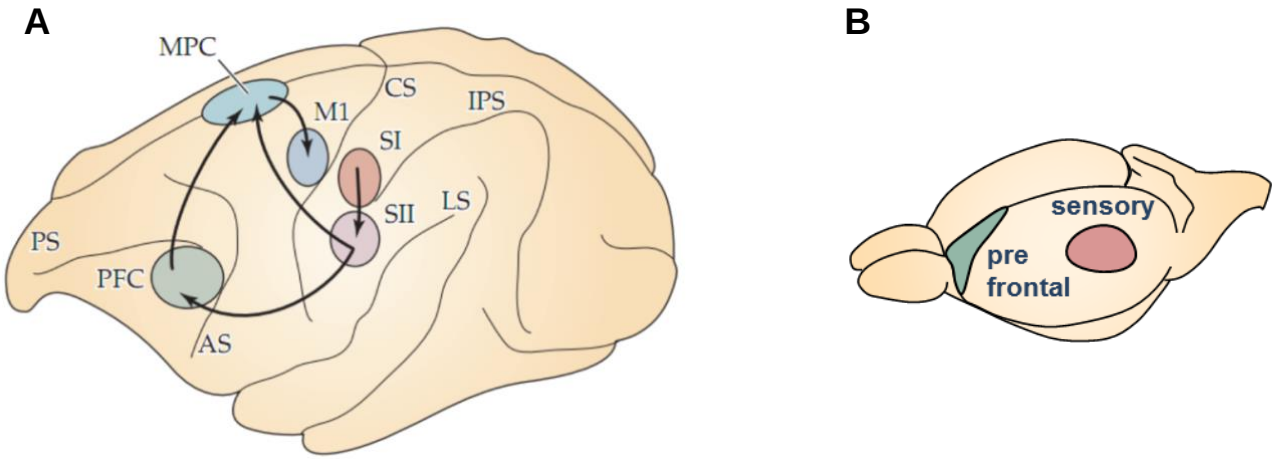

Figure 5. Working memory network in primates and rats brain (A) Cortical Regions Involved in the Vibration Comparison Task. The drawing shows the location of each cortical region (dashed lines). Gray arrows indicate the proposed flow of tactile information. AS, arcuate sulcus; CS, central sulcus; IPS, intraparietal sulcus; LS, lateral sulcus; MI, primary motor cortex; MPC, medial premotor cortex; PFC, prefrontal cortex; PS, principal sulcus; SI, primary somatosensory cortex (Romo & Salinas 2003, Nature Reviews). (B) Schematic of rats' brain with homologue brain regions that are possibly engaged in a similar task.

Medial prefrontal cortex organization in rats

The rat prefrontal cortex (PFC) consists of cytoarchitecturally and functionally distinct areas located over the medial, orbital, and insular surfaces of the rostral cerebral hemispheres (Cechetto & Saper, 1990; Neafsey, 1990; Neafsey et al., 1993; Thierry et al., 1994; Paxinos et al., 1999; Uylings et al., 2000, 2003; Westerhaus & Loewy, 2001 and Bohn et al., 2003). The medial PFC (mPFC) is strategically involved in both cognitive and autonomic visceromotor functions (Neafsey et al., 1986, 1993; Loewy, 1991; Verberne and

Owens, 1998; Groenewegen and Uylings, 2000 and Uylings et al., 2003). In contrast, the ventrolaterally located orbital cortices mediate aspects of reward associations that underlie discriminatory behavior (Schoenbaum et al., 2003). By comparison, the insular cortex is primarily a viscerosensory region directly involved in the processing of afferent cardiovascular, cardiopulmonary, gastrointestinal, gustatory, and related sensory information (Cechetto & Chen, 1990; Allen et al., 1991; Zhang & Oppenheimer, 1997 and Jasmin et al., 2004).

The mPFC consists of four main subdivisions which are, from dorsal to ventral, the medial agranular (AGm) (or medial precentral), the anterior cingulate (AC), the prelimbic (PL) and the infralimbic (IL) cortices (Berendse & Groenewegen, 1991; Ray & Price, 1992; Ongur & Price, 2000 and Heidbreder & Groenewegen, 2003).

The IL cortex has been shown to profoundly influence visceral/autonomic activity. IL stimulation produces changes in respiration, gastrointestinal motility, heart rate, and blood pressure (Terreberry & Neafsey, 1983; Burns & Wyss, 1985; Hurley-Gius & Neafsey, 1986; Verberne et al., 1987 and Hardy & Holmes, 1988). IL is viewed as a visceromotor center (Hurley-Gius & Neafsey, 1986 and Neafsey, 1990). PL cortex, on the other hand, has been implicated in cognitive processes. PL lesions have been shown to produce pronounced deficits in delayed response tasks (Brito & Brito, 1990; Seamans et al., 1995; Delatour & Gisquet-Verrier, 1996, 1999, 2000; Floresco et al., 1997 and Ragozzino et al., 1998), similar to those seen with lesions of the dorsolateral PFC of primates (Kolb, 1984; Goldman-Rakic, 1994; Barbas, 1995, 2000 and Groenewegen & Uylings 2000).

Each of the subdivisions of the mPFC receives a unique, but partially overlapping, set of afferent projections. There is a shift dorsoventrally along the mPFC from predominantly sensorimotor (non-limbic) cortical and thalamic input to dorsal mPFC, to limbic cortical and thalamic (midline thalamus) input to the ventral mPFC. Each division of mPFC strongly communicates with immediately adjacent regions, and with the possible exception of IL, each division interconnects with all others. The hippocampus (CA1/subiculum) projects heavily to IL and PL, and considerably less so to dorsal regions of the mPFC. Sites projecting commonly to the four divisions of mPFC include insular cortex, claustrum, amygdala, parts of the midline thalamus, supramammillary nucleus, ventral tegmental area, periaqueductal gray, dorsal raphe nucleus, median raphe nucleus, and locus coeruleus of the brainstem.

Somatosensory information can reach prefrontal areas via several channels (Eden et al., 1992; Conde et al., 1990 and Hoover & Vertes, 2007). Direct projections of somatotopically organized regions: Projections from SI to prefrontal areas are sparse and negligible, and most of them are mediated either via the dysgranular somatosensory cortex or via SII. These areas project mostly to the dorsal part of the mPFC, comprising the AGm and dorsal AC. These areas receive a vast array of information both directly and indirectly from all sensory modalities and presumably utilize this information in situations demanding immediate attention for appropriate actions. As discussed, Reep et al. (1990) view AGm as a multisensory integration region. Stimulation of AGm (and dorsal AC) produces movements (and generally coordinated movements) of the head, eyes and vibrissa, having the characteristics of orienting responses. AGm it is thought to be homologous to the premotor, supplementary motor and frontal eye fields of primates (Vertes, 2006 and Erlich et al., 2011).

Indirect connections relaying somatosensory information to PFC, probably in a highly processed form, come from the perirhinal cortex and reach PL and IL. There is a dramatic shift in sources of afferent information from the AGm/dorsal AC to PL (and ventral AC), from multisensory afferents dorsally, to a combination of sensory and limbic input (subcortical/cortical) ventrally. PL is strategically positioned to integrate information across modalities and compare present and past events for appropriate actions. In this regard, cells of PL (and ventral AC) respond selectively during the delay period of delay response tasks, and PL lesions produce marked deficits in delayed responses tasks involving short and long delay—as do lesions of major PL targets (or the PL circuit) (Vertes, 2006). PL area in rat is thought to be homologous to the lateral/dorsolateral PFC of primates (Vertes, 2006 and Hoover & Vertes 2007).

The mPFC of rats, like the prefrontal cortex of primates, would appear to be directly involved in higher order cognitive functioning, and through interconnections among the four divisions, would be capable of exerting control over all aspects, including affective components, of goal directed behavior. If PL is the homologous of the dlPFC in primates, we would expect to find neurons that encode and store the stimulus during the delay period following the stimulus offset. In this project we have investigated this idea in a delayed comparison task involving parametric working memory.

Neuronal communication through coherent oscillations

As described earlier, working memory, like every cognitive operation, entails participation of widely distributed cortical areas including parietal and frontal areas of the brain and different sub networks within

the same area. What are the modes of transferring information between neuronal populations? How do these distant brain areas communicate? With the axonal projections and anatomical connections forming the structural basis for communication, neuronal coherence has been hypothesized to be an important mechanism for optimizing the efficiency of communication between structurally connected brain areas (Engel et al., 2001; Fries, 2005 and Varela et al., 2001).

The central argument is that activated neuronal groups have the intrinsic property to oscillate (Kopell et al., 2000 and Tiesinga et al., 2001). Those oscillations constitute excitability fluctuations that do not only affect the output of the neuronal group, but also its sensitivity to input (Burchell et al., 1998 and Volgushev et al., 1998). Thus, oscillations of a neuronal group rhythmically open and close the group's windows for communication. It is obvious that different groups of neurons can only communicate effectively with each other if the rhythmic opening of their communication windows is coordinated between the groups. In other words, oscillatory activity in different areas can be phase-coupled, i.e., display systematic phase-delays, a phenomenon called phase-synchronization. In support of this hypothesis, correlations between cognitive functions and long-range phase synchronization have been demonstrated in many different areas and species, e.g. (Benchenane et al., 2010; Buschman and Miller, 2009; Gregoriou et al., 2009; Pesaran et al., 2008; Roelfsema et al., 1997; Siapas et al., 2005; von Stein et al., 2000 and Womelsdorf et al., 2007).

When performing a cognitive task (e.g. vibration discrimination task), rats require integrating two streams of data, those coming from the environment (i.e. stimuli) and, from reference memory representing the task goal that entails how to map stimuli onto responses. This task set information serves as a critical top-down signal that biases how efficiently and accurately sensory inputs are processed and mapped onto actions. These top-down influences refer to the fact that many aspects of cognition and behavior are not stimulus driven in a reflex-like manner, but are to a large degree based on expectations derived from previous experience, and on generalized knowledge stored in the architecture of cortical and sub-cortical networks. Accordingly, Singer and colleagues proposed that synchronous oscillations are particularly important in this process (Engel et al., 2001), building in this way a more complete scenario on the role of oscillations in the brain. Recent studies have begun to map this preparatory top-down state onto brain areas in the prefrontal and parietal cortex (Summerfield & Egner, 2009; Bollinger et al., 2010 and Passingham et al., 2010).

These studies have shown that selective preparatory states indicative of anticipatory attention and working memory retention are associated with selective long-range phase synchronization at various time scales and frequencies (Deco & Thiele, 2009; Canolty et al. 2010; Womelsdorf, Vinck et al., 2010; Fell & Axmacher,

2011; Bosman et al., 2012; Salazar et al. 2012 and Siegel et al. 2012). Large-scale phase coupling could thereby provide a critical window into the mechanisms underlying the coordination and integration of distributed top-down information during task performance (Fries, 2005; Womelsdorf et al., 2007; Arnal & Giraud, 2012; Battaglia et al., 2012 and Jensen et al., 2012).

As synchronous oscillations would be particularly important in top-down modulation, the study of somatosensory processing in the context of attention and working memory paradigms is a valuable approach to the highlighting of pioneering theories.

Materials and Methods

The behavioral methods of the delay comparison task here have been previously described in the paper attached in the Appendix, of which the PhD candidate is co-author (Fassihi et al., 2014). In this chapter we shortly explain the main parts; further details of the behavioral methods can be found in the paper. Neuronal recordings and analysis are explained later in this chapter.

Subjects

Eight Wistar male rats (Harlan Laboratories, Italy) were housed in pairs or individually and maintained on a 12/12-h dark/light cycle till the moment of surgery. Rats were habituated to the researcher (handling procedure) for five days before the experiments started. All experiments were conducted during the dark phase. Food was ad libitum throughout the experiment. Rats were water restricted and were trained to perform tactile delay comparison tasks for a pear juice reward diluted with water (1 unit juice : 3 units water). The water restriction schedule allowed access to water *ad libitum* for 10 min/d after each training session.

At the start of the experiment rats were 6–8 week old and weighed 225–250 g; they gained weight steadily throughout the study. They were examined weekly by a veterinarian. Protocols conformed to international

norms and were approved by the Italian Health Ministry and the Ethics Committee of the International School for Advanced Studies.

Apparatus

The behavioral apparatus consisted of a custom-built Plexiglas chamber measuring 25 × 25 ×38 cm (H × W × L) attached to a stimulus delivery port (Figure 6). In the front wall, a 3.8 cm (width) by 5 cm (height) head hole allowed the animal to extend its head from the main chamber into the stimulus delivery port. Within the stimulus delivery port a 0.85-cm-diameter nose poke was centered in front; the nose poke contained an optic sensor illuminated by an infrared photo beam to detect the rat's snout. Above the nose poke, a blue LED was fixed. LED illumination signaled to the rat that the next trial may begin.

The stimulus was delivered through a permanent magnetic vibration exciter (type 4808, Bruel & Kjaer) which was placed on its flank in order to produce motion in the horizontal dimension. The motor was selected due to its ability to deliver displacements of up to 12.7 mm peak-to-peak (1.4 m/s max velocity) and with frequency content of 5Hz to 10 kHz, depending on the attached weight to it. Since the motor produced constant acceleration above certain frequencies, its velocity range was reduced for large frequencies. To make the motor output compatible with the desired stimulus velocity patterns, described below, we first low-pass filtered the signal to remove the frequencies higher than 110 Hz.
Since the motor itself applies another filter to the signal, the motor motion was assessed empirically to determine the exact pattern of the stimulus delivered to animal's whiskers. We tested the motor before installing it in the apparatus by fixing a position transducer (LD 310-25; OMEGA Engineering) to a rod and then executing the entire stimulus library while recording 1,000 frames per s video clips (Optronis CamRecord 450). At this point, we could install the motor in the behavioral apparatus with full knowledge of its output. Descriptions of the stimulus are based on the true measured output of the motor.

A lightweight aluminium rod was fixed to the diaphragm of the shaker, projecting the motor's translation into the stimulus delivery port. On the end of the rod, a 20 x 30 mm plate was attached with vertical orientation. The rat received the stimulus by placing its whiskers on the plate with an approximately orthogonal orientation. Double-sided sticky tape was placed on the plate prior to each session to make the whiskers remain in contact and to "follow" the motor during stimulation. Using the miniature nose poke as a reward port during shaping, the rats learned to place their head between the head hole and nose poke; at

this point, head movement was reduced and the natural position of the whiskers was to rest in contact with the stimulator plate (Fassihi et. al, 2014).

An infrared light emitting diode (LED) illuminated the stimulus delivery port to permit video recording. In some sessions, high speed video images (Optronis CamRecord 450) were taken at 1,000 frames per second through a macro lens (Kawa CCTV Lens, LMZ45T3) to monitor head and whisker position and movement during behavior.

The chamber also contained left (L) and right (R) reward spouts mounted on 8-cm–high pedestals (Figure 6A). Each spout housed a custom-made infrared LED-based contact sensor. An AVR32 board (National Instruments) acquired all sensor signals and controlled the liquid syringe pump (NE-500 programmable OEM; New Era Pump Systems) for reward delivery. Three audio speakers were positioned just outside the walls of the apparatus. The central one, located at the back of the apparatus, delivered the go cue. The two lateral speakers were positioned near the two reward spouts to present a "reward delivery cue" as a reinforcer of the release of juice.

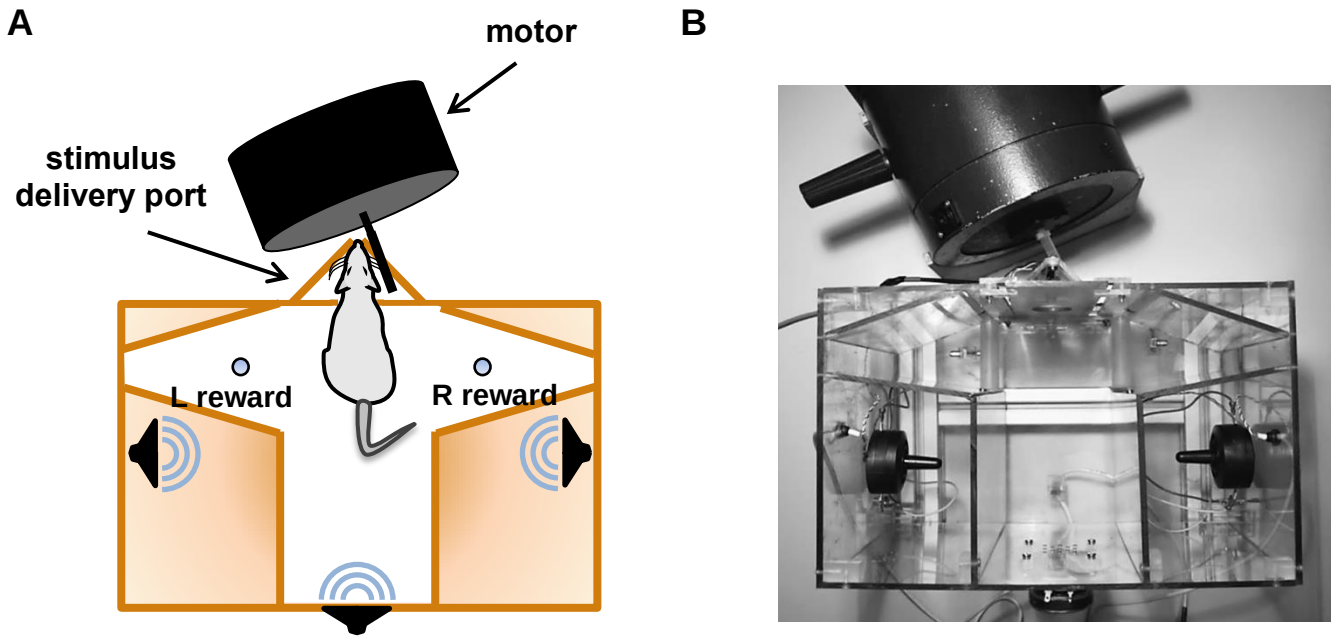

Figure 6. Behavioral apparatus. (A) Dark boundaries represent Plexiglas walls. The rat is sketched with snout extended through the head hole into the stimulus delivery port, and placed its whiskers in contact with the plate. Left (L) and right (R) reward ports are indicated. The plate's surface is approximately vertical and is seen as a line segment from above. Reward spouts are visible laterally. (B) Photograph of the apparatus from above. The configuration mirrors the sketch in A.

The experiment ran automatically using software written in LabVIEW (National Instruments). During the shaping sessions of the training procedure, experimenters set variables such as reward size, task difficulty (the difference between the two stimuli to be discriminated), and interstimulus delay according to the progress of the rat. Once the animal learned the task, the experiment could run without any manipulation by the experimenter. Nevertheless, the experimenter monitored the session to detect and react to tendencies such as left/right bias or satiety.

Stimuli

Stimuli were irregular "noisy" vibrations, consisting of changes in the plate position in the rostral/caudal direction. The sequence of velocity values was taken from a normal distribution with 0 mean, and SD denoted by σ. Velocity distributions and time series for two example stimuli are illustrated in Figure 7A. Figure 7B shows the task structure. When the rat positioned its snout in the nose poke, the trial began with the prestimulus delay. At the conclusion of the delay, the first stimulus was presented, characterized by σ1. After the interstimulus delay, the second stimulus was presented, characterized by σ2. The rat had to remain in the nose poke for the entire trial, including the poststimulus delay. When the "go" cue sounded, the rat withdrew and selected the left or right spout according to the relative values of σ2 and σ1. As for any discrimination task, difficulty increased as the stimulus difference decreased. Difficulty depended on the difference between σ1 and σ2, quantified by the SD index (SDI):

$$SDI = \frac{\sigma 2 - \sigma 1}{\sigma 2 + \sigma 1} \qquad (1)$$

On a typical trial, a well-trained rat (Figure 7C) placed its snout in the stimulus delivery port to initiate the trial and receive stimuli (Figure 7C, Left); it withdrew from the nose poke after the go cue (Figure 7C, Center) and turned to one of the two reward ports (Figure 7C, Right). In well-trained rats, the self-generated motion known as "whisking" was suppressed throughout the trial, indicating that the sensorimotor system entered a "receptive sensing" mode of operation (Diamond & Arabzadeh, 2013; Prescott et el., 2011).

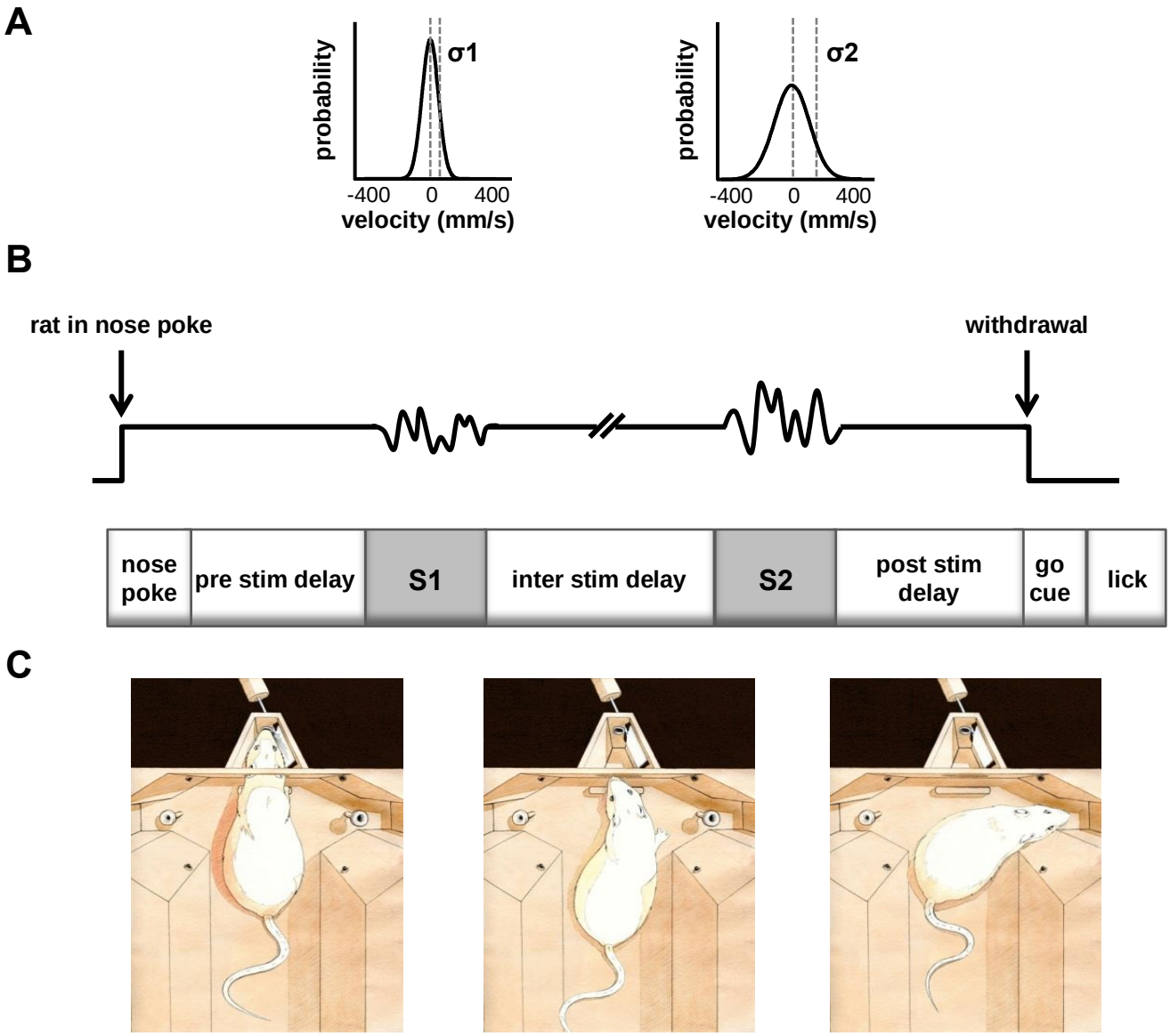

Figure 7. Structure of a single trial. (A) Stimuli were composed of a series of velocity values where the sampling probability of a given velocity value was given by a normal distribution with mean = 0 and SD = σ. Example schematic stimuli are illustrated, resulting from the sampling of the distribution shown above each stimulus. For illustration purposes stimuli are downsampled; the real stimuli have higher frequency contents. (B) Upper trace indicates the presence of animal in the nose poke, the arrows demonstrate the time of entry of the rat in the nose poke (at the far left) and the time of withdrawal (at far right). Below, key events of the trial are given. (C) Sketches depicting one trial. (Left) The rat places its snout in the stimulus delivery port to initiate the trial and receive stimuli. (Center) Upon hearing the go cue, the rat withdraws. (Right) The rat selects the right reward port.

Stimulus Generalization Matrix

To ensure rats perform a working memory task, the set of stimuli used was of great importance. If the first stimulus were fixed across all trials and only the second stimulus shifted, the rat might solve the task by ignoring S1 and applying a constant threshold to S2. Likewise, if the second stimulus were fixed across all trials, the rat might simply apply a constant threshold to the first stimulus. To avoid such shortcut strategies, we used the stimulus generalization matrix (SGM). The SGM, adapted from Romo and coworkers (Hernández et al., 1997; Romo et al., 1999), consisted of stimuli spanning a wide range of σ values (Figure 8). Neither the first stimulus nor the second stimulus, taken alone, contained sufficient information to solve the task, so the rat was required to execute a direct comparison between the two stimuli on every trial.

In the final stage of training (Fassihi et al, 2014, SI Text), rats proceeded to an SGM with 14 [σ1, σ2] stimulus pairs (Figure 8). The σ values were evenly distributed in a logarithmic scale and the absolute value of the SDI was kept equal for all stimulus pairs (SDI = 0.25), ensuing an equal difficulty level. The diagonal line represents σ1 = σ2; all the pairs on one side of the diagonal were associated with the same action. The delay period was variable during the training phase to prevent the animal developing timing strategies for delay duration. The values of delay were taken from the set 0.5, 1, 2, 3 and 4 s; trials with different delays were randomly interleaved.

Exclusion of non-tactile Signals

Test sessions were run under dim ambient or red light that did not allow visualization of the stimulator motion. No potential olfactory or gustatory cues about the vibrations were available. However, the motor generated acoustic signals (easily heard by humans), and precautions were taken to ensure that rats did not use such signals to judge the stimuli, as described in supplementary information text and Figures S4 and S5 of the paper in appendix (Fassihi et al., 2014).

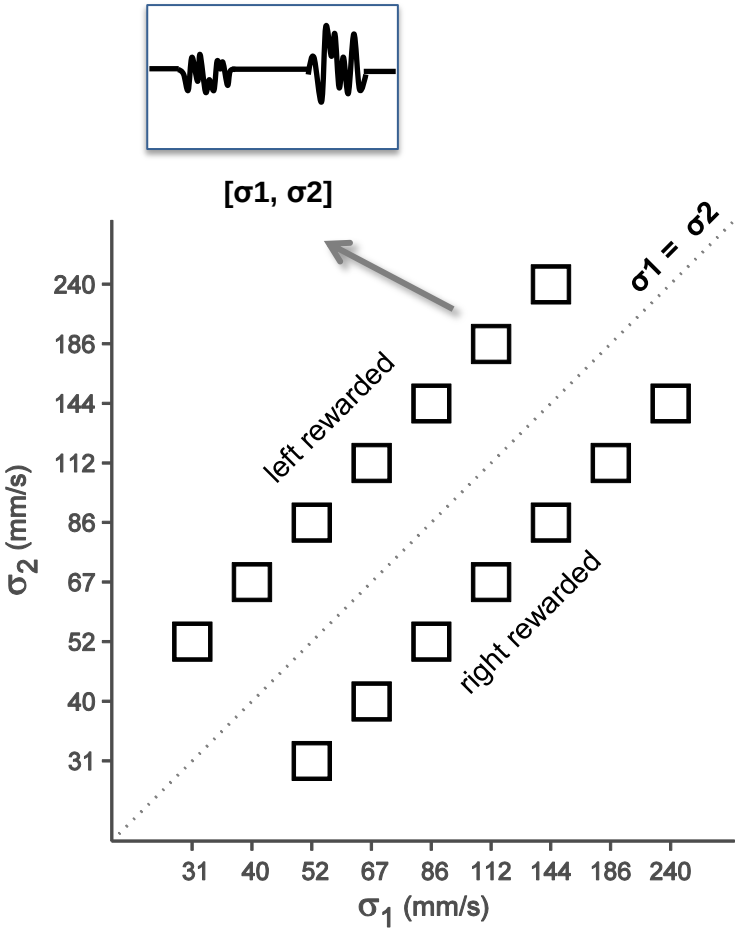

Figure 8. Stimulus generalization matrix. The [σ1, σ2] pair for each trial was selected randomly from among those represented by the boxes. S1 values are distributed along the abscissa, and S2 values are distributed along the ordinate; note logarithmic scales. Diagonal line separates σ2> σ1 (reward left) from σ2 < σ1 (reward right) stimulus pairs.

Surgery

Once rats reached a stable performance in the working memory task (>75% correct trials, statistical proof for working memory), they underwent a surgery for electrode implantation. Animals were anesthetized with Isoflurane (2.5% for induction and craniotomy, 1.5% for maintenance) delivered through a snout mask. Three small screws were fixed in the skull to support the dental cement. One of the screws was touching the Dura and served as the reference and ground electrode (reference and ground were shorted). Two craniotomies were made, one over barrel cortex, centered at 2.5 mm posterior to bregma and 6 mm lateral to the midline, the other over medial prefrontal cortex, centered at 3.2 mm anterior to bregma and 0.6 mm

lateral to the midline. To minimize brain dimpling, we performed a few steps. First, Dura mater was removed over the entire craniotomy using the tip of small syringe needle. The tip of the needle was bended to make a small hook. Then a drop of sterile ointment in the middle of craniotomy and the surgical cyanoacrylate adhesive (Histoacryl, B.Braun) was applied directly to the pial surface bordering the edge of the cranial opening. This procedure fastens the top layer of the brain, the pia mater, to the overlying bone and the resulting surface tension prevents the brain from depressing under the advancing electrodes.

With the brain anchored to bone, the 16 or 32 channel microwire arrays (Tucker-Davis Technologies) were inserted in each area by slowly advancing a Narashige micromanipulator. Once at the right depth, the remaining exposed cortex was covered with biocompatible silicon (KwikSil, World Precision Instruments). The array was then attached to the skull by dental cement (SEcure Starter Kit, Sun Medical). Rats were given the antibiotic enrofloxacin (Baytril; 5 mg/kg delivered through the water bottle) for a week after surgery. During this recovery time, they had unlimited access to water and food. Recording sessions in the apparatus began thereafter.

Electrophysiological recordings

The microwire array (Tucker-Davis Technologies) was comprised of 16 or 32 polyimide-insulated tungsten wires of 50 μm diameter, 250 μm electrode spacing and 375 μm row spacing. The impedance of the each wire was 20 kΩ, at 1 kHz, measured in saline, and around 150-200 kΩ when measured in vivo (Prasad and Sanchez, 2012). While lowering the arrays, the quality of raw signals was monitored and the detected spikes were clustered and sorted online using the OpenEx toolbox (Tucker-Davis Technologies). The barrel cortex array was fixed at a depth of around 900 μm, where it became possible to distinguish action potential waveforms evoked by manual whisker deflections. The depth of the recording sites, together with the small receptive fields, is consistent with an electrode tip position in layer 4. However our analyses and conclusions do not depend on the precise laminar localization of the neurons. The medial prefrontal cortex array was designed in a way that wires with two different lengths were interleaved. This resulted in half of the electrodes having 600 μm tip-spacing with the others. So we recorded from two different depths with a single array, one around 2800 and the other 3400 μm.

After passing through a unity-gain headstage, signals were transmitted through a cable to PZ2 preamplifier (Tucker-Davis Technologies). Signals were then digitized at a sampling rate of 24 kHz and sent through an optical fiber to RZ2 amplifier (Tucker-Davis Technologies) were they were amplified and stored. Data were

then analyzed offline using custom-build Matlab codes (MathWorks). To remove the common artifact and improve signal to noise ratio, we performed local referencing on each array. This was achieved by visualizing bandpass filtered (300Hz – 3 kHz) signals of multiple channels and selecting the most silent channel, which then served as the reference for all the other channels on the same array. For the analysis of neuronal data, spike detection and sorting were performed using clustering algorithms (Wave-Clus, Quian Quiroga et al., 2004). Only well separated units together with multiunit with stable waveform and firing rate over the course of a session were included in the analysis. In total, we identified 153 multiunit clusters in barrel cortex, and 69 clusters in PFC.

Data analysis

Spike density functions. In the analysis of neuronal responses we carried out a continuous-time data analysis approach. We first convolved the spike train of each neuron (with 1 ms resolution) with Gaussian kernels to obtain spike density functions. To avoid the leakage of data from stimulus period due to smoothing, this period was convolved separately from other periods. The kernel sigma used for stimulus period was narrower (σ=50 ms) comparing to other periods (σ=150 ms) to better examine the temporal dynamics of response during vibration stimulus. Kernels were corrected for the edge effect. The time-dependent spike density functions which give an estimate of the instantaneous firing rate were used for the rest of the analysis explained below.

Generalized Linear Model. We first examined the linear relation between the stimulus velocity standard deviation and neuronal responses. The response of the neuron at each point in time was defined as its instantaneous firing rate taken from the spike density function. Employing a standard linear regression was not appropriate because it uses a squared-error loss function, and assumes that the noise (residual of the fit) is Gaussian distributed which is not valid for neuronal activity. Instead, we fitted a generalized linear model (Nelder & Wedderburn, 1972) to linearly map the stimulus standard deviation to the response of the neuron through a Poisson link function which better captures the statistics of neural firing. We estimated the optimal slope parameter of the linear fit with a maximum likelihood-based iteratively reweighted least squares method. This was implemented using *glmfit* in Matlab (MathWorks).

Test of significance for the slope of the fit. We performed a non-parametric test for evaluating whether the slope of the fit was significantly different from zero. To estimate the reliability of the estimated GLM parameter, we first built a bootstrapped distribution of slopes by resampling (with replacement) 1000

times from different observations (trials) and fitting a GLM model. To obtain a baseline comparison, we then shuffled the stimulus tag across trials 1000 times and estimated the slope of the GLM fit in each iteration resulting in a shuffled distribution. We compared both distributions by computing a difference distribution and calculating the proportion of differences greater than zero. This provides us with a p-value for the statistical test. The neuron was tagged as having a significant slope if the p-value of the non-parametric test was smaller than 0.05. To build the temporal profile of the neurons having significant slope we sampled from the spike density function of the neuron every 20ms.

Information theoretic analysis. Our hypothesis was that barrel and prefrontal cortex neurons participate in the on-line encoding and storage of stimulus in the delay comparison task. Moreover they might contribute to the comparison of the two stimuli. Therefore, we needed to estimate the quantity and statistical significance of the signal carried by the firing rate modulations of individual neurons on single-trials about each of these task parameters. We computed Shannon's Mutual Information (Shannon 1948), hereafter referred to simply as information, for this purpose.

In this formulation, the amount of information which can be extracted from the firing rate of a neuron R, about the task-related parameter X can be computed as:

$$I(X;R) = \sum_{x} P(x) \sum_{r} P(r|x) log_2 \frac{P(r|x)}{P(r)} \qquad (2)$$

Where $P(r|x)$ is the conditional probability of observing a neuronal response r given the presentation of the task parameter x, $P(r)$ is the marginal probability of occurrence of neuronal response r among all possible responses, and $P(x)$ is the probability of task parameter x. For example when measuring information about stimulus standard deviation, $P(x)$ is the proportion of trials where a stimulus with σ=x was presented. Intuitively, mutual information measures how much knowing the neuronal response reduces uncertainty (or entropy) about the parameter of interest.

When estimating the information in the neuronal response, we were concerned about spurious information values caused by the inherent correlations between task parameters. This correlation comes from extreme [S1, S2] pairs of SGM, where a unique S1 (or S2) value could lead to only one possible decision. So that a neuron encoding (and so having only information about) S1 will necessarily have information about the decision, and vice versa. In particular, since our main interest was determining neurons that encode the stimulus in a graded manner (i.e. parametric working memory), we took special care to compute the

information that neurons carry about S1 that could not be explained by other possible parameters (like future action of the animal).

For this purpose, we used conditional information to disentangle the information about stimulus from the information about the difference of the two stimuli which leads to animal action:

$$I(S1;R|D) = I(S1;\{R,D\}) - I(S1;D) = I(R;\{S1,D\}) - I(R;D) = I(R;\{S1,S2\}) - I(R;D) \qquad (3)$$

Where S1 and S2 are the first and second vibration standard deviations, R is the neuron's firing rate and D is the sign of the difference between two stimuli (S2-S1) which in the correct trials studied here is equivalent to the action of the animal. In simple words, we measured information in the response of a neuron about S1 that was extra to the information that could be extracted merely by knowing decision. Or in other words, for a given value of D, we measured whether there is still statistical dependence between R and S1. In the particular case of the SGM, this is equivalent to measuring information about S1 across the [S1, S2] pairs of SGM that correspond to similar action, i.e. lying below (or above) the diagonal (Figure 9A). Note that the last equality in (3) is due to the fact that knowing S1 and D is equivalent to knowing S1 and S2.

Similarly, for information about the difference at different parts of the trial we computed the conditional information given S1 or S2:

$$I(D;R|S1) = I(D;\{R,S1\}) - I(D;S1) = I(R;\{D,S1\}) - I(R;S1) = I(R;\{S1,S2\}) - I(R;S1) \qquad (4)$$

$$I(D;R|S2) = I(D;\{R,S2\}) - I(D;S2) = I(R;\{D,S2\}) - I(R;S2) = I(R;\{S1,S2\}) - I(R;S2) \qquad (5)$$

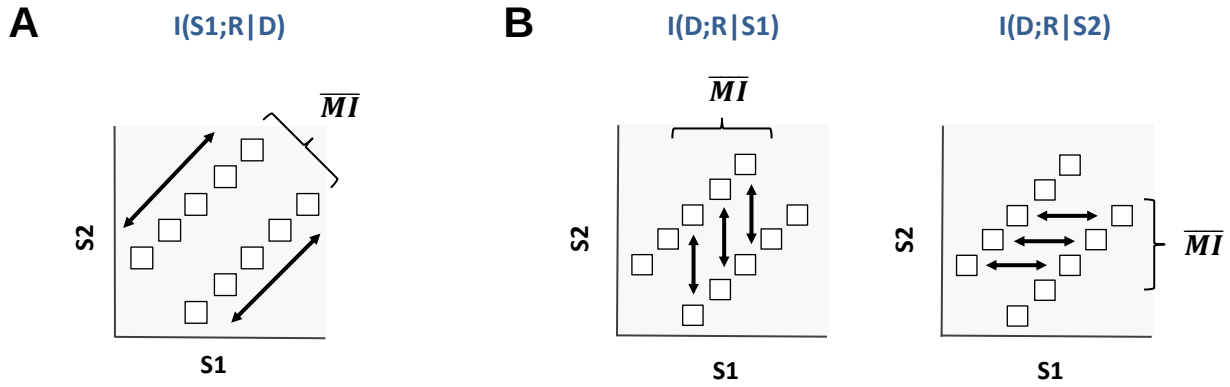

Figure 9. Conditional information demonstration on the SGM. (A) I(S1;R|D) can be estimated by measuring information about S1 across the [S1, S2] pairs of SGM that correspond to each of the two possible actions, i.e. lying below and above the diagonal, separately and then averaging between the two values. (B) Similarly I(D;R|S1) and (ID;R|S2) can be estimated by averaging between the MI values calculated among pairs of SGM with equal S1 and S2 respectively.

Equations 4 and 5 quantify the information in the firing rate about the difference of the two stimuli with equal S1 (Figure 9B left) and S2 (Figure 9B right) respectively.

The response of the neuron at each time was defined as its instantaneous firing rate. To build the temporal profile of information we measured the information by sampling from the spike density function of the neuron every 20ms. This is similar to using a sliding Gaussian kernel with step size of 20 ms. The convolution of this kernel with the spike train of the neuron results in an estimate of the instantaneous firing rate. Thus, we investigated the information afforded by the "rate" code only. Additional information, not captured by rate, may be present in the precise timing of spikes of neurons in each area (Panzeri & Schultz, 2001; Panzeri et al., 2001; Petersen et al., 2001).

The probabilities in equation 3-5 are not known a priori and must be estimated empirically from a limited number, N, of experimental trials for each unique x and r value. For some recordings in our dataset, N could be as low as 20. Limited sampling of response probabilities can lead to an upward bias in the estimate of mutual information (Optican et al. 1991; Panzeri & Treves 1995). One correction method for this bias has been proposed (Panzeri & Treves 1995) and can be subtracted from the direct information estimates (Equation 1), provided that N is at least two to four times greater than the number of different possible responses (Panzeri and Treves, 1995). To obtain unbiased estimates we reduced the dimensionality of the response space by grouping the firing rates into 3-4 classes. All of the information values in equation 3-5 were computed using Information Breakdown Toolbox (Magri et al., 2009).

Test of significance of information. We built a non-parametric permutation test to determine the epochs of behavioral trial in which the recorded neurons had values of information significantly greater than zero. This was achieved using a bootstrap procedure that consisted of random pairing of stimuli and responses in order to destroy all the information that the responses carry about the stimulus. We repeated this procedure 1000 times and we compared the original response against the bootstrapped distribution. The neuron was called significantly informative in one epoch if the original response value exceeded the 95% percentile of the bootstrapped distribution. ($p<0.05$).

Linear Discriminant Analysis. To quantify the information carried in the response of a population of simultaneously recorded neurons we used decoding algorithms which are more data-robust in case of limited samples (Quiroga & Panzeri, 2009). Time-dependent population density vectors were constructed from the spike density functions of the jointly recorded neuronal clusters at each region. To evaluate the

information provided by the population vector, we decoded task related parameters (S1, S2 and S2-S1) at each time.

Linear discriminant analysis (LDA) was implemented to find the optimum weight vector for population decoding. LDA finds the optimized projection directions that the between-class variance in the data is maximized relative to the within-class variance (Fisher, 1936; Duda, 2012).

However, in the case of high dimensional (large number of neurons), low sample size data (limited number of trials per condition), LDA suffers from overfitting. This term describes a situation where the decoder weights are determined to a large extent by the noise in a particular data set, instead of the structure of the generating process. Such a decoder classifies the current data, seemingly "correct" but as a consequence of over-fitting, it is unable to predict future data originating from the same process. To deal with such a situation, regularization techniques are proposed (Friedman, 1989). Regularization prevents over-fitting by introducing a penalty on the complexity (i.e. number and values of weights) of the decoder. Here, we used a pair of regularization parameters *Gamma,* the constraining (or shrinkage) parameter on the weight values, and *Delta,* a threshold below which weights were set to zero (Guo et al., 2006). Delta and Gamma could vary from zero to one.

The performance of the decoder was validated using cross validation methods; the optimal set of weights were obtained on a subset of data (training set) and then tested on the other part of data that was untouched. The regularization parameters were first optimized with cross validation within the training set itself. For this purpose, the training data were further subdivided into five folds. The decoder was trained on four CV-folds and tested on the remaining one. This was repeated with all permutations of training and test folds resulting in an estimate of the likelihood for the training data set at a fixed regularization parameter pair (in this process the independent test data set remains untouched). The procedure was reiterated with different values of the regularization parameter pair. The optimal pair was chosen as to maximize the decoder performance during testing with maximum of 5 non-zero weights.

To validate the performance of the decoder using selected pair of *Gamma* and *Delta* and optimized set of weights, leave-one-out cross-validation method was used. The p value of the decoding performance was estimated in two ways: first analytically by comparing the number of hits to the number of correct guesses obtained from a binomial distribution (Quiroga et al., 2007); and with a nonparametric permutation test. In each permutation, the stimulus tags were shuffled, and the same linear discriminant analysis was implemented. This procedure was repeated 1000 times, thus producing a distribution of number of hits

under the null hypothesis. The *p* value was estimated as the proportion of times that the number of hits from the shuffled distribution exceeded the observed one.

Local Field Potentials. All the time-frequency analysis was performed using Fieldtrip toolbox (Oostenveld et al., 2011) and custom-build Matlab codes. Local Field Potentials (LFPs) were obtained offline by filtering the raw signal between 1-300 Hz and then downsampling to 1000 Hz. Continuous recorded data were divided into trials starting 5 seconds before nose poke until 5 seconds after the go cue when animal was free to leave the nose poke.

LFP power spectrum. The power spectrum of the LFPs was estimated using a continuous wavelet transform using complex Morlet wavelets of 4 cycles length. This results in shorter wavelet duration for larger frequency values. To avoid redundancy in measuring power, we considered a logarithmic set of frequencies, starting at 2 Hz and increasing by $2^{1/4}$. Time-frequency power maps were log-transformed and averaged across trials and then normalized by the mean power during a least active period during the behavioral task which we call baseline hereafter (1.5 - 2.5 seconds after the go cue).

LFP-LFP phase coherence. To quantify the phase synchronization between the LFPs recorded from separate electrodes in barrel cortex and prefrontal cortex, we computed the Weighted Phase Lag Index (WPLI) (Vinck et al. 2011). The WPLI is a measure of phase coherence that is based exclusively on the imaginary component of the cross-spectrum, and is not spuriously affected by the volume conduction from a single source's activity to two separate sensors, or by a common reference. The WPLI has increased robustness to noise compared to other measures that are based on the imaginary component of the cross-spectrum (Nolte et al., 2004 and Stam et al., 2007). A direct estimator of the WPLI can be biased by sample size. Therefore, we estimated the squared WPLI by using the debiased WPLI estimator (Vinck et al., 2011), ranging from zero (no phase coupling) to one (maximum coherence). The debiased WPLI has no sample size bias if the asymptotic WPLI value equals zero, hence does not spuriously indicate interactions.

Statistical test of WPLI and FDR control for multiple comparisons. To test whether the debiased WPLI significantly exceeded zero (i.e., significant phase-coupling) we build up a non-parametric permutation test. Trials in one of the areas under investigation were shuffled randomly (N times) and a distribution of shuffled time-frequency coherence values was computed. Time-frequency values of observed coherence were compared to the N × P highest value of the permutation distribution across all time-frequency bins (where N is the total number of permutations and P is the desired "P value"). Thus, we tested for coherence against a null hypothesis of complete independence and corrected for the multiple

comparisons (one per frequency and time-bin) by using the maximum coherence value as the test statistic (Maris & Oostenveld, 2007; Maris et al., 2007; Nacher et al. 2013).

LFP-LFP phase shifts. In order to analyze for a possible directional influence of activity from one area to the other, we calculated the phase difference between areas across the frequency range of interest (4-10 Hz). The instantaneous phase of each signal was estimated using a Hilbert transform and the phase difference between pairs of electrodes in barrel cortex and prefrontal cortex was computed at each time. The significance of phase shift being different from zero was tested using a Rayleigh test implemented in CirStat toolbox in Matlab (Batschelet, 1981; Berens, 2009).

Results - Behavioral Performance

Eight rats were trained to perform a tactile working memory task. Their performance was monitored across different pairs spanning the entire SGM. Figure 10A shows the performance, as percent correct, for each stimulus pair, averaged across all rats. For each rat the performance was computed by averaging across all trials of the last month of training prior to surgery. The color indicates percent of trials that animal judged S2 > S1: the performance of a perfect subject would yield dark blue and dark red for all the pairs above and below the diagonal, respectively. Performance was good across all stimulus pairs and across all rats (Figure 10). However, there were two apparent biases in the behavior. First, there was a trend for diminished performance for the lower values of stimulus. While we do not have any explanation for the poor performance on smaller values, one clue might arise from the second bias: rats more frequently made errors on low-to-high stimulus comparisons (pairs above the diagonal) (Figure 10A and 11). In (Fassihi et al., 2014), we have attributed such errors to "contraction bias," a phenomenon known in psychology for more than a century. When two sequentially presented stimuli are small in magnitude compared to the mean value of the entire stimulus set, subjects usually overestimate the first stimulus and judge it as larger than the second; compatible with this in our data set, rats in average made more incorrect choices at [3.1 3.8] pair compared to [3.8 3.1] (Wilcoxon rank sum test pvalue<0.001). In contrast, the first stimulus is underestimated when the two stimuli are relatively large. Therefore they report the second stimulus more

frequently as larger in such pairs (higher performance for [4.5 5.5] vs. [5.5 4.5], Wilcoxon rank sum test pvalue<0.001). One account for contraction bias is that during the delay the memory trace of the first stimulus drifts toward the expected value of the entire stimulus distribution (Akrami et al., 2013).

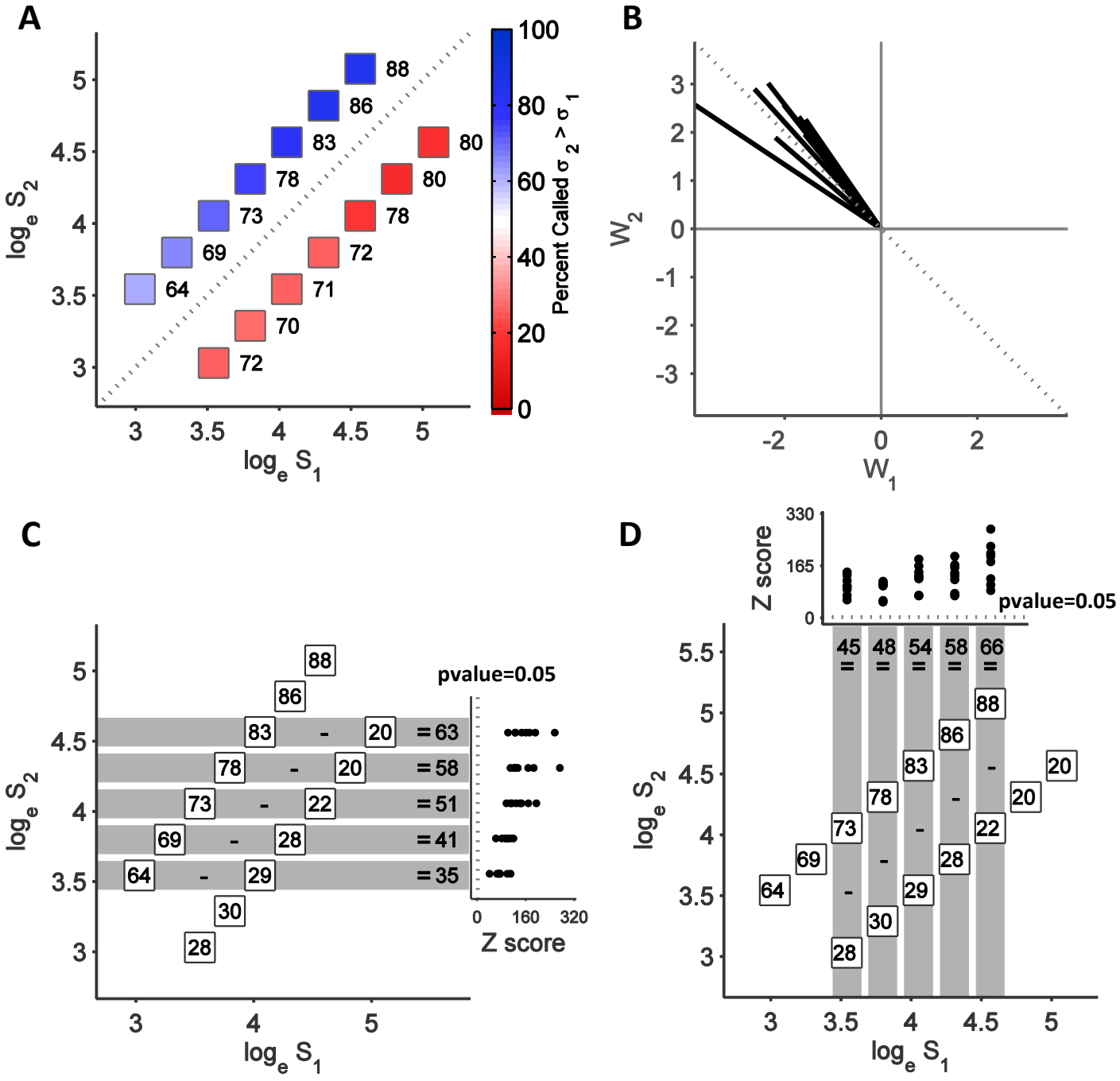

Figure 60. Working memory performance. (A) Data from final month before surgery of 8 rats are separated by [S1, S2] pair but averaged across rats; SDI was 0.25 and inter stimulus delay was variable, from 1 to 4 seconds. (B) Weights of S1 and S2 in animal choice are represented by W1 and W2. Each (W1, W2) vector represents data from one rat. (C) Statistical test for the effect of S1 in rat's behavior. Values in the boxes give the percent of trials in which rats judged S2 > S1. The difference between paired boxes in a gray band represents the dependence of choice on whether S2 was preceded by smaller or larger S1. The statistical significance of the choice for all single rats is given as a Z-score on the right. (D) Same analysis but for the effect of S2.

To evaluate whether rats truly performed a sensory delayed comparison task, as opposed to the alternative of applying a threshold to a single stimulus (either the S1 or S2), we did two separate tests. The tests were aimed at quantifying the effect of each of the two stimuli on the rats' decision.

Weights of S1 and S2 in the animal's choices. The first test was to weigh the contributions of S1 and S2 to the animal's choice. We fit the animal's choice using a generalized linear model. This model posits a linear combination of S1 and S2 which is mapped nonlinearly through a logistic link function, onto the animal's choice (i.e., percent of trials in which the rat judged S2 > S1):

$$percent\ of\ trials\ judged\ S2 > S1 = \frac{1}{1 + e^{-(C + W1 log S1 + W2 log S2)}} \qquad (6)$$

where W1 is the S1 regressor, W2 is the S2 regressor, and C captures the overall bias of the subject in calling S2 >S1 (for instance, a bias towards turning to the left reward spout).

The coefficients W1, W2, and C were derived to most closely reproduce the observed performance by an iteratively reweighted least squares algorithm implemented in MatLab. The W1 and W2 regressors quantify the strength of the relationship between S1and S2 respectively, and the animal's choice. If the regressors are plotted in Cartesian coordinates, the critical issue becomes the direction of the vector formed by W1 and W2. An ideal performer – one who precisely encodes the first stimulus, holds it in the memory, precisely encodes the second stimulus, and then accurately judges the difference between S1 and S2 – would yield W1= -W2, corresponding to the dashed line. Any possible bias C is independent of stimulus weighting and would not affect the angle. W1 and W2 regressors for the data from one month of all rats are illustrated in Figure 10B. All the (W1, W2) vectors lie very closely to the dashed line. These data show that rats gave relatively equal weights to S1 and S2 when they were choosing to go to one or the other reward spout.

Statistical test for effect of S1 and S2 on behavior. We performed an additional statistical test to show that rats attended to the first stimulus and stored it in memory. We computed the percent of trials judged as S2>S1 for each pair within the SGM (Figure 10C). If the values in the paired boxes along a gray iso-S2 band were equal, we would conclude that choice was unaffected by the value of S1. Instead, the large differences (right side of the gray bands) indicate that choices depended on S1.

To test the significance of the observed values, for each rat and each fixed S2 value, we computed the choice differences by taking a sample of 1,000 trials (with replacement) from each rat. By repeating the resampling 1,000 times, we generated a new bootstrap distribution of differences. Next we compared this

resampled difference distribution to a difference distribution obtained after randomly shuffling the S1 labels on each trial. The shuffled distribution simulated the expected choices of rats if those choices were ***not*** determined by comparing sigma values. The distance between the mean of the resampled difference (obtained from real observations) and the mean of the simulated, shuffled distribution, divided by the SD of the distributions, gave a Z-score. On the right side of Figure 10C, the Z scores are aligned by S2 value, with each rat plotted as a point. Conventionally, Z scores > 2 are considered significant (dashed line), and in this analysis, Z scores were found to be much higher. For most S2 values, the effect of S1 on animal choice exceeded 10 SDs and was thus strongly significant.

The same analysis was applied to quantify the effect of S2 on the animals' decision (Figure 10D). Gray shading links trials with the same value of S1 followed by one of two values of S2. The significant difference between the paired boxes represents the dependence of choice on the value of S2.

To summarize, these findings demonstrate that rats encoded the first stimulus, stored it in memory and compared it with the second stimulus, and thus executed the true delayed comparison.

Data from individual rats are illustrated in the format of Figure 10A in Appendix 1.

Appendix 1. Working memory performance of individual rats

Data from each rat is illustrated in separate plots. All rats had a high performance (>70% correct) across the last month of training. Separating the frequency of correct response for different pairs of [S1, S2] demonstrates similar trends across most of the rats; a decrease in performance for smaller sigma values which is stronger for the pairs above the diagonal and an enhanced performance for largest sigma values also above the diagonal. The analysis for proof of working memory was done separately for each rat and is already depicted in Figure 10.

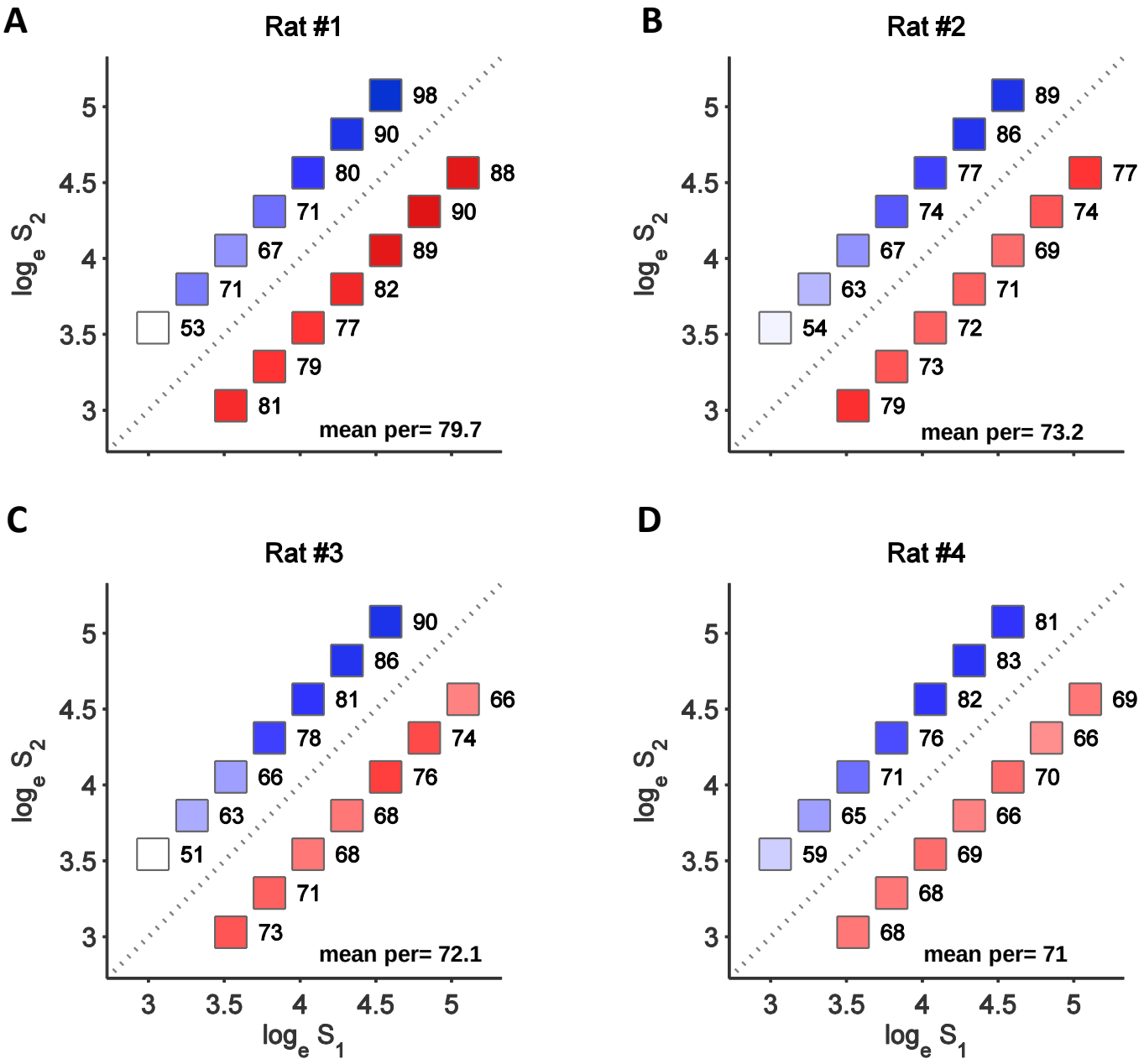

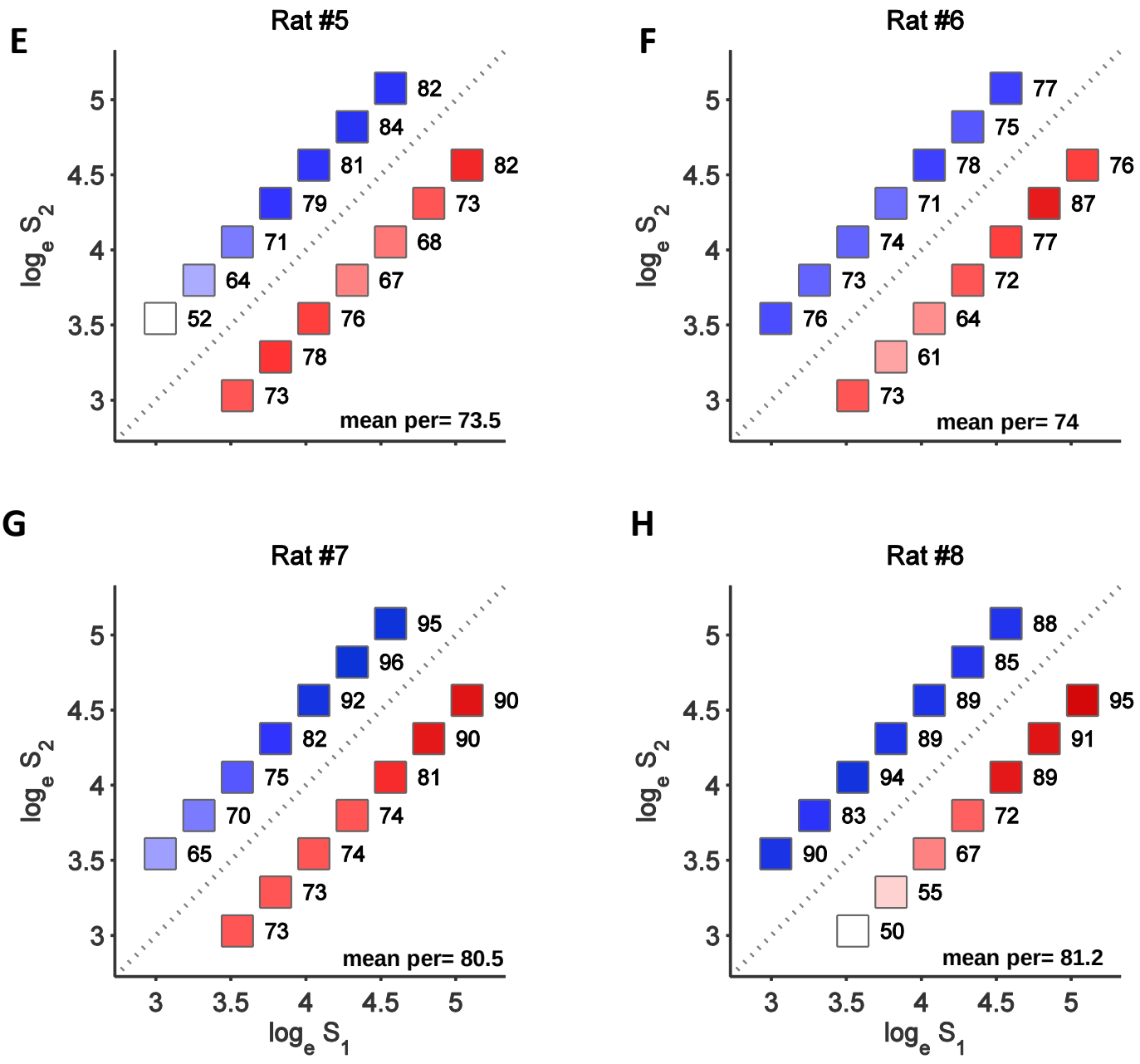

Figure 11. Working memory performance of each rat. (A to H) Data similar to Figure 10A but illustrated for each rat separately. Color bars are similar to Figure 10A.

Results – Neuronal Analysis

We simultaneously recorded the activity of neurons from primary somatosensory "barrel" cortex (BC) and prelimbic area of medial prefrontal cortex (mPFC). Microwire arrays comprising 16 or 32 electrodes were implanted in the brain of each animal (one array per area). The average performance of the rats across SGM pairs and statistical tests for the proof of working memory is demonstrated previously in the Behavioral Analysis section. The structure of the stimulus generalization matrix (SGM) in the recording sessions remained the same as that used during training except for two modifications illustrated in Figure 12; fewer [S1, S2] pairs to increase the number of trials per stimulus condition, and reduced difficulty (SDI=0.33) to keep the animal's performance elevated across trials.

As explained in the Materials and Methods, each trial was initiated by the animal positioning its snout in the nose poke. Figure 13 shows the structure of the trial in the electrophysiological sessions. Each stimulus lasted 500 ms and delay duration was fixed at 2 seconds.

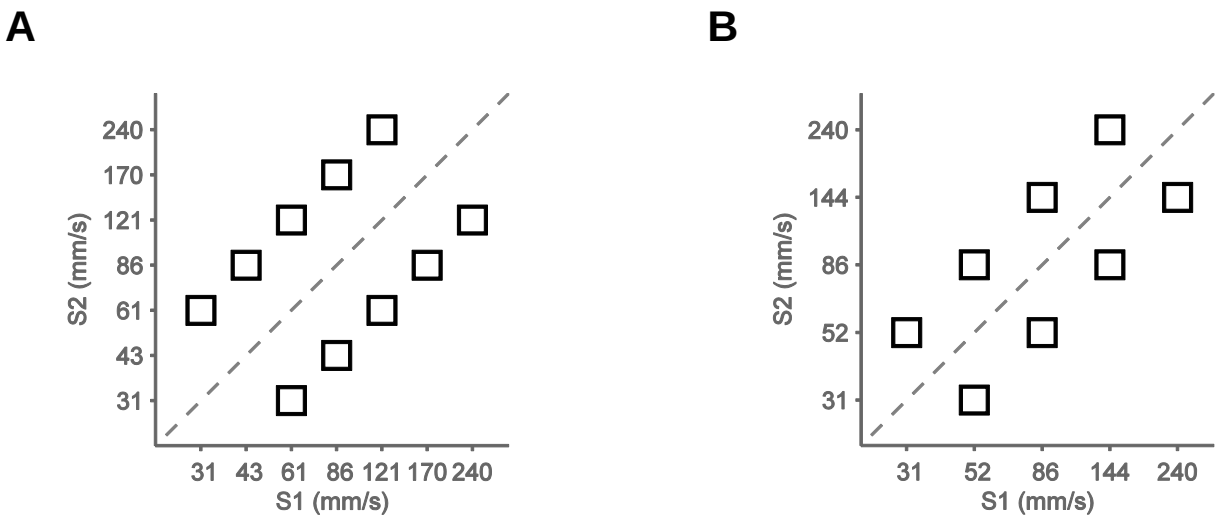

Figure 12. Stimulus set of the recording sessions. (A) The Stimulus Generalization Matrix used in the recording sessions. Each box presents a pair of [S1, S2]. The nominal velocity standard deviation of each noisy vibration varied from 31 to 240 mm/s. The Standard Deviation Index was equal for all the pairs of stimuli (SDI=0.33). (B) The same as (A) but with fewer pairs. This configuration was used in two rats which performed fewer trials, however to span the same range of sigmas the SDI was set to 0.25.

The electrophysiological data presented here are from eight rats. In order to eliminate the risk of counting the same neuron in the analysis twice, we took data from one session of each rat. The selection of sessions for inclusion in the analysis was based on a few parameters, such as number of trials, stable performance of the rat over the course of the session and quality of the recording in that session.

The criteria for including neurons in the analysis included:

- spike waveform quality (i.e. action potential shape and signal to noise ratio),
- average firing rate of at least 1 Hz during trials,
- stable firing rate over the course of a session.

In total we included 153 neuronal recordings in barrel cortex and 69 in medial prefrontal cortex.

Encoding of task parameters by neuronal firing

Successful completion of the task requires the cognitive operations illustrated in Figure 13:

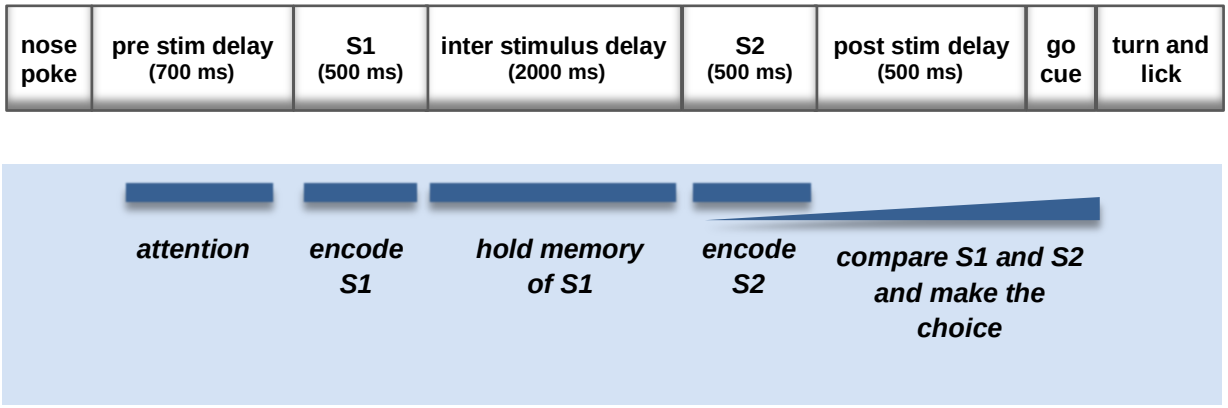

Figure 13. Trial Structure. Timeline of a trial in the recording session is depicted in the upper panel. The lower panel represents the cognitive structure of a trial.

Given this set of operations, our intuition is that neurons in the sensory-perceptual networks of the neocortex must encode the standard deviation of S1, the memory of S1, standard deviation of S2 and the difference between the stimuli. Our examination of neurons in the barrel cortex and the medial prefrontal cortex therefore focused on the search for such properties (see Materials and Methods for details).

To visualize the characteristics of neurons we first illustrated the activity of each neuron as a raster plot and time-dependent firing rate. Mean firing rates were computed from the set of density functions (spike trains convolved with Gaussian kernels) for each stimulus condition. We then quantified the correlation between the firing rate of the neuron in each time bin and stimulus conditions by fitting a line to the response of the neuron from all trials. A significant relationship between stimulus value and firing rate was revealed by the difference of the slope from zero, as examined with permutation tests. This is referred to as "slope of the fit" in the following sections. We further calculated the Mutual Information between the firing rate of each neuron and the parameter of interest.

In this introductory section, we present a small set of selected neurons in each region that appear to be involved in the cognitive operations summarized above (Figures 14,15 and 17). The initial presentation also serves to illustrate several of our analytical methods. In later sections, we will present the full data set, in

condensed format, so that the distribution of properties across neurons and across brain regions can be appreciated. All the analysis presented here was performed on correct trials.

Representation of the ongoing stimulus. To examine the encoding of the vibration stimulus in neuronal activity, trials were grouped and illustrated by color based on the velocity standard deviation of S1 (from trial start until the end of interstimulus delay) and S2 (from S2 onset until trial ending). Figure 14 demonstrates two example neurons (one per area) whose discharge rate was modulated monotonically as a function of the ongoing stimulus. The firing rate of these example neurons increased for larger values of S1 and S2 velocity standard deviation, during S1 and S2 periods respectively, but not during the interstimulus delay (Figure 14A-D).

The stimulus-response correlation was then assessed using a generalized linear model. At each point in time, the best linear fit to the firing rate as a function of stimulus standard deviation was computed. In the insets of Figure 14C and D, the mean firing rate of the sample neurons at a few points in time versus S1/S2 velocity SD are demonstrated. The positive slope of the best linear fits indicates the monotonically increasing encoding of stimulus.

When measuring the Mutual Information (MI) between firing rate and S1, we compared responses for stimulus values for a given decision (D) taken, i.e. MI(FR,S1|D). For the set of correct trials, this procedure is similar to grouping all the SGM pairs located below or above the diagonal together and measuring information about the stimulus in each group separately. Similarly for information about S2, MI(FR,S2|D) was computed. This grouping serves to obviate the possible effect of the future decision of the animal (insets in Figure 14E, F). In other words, the future choice of the animal could bias or influence the encoding of the current stimulus. To avoid such effects, comparisons were made of the stimulus-dependent activity across trials in which the final action was the same.

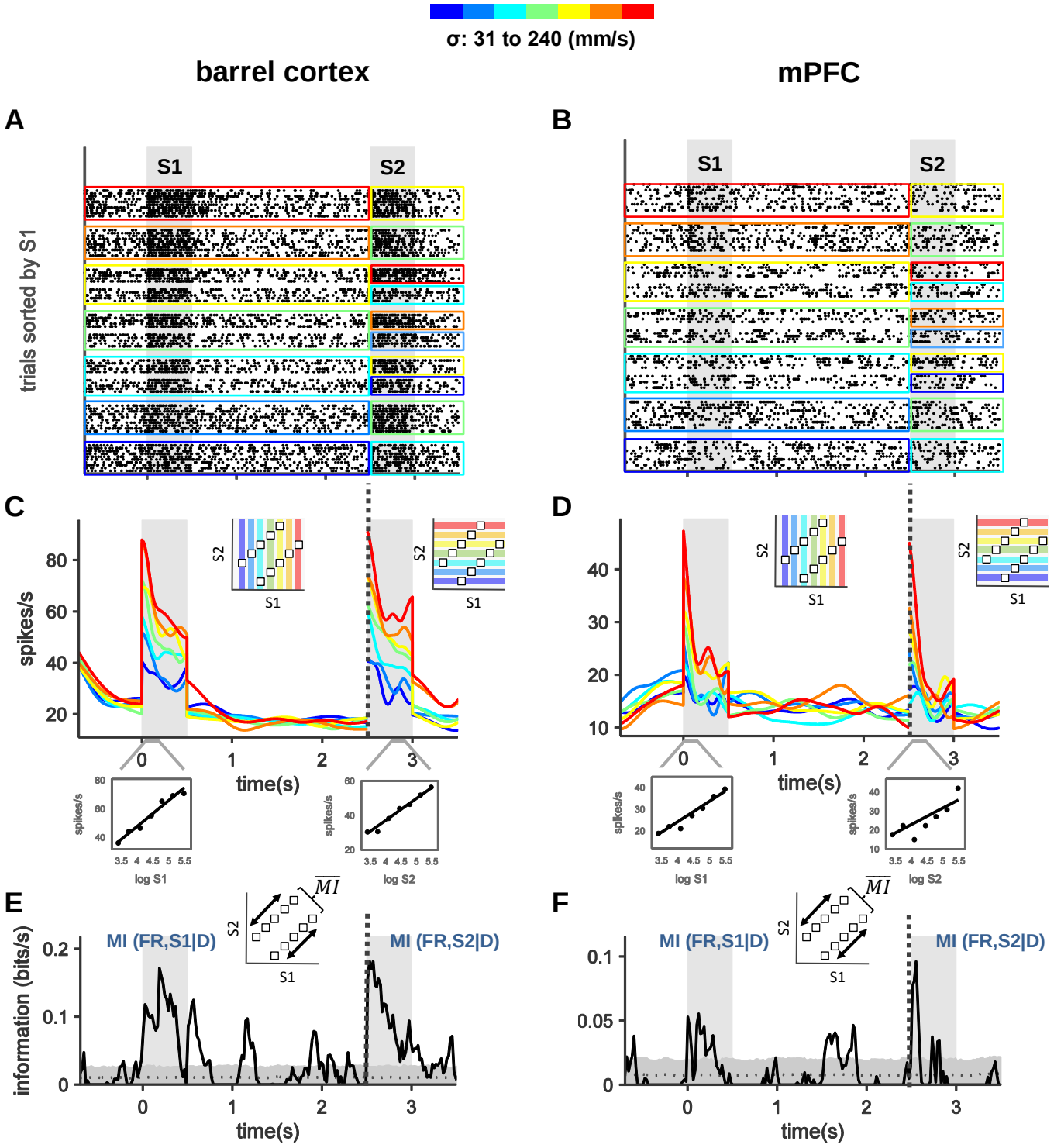

Figure 14. Representation of ongoing stimulus. All the plots are aligned to the beginning of the first stimulus. Data from one example neuron in the barrel cortex (left) and in the mPFC (right) are represented. Gray vertical bars mark the duration of stimuli. (A, B) raster plots. Trials are sorted and grouped by S1; each dot denotes an action potential. Color boxes demonstrate the trials with same velocity standard deviation of S1 until the termination of the delay (vertical dashed line); thereafter they depict S2. (C, D) temporal dynamics of firing rate. Mean firing rate of the neuron for each stimulus condition is plotted across time. The insets illustrate the grouping of the trials on the SGM. (E, F) Time course of information. Mutual information between the firing rate of the neuron and stimulus is plotted. The dark gray band is the 95 percent confidence interval resulted from the shuffled distribution.

Memory of the first stimulus. One of our main interests in this thesis was to identify neurons that store the memory of the first stimulus during the interstimulus delay period. Stimulus-related activity of neurons during the delay was analyzed similarly to what is outlined in previous section, but the main interest was on working memory neurons.

Figure 15 illustrates two neurons in barrel cortex and prefrontal cortex that represented S1 both during S1 and during some parts of the delay period. The barrel cortex neuron encoded the first stimulus standard deviation in a graded manner in its discharge rate. The slope of the fit at the end of delay was positive as depicted in Figure 15C, implicating that firing rate increased for larger SD values. The response of the mPFC sample neuron reliably encoded S1 across the whole retention interval.

In searching for neuronal correlates of parametric working memory, we took special care in quantifying the stimulus signal carried in the response of neurons during the delay period. Thus, we computed conditional information, MI(FR,S1|D), which quantifies the amount of working memory information in the neuronal response (See Materials and Methods). Although this method of analysis underestimates the stimulus signal present, the information values would not increase spuriously due to possible correlations between other (non-stimulus) task parameters (e.g. animal future choice) and specific stimulus values (e.g. extreme pairs).

Response modulation in different neurons. In the previous sections we defined our approach in searching for the stimulus encoding in the neuronal activity of single clusters. In the following sections we summarize the results of those analyses on the whole data set (153 clusters in BC, 69 clusters in mPFC) in a compact format. Figure 16 illustrates the percentage of neurons, in each area, with significant slopes of the fit (different from zero) at different time epochs.

Our expectation was that a large proportion of neurons in barrel cortex would encode S1 and S2 online, that is, during the online presentation of each stimulus (Fassihi, doctoral dissertation, 2012). Accordingly, in barrel cortex, around 53% of neurons had a significant slope of the fit during S1, meaning that they significantly modulated their discharge rate as a function of the SD of the first stimulus (Figure 16A). These neurons mostly encoded the ongoing stimulus by a significantly *increased* discharge rate for larger values of S1 (~42%); only a smaller proportion of these neurons had a negative slope of the fit, that is, a significantly *decreased* discharge rate for larger values of S1 (~11%) (Figure 16C). These neurons had narrower spike waveforms (0.22 ms, median spike half width) suggesting that they mostly belonged to the category of fast-spiking units (FSUs), putative inhibitory neurons. In contrast, positively encoding neurons seemed to be

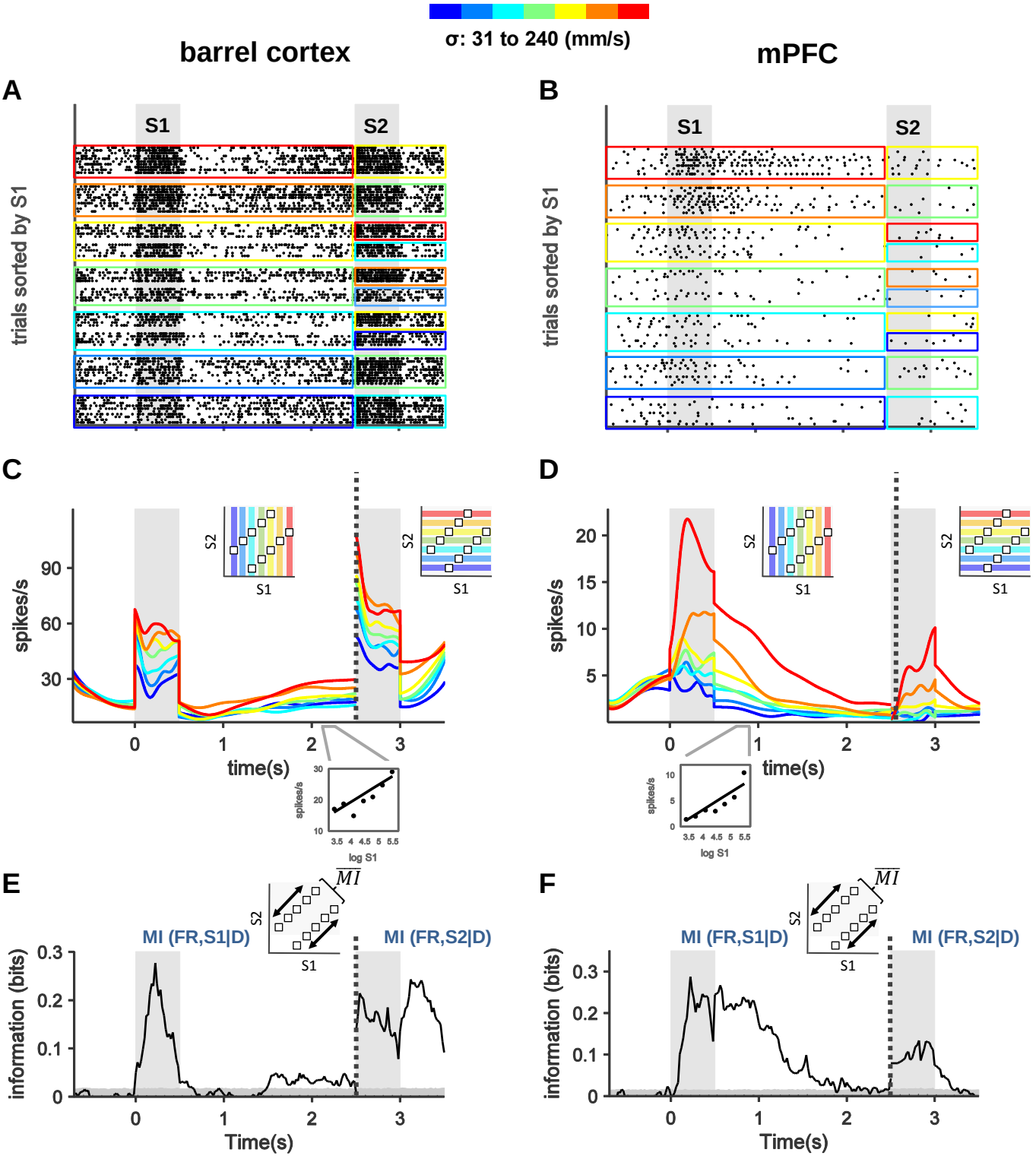

Figure 15. Memory of stimulus. Plots are in the same format as Figure 14 but for two example neurons that keep the trace of S1 during some portion of the delay. The insets in (E, F) represent how the information about S1 and S2 was measured at different time epochs.

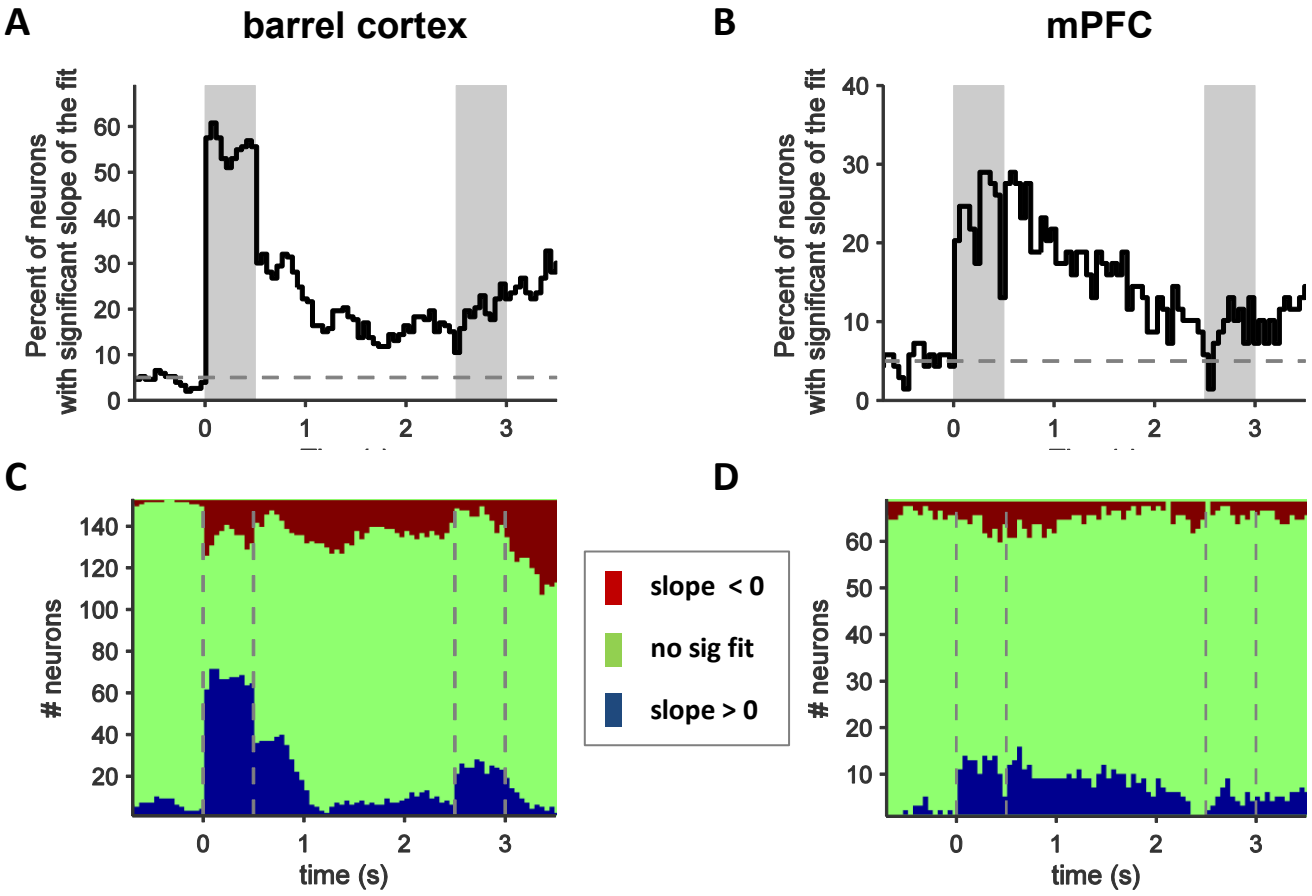

Figure 16. Significantly encoding neurons. (A, B) Fraction of neurons with significant slope of the fit at barrel cortex (left) and mPFC (right). (C, D) slope of the fit sign of all the recorded neurons from each region.

mostly excitatory regular-spiking units (RSUs) with longer spike durations (0.36 ms, median spike half width) (Simons, 1978; Bruno & Simons, 2002, Bean, 2007).

The proportion of positively encoding neurons remained the same at early delay, but reversed in the middle of the delay interval. This might be partly explained by adaptation mechanisms. Interestingly, the number of neurons with positive slope increased at the end of delay. This finding suggests that the memory of the first stimulus was re-encoded in a few neurons just at the end of delay.

Using a similar experimental design, Romo and collaborators found that only a negligible proportion of monkey primary somatosensory cortex neurons carried signals about S1 during the delay (Hernández et al., 2000). If barrel cortex function were analogous to that of primate somatosensory cortex, one would expect

no significant trace of the first stimulus in barrel cortex during the delay. On the contrary, we found that for 30% of neurons in this region, early in the delay period the discharge rate varied with a monotonic function according to the previous stimulus. This percentage decreased gradually and reached 15% at the end of the delay period. The barrel cortex neuron of Figure 15 is one that carried S1 information late in the delay.

In mPFC neurons exhibited a more heterogeneous functionality. Nevertheless, 26% of neurons in this region showed a firing rate modulation according to the ongoing stimulus (Figure 16B). 16% of these neurons had positive slope of the fit during the S1 period in comparison to 10% with a negative slope (Figure 16D). Thus, the preponderance of positively stimulus-correlated neurons found in barrel cortex was reduced.

Similar to S1 period, 26% of neurons in mPFC showed significant slopes at the beginning of delay, indicating that the same percentage of neurons that represent the ongoing stimulus keep the memory trace at least in some parts of delay period (Figure 16B). This percentage decayed gradually to 10% at the end of the delay interval. Early at the delay, most of the significant encoding neurons had a positive slope, but at the end there were only neurons with negative slope (Figure 16D).

Representation of action. The final step in the task is to compare the two stimuli, i.e. evaluate whether S1>S2 or S2>S1. This corresponds to rat's two possible actions. We explored the correlates of this in neuronal activity. Thanks to our SGM, we could dissociate the encoding of animal action from stimulus information. This was achieved by including separate parts of the SGM during S1 and delay in comparison to S2 period (dashed line and insets in Figure 17). For the first part of the trial (left side of dashed line) only trials with S1 values that could be followed by two different S2s (and consequently two different actions) were considered; therefore any information about choice in this period could not be explained by S1. After the start of S2, only trials with S2 values that could be preceded by two different S1s were analyzed. Similarly, distinct response rates of neuron for S1>S2 comparing to S2>S1 trials could not be due to encoding of S2 - rather it is an indication of action representation. Any diverging pattern in the mean firing rate of the neuron while animal was in the nose poke is the correlate of comparison and the decision of the animal to take one of the two possible actions.

Example neurons in BC and mPFC carrying decision signal are demonstrated in Figure 17. Trials are grouped and demonstrated with color codes based on the sign of S2 – S1. The firing rate of these neurons is modulated as function of this sign, thus encoding the animal action.

To quantify the information neurons carried about the decision which could not be explained by stimulus, we measured conditional Mutual Information (see Materials and Methods). From the start of the trial until the end of delay period MI(FR,D|S1) was computed; from S2 afterwards MI(FR,D|S2) was calculated. This is similar to the same grouping that we used for Figure 17C and D, but here MIs were computed separately for two pairs of [S1, S2] with equal S1 (arrows in the insets of Figure 17E, F). Using this method we avoid measuring spurious information caused by the inherent correlations between decision and S1 and S2 in some extreme pairs of the SGM.

The significance of information was checked versus a shuffled distribution. The action information in the example neurons was present just after the presentation of the second stimulus (Figure 17E, F).

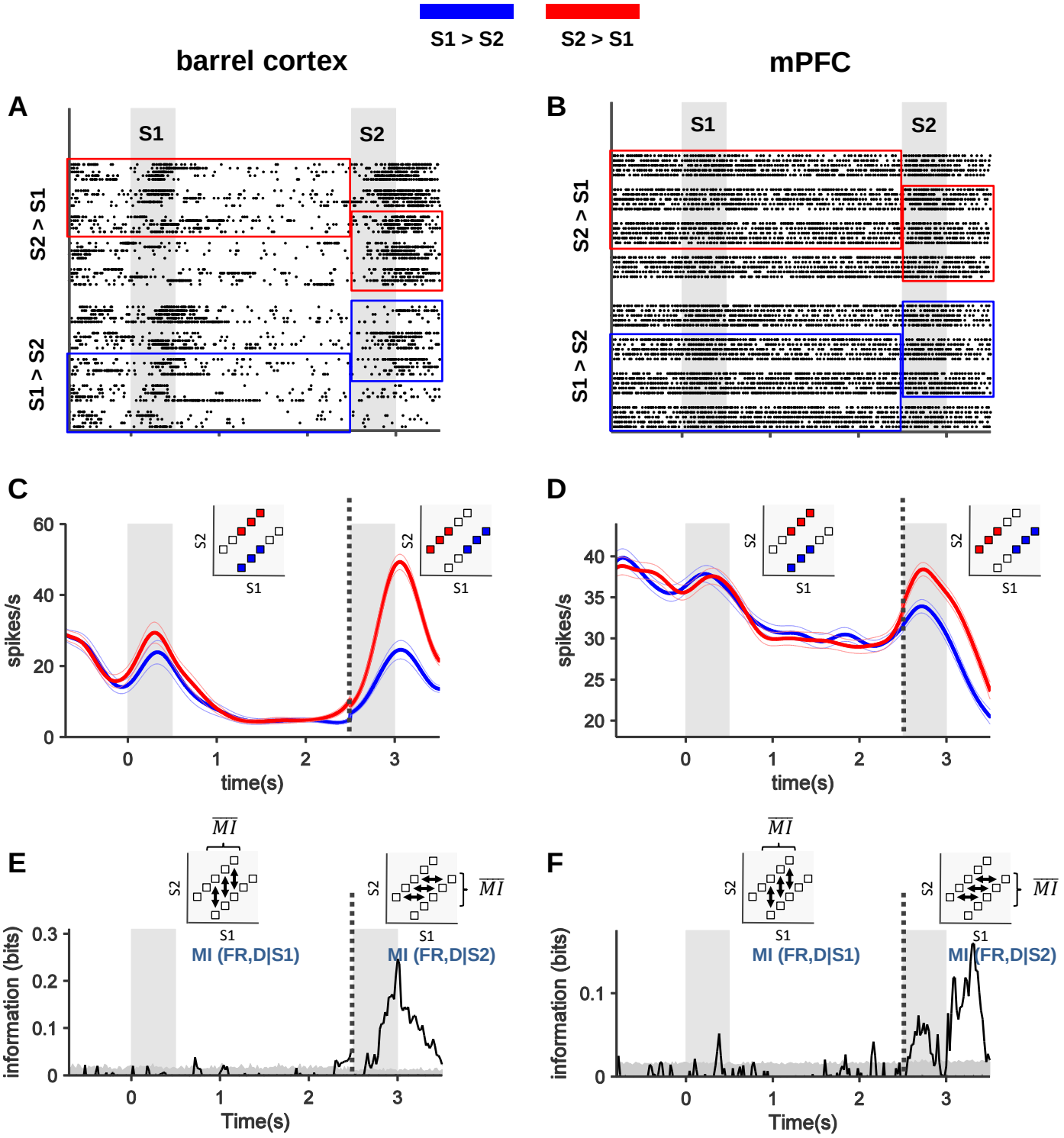

Figure 17. Coding of the desired action of the animal. Similar to Figure 14 and 15 plots are aligned to the beginning of the first stimulus yet trials are grouped by the sign of S2-S1. (C, D) Only parts of SGM are included in the analysis as illustrated by the insets and by the colored boxes over the raster plots. Until the second stimulus only trials with a S1 that could be followed by two different S2 values are considered; thereafter trials with a S2 that could be preceded by a smaller or larger S1 are included. (E, F) Time course of information. Conditional Mutual Information between the firing rate of the neurons and sign of S2-S1 are shown. The same group of trials as in C and D are used in these plots.

Proportion of informative neurons. In previous sections we described our approach in examining the encoding of task parameters, in particular stimulus and action, in spiking activity of neuronal clusters. We also reported the linear stimulus-response correlations in barrel cortex and mPFC neurons. The advantage of computing conditional mutual information to disentangle the stimulus and action signals was also discussed and demonstrated over the stimulus generalization matrix (Figures 14, 15, 17).

Here, the proportion of neurons at each point in time that carried a significant signal about S1, S2 and S2-S1 are demonstrated in the compact format (Figure 18A-D). To examine if each neuron was significantly informative about the parameter of interest, at a specific time bin, a permutation test was performed. The task parameter (stimulus or action) was shuffled randomly across trials 1,000 times and MI was calculated each time. If the MI obtained from the real data was greater than 95% of the shuffled MI values the neuron was considered as having significant information in that time bin.

Figure 18 summarizes this analysis for all the recorded neurons for each region separately. In barrel, around 40% of neurons carried a stimulus signal during presentation of S1 and S2 periods. 30% of neurons kept the trace of S1 at early delay after the termination of stimulus, consistent with a possible role of barrel cortex in working memory. Note that since conditional MIs were considered, the computed information about S1 *cannot* be explained by other non-stimulus parameters. This percentage decayed by time and became 10% at the end of delay period.

Medial prefrontal cortex seems to be also involved in the short term memory storage of velocity standard deviation of vibrations in the delay comparison task. More than 20% of neurons encoded stimulus during the presentation of S1 and S2; a similar percentage represented the stimulus in their firing rate at early delay. The proportion of neurons involved in working memory, similar to barrel cortex, decreased toward the end of delay period.

In neither of the two areas did we observe a decision signal before the presentation of S2. In barrel cortex, a small but significant proportion of neurons carried information about animal decision soon after S2 presentation. This percentage increased at post stimulus delay and reached to 40% before the go cue was sounded, when the animal was still in the nose poke and needed to postpone his action. This suggests that barrel cortex in rats, similar to secondary somatosensory in primates, might participate in comparing S1 and S2 and decision making process.

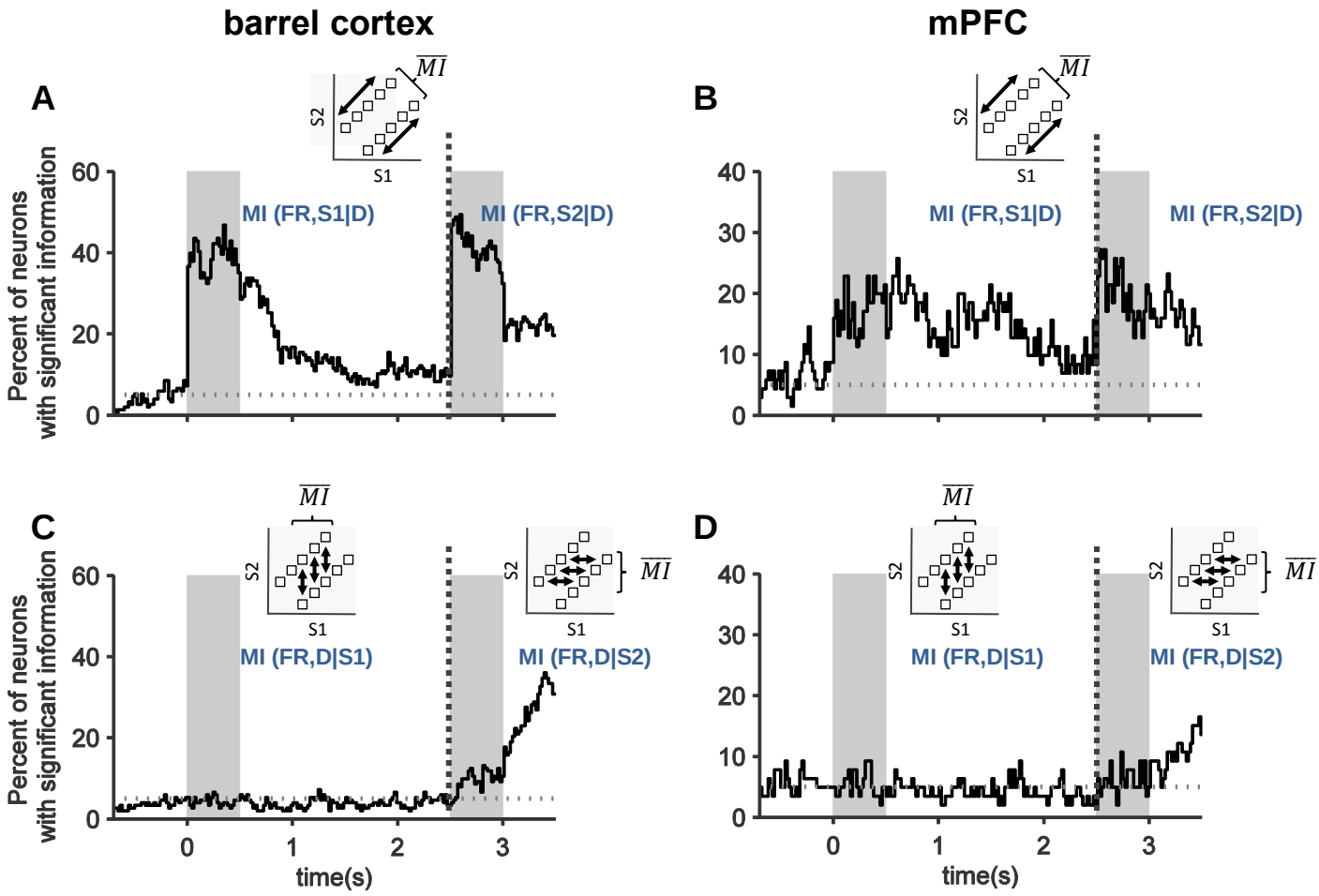

Figure 18. Percentage of neurons with significant information. (A, B) Information about stimulus. Percent of neurons with significant information about S1 in barrel cortex (A) and mPFC (B) are plotted on the left of the dashed line. On the right of the dashed line neurons with S2 information are shown. The method used at each analysis is shown in the insets. (C, D) Information about action. The proportion of neurons that carry significant information about the sign of S2-S1 at barrel cortex (C) and mPFC is depicted.

Neurons in mPFC represented the animal action mainly after the termination of the second stimulus. Around 20% of these neurons had action information before the go cue was presented. After the animal left the nose poke to report his decision, a higher percentage of neurons in barrel cortex (probably due to different engagement of whiskers when turning left or right) and in mPFC represented the action signal (not demonstrated here).

Decoding of task parameters from populations of neurons

In previous sections, the functional characteristics of all neuronal clusters in barrel cortex and prefrontal were explored by assessing the linear relationships between the activity of each neuron and the stimulus. Using information theoretic measures, we also quantified the amount of information each neuron carries about the task parameters. However, the variability of neuronal response to repetition of same stimulus is considerable and constrains the reliability of stimulus decoding from individual neurons. On the other hand different neuronal subpopulations represent the information about stimulus in their spiking activity in different epochs of the trial. The brain typically makes decisions based on the activity of large neuronal populations.

To expand our analysis from single-clusters to populations of neurons, we considered linear decoding methods as an alternative to information measures. Computing mutual information for a population of neurons in experiments with a behaving animal can lead to "limited sampling bias" problems and can generate spurious values of information because the stimulus/response matrix is not adequately populated. Other forms of decoding algorithms are more data-robust and can be applied to large populations of neurons (Quiroga & Panzeri, 2009).

We implemented linear discriminant analysis (LDA), which seeks to build a function of neuronal responses with a linear relationship to the stimulus. The idea behind LDA is to find the optimized projection directions so that the between-class (i.e. between stimuli) variance in the data is maximized relative to the within-class variance (Fisher, 1936; Bishop, 2006; Duda, 2012).

However, in the case of high dimensional space (in our data large number of neurons), low sample size data (few trials per condition), LDA suffers from overfitting and results in poor classification of the test trial (Friedman, 1988). We implemented a regularized version of LDA, which we refer to as RDA, to overcome this problem (see Materials and Methods). In this section, we compare the stimulus signal decoded by the standard (non-regularized) LDA and RDA (using the optimal set of weights and neurons) and compare them to the resulting signal with a LDA based on observation of single clusters. Since it is not possible to integrate data from different rats and different sessions, representative sessions are demonstrated here. Similar results, concerning what is presented here, were observed when analysing data from other sessions. Obviously, the presence of more informative individual clusters tended to result in a more informative population.

Time-shifting population density vectors were constructed from the spike density functions of the jointly recorded neuronal clusters at each region. To evaluate the signal available within the population vector, we decoded task-related parameters (S1, S2 and S2-S1) in each time bin. To validate the decoding performance, the leave-one-out cross-validation method was used. The p-value of decoding performance was estimated in two ways: first analytically by comparing the number of hits to the number of correct guesses obtained from a binomial distribution (Quiroga & Panzeri, 2009); and with a nonparametric permutation test. We observed similar results from the two methods (See Materials and Methods).

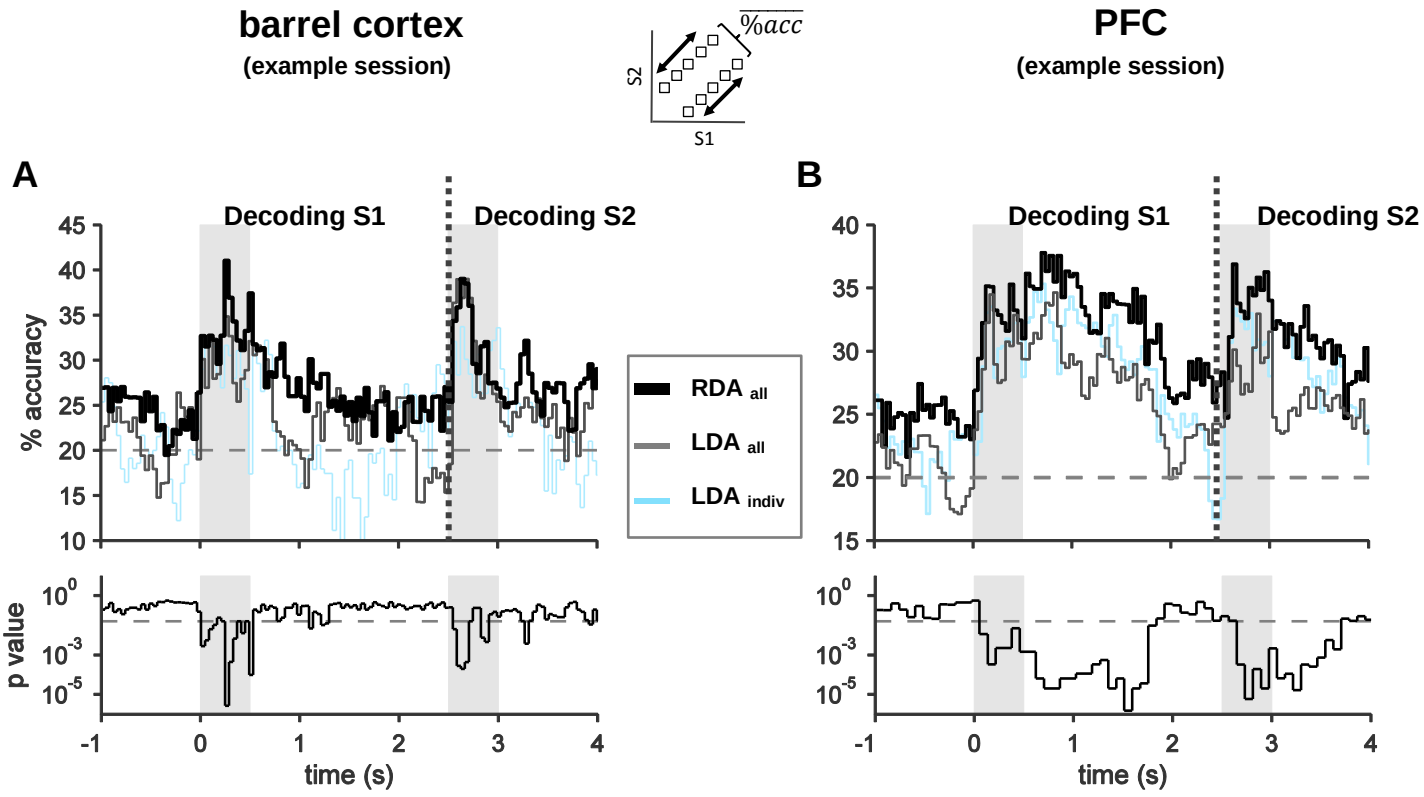

Figure 19. Population decoding of stimulus. (A) The prediction performance of the standard LDA for one individual cell (blue) and all cells (gray) compared to the RDA method. Data are from an example session with a population of 22 neurons in barrel cortex. (B) Similar to (A) but for a population of 12 neurons in PFC. Performance was calculated separately for [S1, S2] pairs associated with same actions (inset) and then averaged. The lower panels show the p-value of the significance test for each of the plots. The dashed line represents p-value=0.05.

The accuracy of the standard LDA and the regularized LDA (RDA) for a population of 22 neurons in barrel cortex is demonstrated in Figure 19A. We also compared the performance of the two population decoding

methods to the performance of a similar LDA based on the activity of one of the best predictive single-neurons. For the example session depicted here (Figure 19A), the individual neuron significantly predicted the stimulus during the presentation of S1 and S2 and also towards the end of the delay period. The performance of standard LDA including all neurons was slightly above chance in the middle of the delay period but worse than the individual neuron at late delay. This is an outcome of the overfitting problem we described above. The RDA decoder obviates this effect and outperforms all the individual neurons (not all shown here) and the standard LDA. This was true across the time course of the trial.

Similarly, we looked at an example neuronal population at prefrontal cortex consisting of 12 simultaneously recorded neurons (Figure 19B). Consistent with the previous result, the RDA afforded the best decoding from this population. We could reliably predict the ongoing stimulus and the memory of S1 during the delay period.

We used the same approach for quantifying the signal present in the neuronal population about the difference between the two stimuli (S2-S1). Figure 20 summarizes this analysis on the same example populations from barrel and prefrontal cortices. The main observation is that the information about the difference built up in BC at the beginning of the second stimulus, suggesting that comparing the stimuli starts from primary sensory cortex in this task. In PFC difference signal was represented after the offset of the second stimulus. In agreement with stimulus decoding results, RDA performed with the highest accuracy rates for predicting the S2-S1 which leads to animal decision.

These analyses indicate that, in our data set, jointly recorded groups of clusters in BC and PFC outperformed individual clusters; they were able to decode task parameters at a significance level even during epochs of the trial where no individual cluster was informative.

In summary, we developed a linear discriminant method to quantify the information of neuronal population in the barrel cortex and prefrontal cortex of rats performing a delayed comparison task. The stimulus and animal's decision could be extracted from population activity simply by linearly weighting the responses of different neuronal clusters. This was particularly remarkable given that recorded populations were not selected on the basis of a strong stimulus or decision-dependent response. Thus, the population signal was present even in epochs of trial where the single clusters were not informative. The functional significance of a linearly decodable population signal is that downstream neurons receiving input from a set of neurons in barrel cortex (or prefrontal cortex) could extract stimulus/decision signal on single trials through simple linear combination of these inputs.

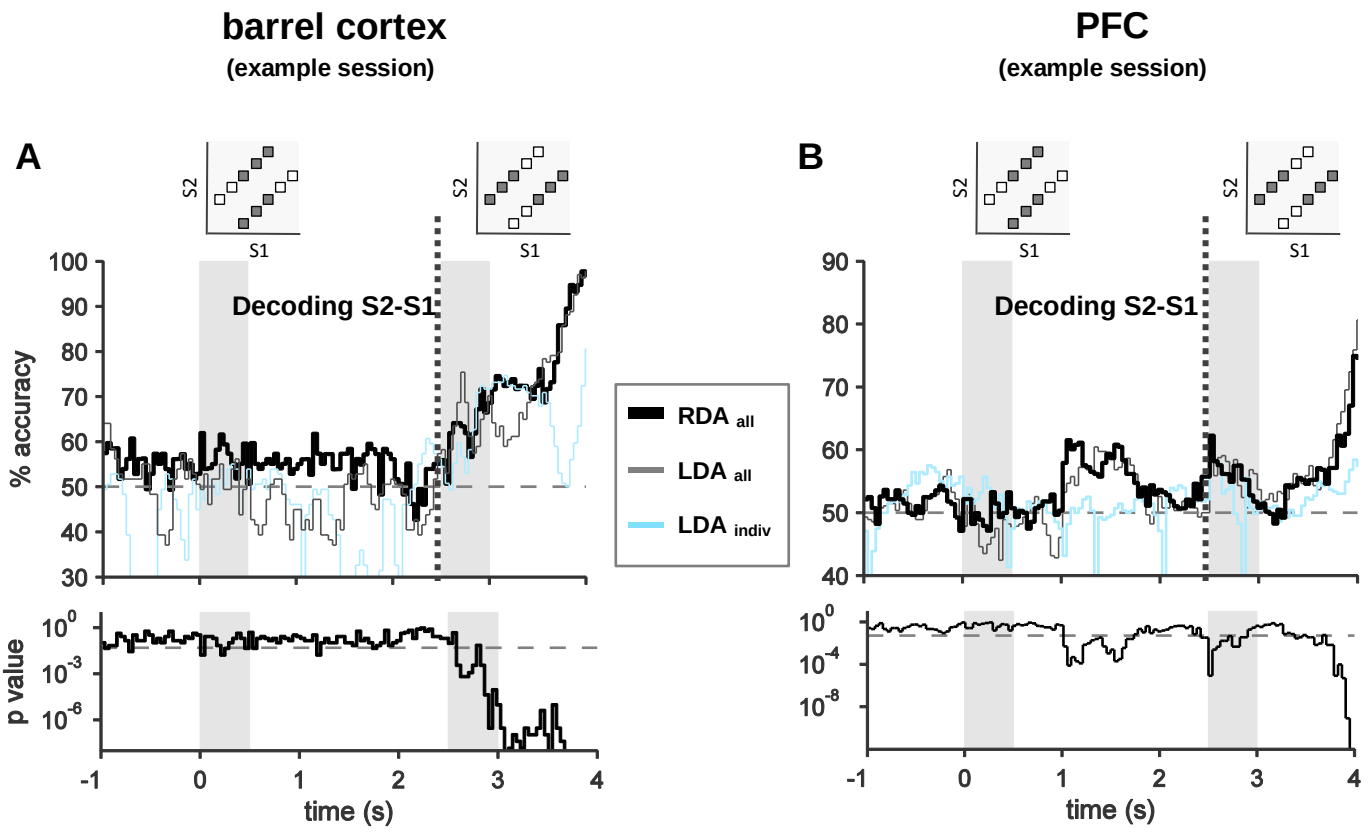

Figure 20. Population decoding of S2-S1. (A) The prediction performance of the standard LDA for an individual cell (blue) and all cells (gray) compared to the RDA method. Data are from the same example sessions in Figure 19. Performance was calculated for a subset of SGM pairs to exclude the stimulus effect in computing decoding performance (inset). The lower panels show the p-value of the significance test for each of the plots. The dashed line represents p-value=0.05.

The majority of neuronal clusters in our data set consisted of multiple units recorded on a single electrode, i.e., of clusters containing more than one neuron. From the point of view of our discriminant analysis, including all spikes from a cluster of multiple units is equivalent to forcibly assigning equal weight to all the separate units contained therein. This is effectively the same operation done in the computation of the discriminability achieved by direct accumulation of the activity of different clusters. Previous works suggest that the inclusion of multi-unit recordings in the population analysis leads to non-optimal weighting of single units, that is, the multiunit clusters are single units summed with the same weights (Safaai et al., 2013). Hence, the discriminability achieved in our analysis must be a lower bound on the achievable by optimal linear decoding of fully sorted single neurons. In sum, our results are likely an underestimate of the total signal that could be extracted from sets of neurons.

Results - Local Field Potential Analysis

Previously we examined the dynamics of task parameter encoding as well as correlates of working memory in the spiking activity of neuronal clusters. We demonstrated that a distributed network of neurons in barrel cortex and medial prefrontal cortex is involved in the encoding and storage of stimulus information in the delayed comparison task. However, how these spatially distant cortical areas communicate with each other and contribute to animal behavior remains unclear.

It has been proposed that coherent oscillations between different brain areas is one possible mechanism for mediating this interaction (Fries, 2005). For instance, there are coherent oscillations between parietal and frontal cortices during the decision-making period of a vibration delayed comparison task in primates (Nácher et al., 2013).

We first looked at the power modulations of the Local Field Potentials (LFP) recorded from representative channels in barrel cortex and prefrontal cortex (Figure 21). The power in barrel cortex electrodes increased mostly in the β (20-35 Hz) range during the presentation of stimuli. Theta power also increased in various epochs of the trial. We also observed an increase in 2-10 Hz range as the animal approached the nose poke and during the licking period after the go cue is sounded.

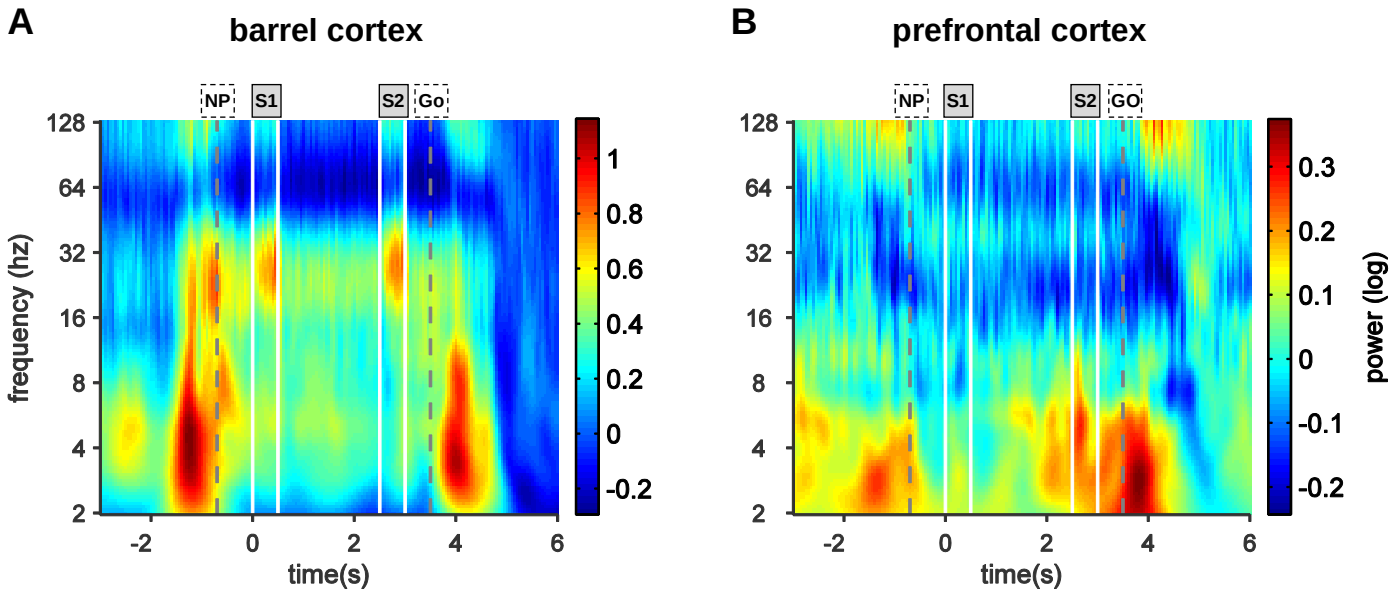

Figure 21. Time-frequency maps of power modulation. (A) barrel cortex. (B) prefrontal cortex. Dashed gray lines represent entry into the nose poke (NP) and go cue (GO) respectively. White lines mark the stimuli onset and offset time. Note that the frequency axis is in logarithmic scale.

In PFC, the increase in the spectral power was found only in the frequencies below 10 Hz during the task. Similarly to BC, power in delta band increased before nose poke and after the go cue, the epochs when animal was not in the stimulus delivery port and was probably moving in the setup.

We quantified the phase synchronization between the two areas using a debiased version of Weighted Phase Lag Index (Vinck et al. 2011). In WPLI the contribution of the observed phase leads and lags is weighted by the magnitude of the imaginary component of the cross-spectrum. We selected the WPLI estimator since firstly cannot be spuriously increased by volume-conduction of independent sources and secondly because it enables increased statistical power to detect changes in phase-synchronization (Vinck et al. 2011).

We measured coherence across the pair of LFP signals recorded from BC and PFC all over the time-frequency plane (Figure 22A). If coherence were a mechanism to facilitate the transfer of information from sensory to prefrontal cortex, we would expect it to be highest during the presentation of stimuli, when relevant task-related information is present. The two signals were mostly coherent at the theta range at the beginning of the two stimuli and interestingly during the pre-stimulus delay period as the rat awaited, or anticipated, the first stimulus. We tested the significance of coherence values with permutation tests corrected for multiple comparisons (See Materials and Methods). Figure 22B shows that the modulations in

the theta range are indeed significant ($p<0.05$). We interpret the high degrees of coherence in the pre-stimulus period as reflecting or underlying preparatory and expectation mechanisms.

To identify the direction of entrainment of the two regions, we examined the phase shifts in the two signals. Synchronization was clearly present when we plotted the two LFP signals filtered in the theta range and overlaid (Figure 22C). We observe that during the epochs of high coherence, PFC led BC with a phase shift of $\pi/2$ (Figure 22D). The fact that the downstream region (PFC) preceded the primary sensory cortical region (BC) suggests that top-down, not stimulus-evoked, modulations might underlie the phase synchronization between the two areas during the delay comparison task.

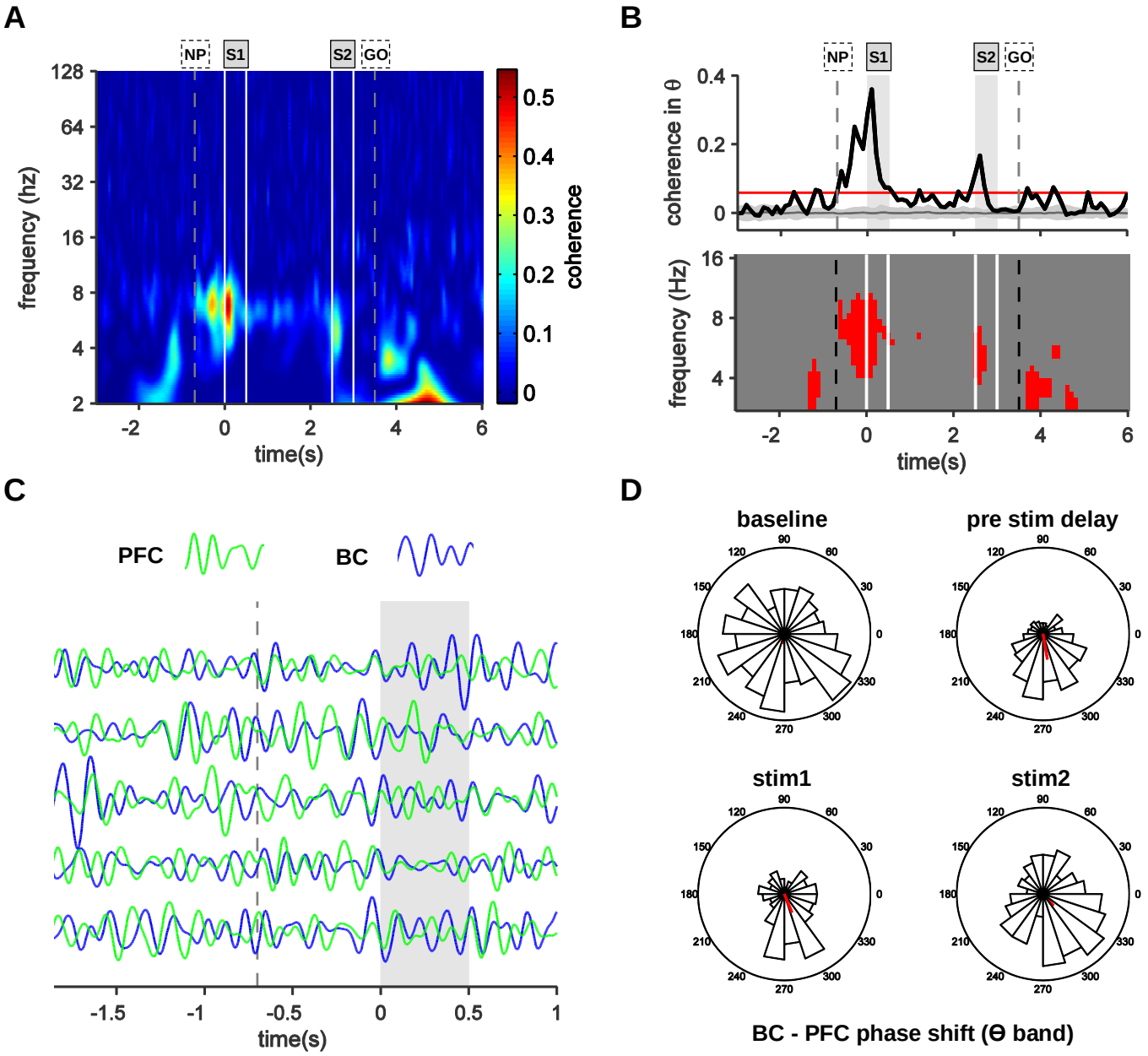

Figure 22. Phase synchronizations of the LFP signals. (A) Time-frequency map of WPLI measure for two simultaneously recorded BC and PFC channel. Data are aligned to the onset of the first stimulus. The white solid lines show the stimulus presentation, dashed gray lines represent entry into the nose poke (NP) and go cue (GO) respectively. (B) The upper panel shows coherence averaged in the theta (4-10 Hz). The red line is the significant level corrected for the multiple comparisons by taking the maximum coherence across all time bins. In the lower panel the time-frequency bins where the coherence was significant ($p<0.05$, See Materials and Methods) are shown in red. (C) Single-trial LFP traces of PFC (green) and BC (blue) overlaid. (D) Histograms of the phase difference across different trials for the same pair of electrodes. The phase difference is consistent at pre-stimulus period and at the beginning of the two stimuli but not in the baseline ($p<0.01$, Rayleigh test of uniformity). The red vector shows the amplitude and angle of the average phase shift across all trials.

Discussion

General observations

Many higher cognitive functions involve working memory (WM), the storage and manipulation of information across limited time intervals. We uncovered the previously unknown sensory WM abilities in rats (Fassihi et al., 2014, in Appendix), setting the stage for exploration of its neuronal coding. Rats received two sequential "noisy" vibratory stimuli on their whiskers, separated by a delay, and had to compare the velocity standard deviation of the vibrations. In this task, a neuronal representation of the first stimulus needs to be maintained during the interstimulus delay. Where in the brain is such a mnemonic trace kept and what is the nature of its representation? Simultaneous multi-electrode recordings are consistent with the involvement of barrel cortex and prelimbic area of medial prefrontal cortex in encoding and storage of vibration information in working memory. Diverse populations of neurons across the delay period encoded the first stimulus parameter in their firing rate.

What are homologous neocortical regions across primates and rats?

Primary sensory cortex is defined as the entryway of ascending sensory pathways into neocortex (Jones, 2007). From this definition, there can be little doubt that barrel cortex in rats is homologous to the hand

region of primate S1 cortex (presumably Brodmann's area 3b; see Kaas, 1983). In spite of their likely homology, we found functional differences between barrel cortex and primate S1 that are discussed later.

A further issue is the homology between primate dorsolateral prefrontal cortex (dlPFC) and prelimbic cortex (PL) in rats, the region we have explored. Anatomical connections and projections supports the view that these two area are related (Uylings, 2003; Vertes, 2006). Functionally the primate and human dlPFC is believed to be involved in excutive functions including working memory, decision making and selective attention. Rat PL, similarly, is strategically positioned to integrate information across modalities and compare present and past events for appropriate actions. Previous studies have reported neurons in this area that respond selectively during the delay period of delay response tasks (Baeg et al., 2003; Batuev et al., 1990; Orlov et al., 1988; Pratt & Mizumori, 2001). Lesions of this area produced marked deficits in delayed response tasks involving short and long delay, similar to those seen with lesions of the dorsolateral PFC of primates (Kolb, 1984; Goldman-Rakic, 1994; Barbas, 1995, 2000; Groenewegen & Uylings, 2000 and Vertes, 2006). Fnctional data indicate that PL is implicated in some dorsolateral-like features (see Uylings, 2003).

For these reasons, we argue, as do other authors (Vertes, 2006; Hoover & Vertes 2007, Seamans, 2008 and Uylings et al., 2003), that prelimbic cortex might be the closest homology to primate dorsolateral PFC. Further comparison of these regions based on the current data and the data presented in a similar task in primates is discussed later in this chapter.

Working memory in rodents

Although there can be no doubt that rodents store short-term memories, it was unclear before now what form of information they could hold in working memory. Rodents express spatial working memory, but navigation tasks do not constrain the modality or entity of stored information; choices could even be held in memory through body posture and other nonneuronal mechanisms (Carruthers, 2013; Dudchenko, 2004). Can rodents perform parametric working memory; that is, can they store a stimulus not according to its identity or quality (Ennaceur, 2010) but only by its position along the scale of a single sensory dimension? Delayed comparison tasks have been an effective means for studying working memory for over 30 years (Kojima & Goldman-Rakic, 1982).

In a published work, we demonstrated that the performance of rats in a tactile delayed comparison task resembles, to a first approximation, that of humans (Fassihi et al., 2014, in Appendix). Here we recount some of the arguments made in our earlier publication. Our study is notable for its parallels to studies of

tactile delayed comparison in monkeys by Romo and Salinas (Romo & Salinas, 2003; Mountcastle et al., 1990). In common with our task, the monkey receives two vibrations separated by a variable delay; it then makes a choice according to the difference between the vibrations (Romo & Salinas, 2003; Mountcastle et al., 1990). There are several distinctions in experimental design. In our task, rather than applying stimuli to the fingertip, we selected the whisker sensory system due to its behavioral importance in rats (Diamond & Arabzadeh, 2013, Prescott et al., 2011; Diamond, 2010; Diamond et al., 2008; Brecht, 2007; Petersen, 2007; Adibi & Arabzadeh, 2011; Harris et al., 1999). Another distinction is the structure of the vibration. Although the studies in monkeys typically use regular, periodic skin deflections in the form of either a sinusoid or a pulse train (Hernández et al., 2000), we opted for a stochastic stimulus composed of filtered noise (Maravall et al., 2007). The choice was motivated by several factors. First, in pilot studies, rats attended to noisy stimuli better than to periodic stimuli and were more likely await the go cue before withdrawing. Second, noisy vibrissal stimuli evoke a more robust cortical response (Lak et al., 2008; Lak et al. 2010), an advantage for neurophysiological studies. Third, the structure of the noise stimulus is well suited to future reverse correlation methods (Ringach & Shapley, 2004) and will provide rich data for studying the kinematic features extracted by sensory neurons (Arabzadeh et al., 2004; Lottem & Azouz, 2011).

The initial discovery (Fassihi et al., 2014) of the perceptual capacity of rats in performing a sensory working memory task was of great interest to us since it opened up the opportunity to study its neuronal correlates.

Neuronal representation of the delayed comparison task

In this thesis we begin to examine the neuronal basis of sensory working memory by recording from populations of neurons in barrel cortex, where the vibration information first enters the neocortex, and prelimbic area of medial prefrontal cortex, which is part of a frontal network for higher cognitive functions in rats. We found that 42% of barrel cortex neurons, mainly categorized as regular spiking units (RSUs), encoded the ongoing stimulus by an increase in firing rate for increasing values of velocity standard deviation, a coding scheme we denote as positive monotonic. Another set of barrel cortex neurons, comprising 11% of the entire sample, and mainly categorized as fast spiking units (FSUs), encoded the stimulus parameter by a negative monotonic code. It was shown previously that the behavior of RSUs and FSUs was opposite when tested with noisy versus regular (periodic) stimuli (Lak et al., 2008, 2010). This finding is important because, in the Romo group's flutter discrimination task, primary somatosensory cortical neurons almost exclusively encoded the online stimulus in a positive monotonic fashion (Hernández et al., 2000; Hernández et al., 2010). If barrel cortex function were analogous in every way to that of primate

somatosensory cortex, one would expect similar results here. Whether this is due to functional differences in the organization of these cortical areas or because of the dissimilarity in the type of stimuli could be the subject of further investigation. Our intuition is informed by the fact that the Romo group found negative monotonic neurons in SII cortex (Romo et al., 2002). From this, we believe that functions that in primates are separated in distinct cortical regions must be in rats "folded into" single regions. In other words, rat barrel cortex seems to embody the second stage of processing, the parsing of the sensory representation into positive and negative codes, an operation that in primates does not occur until SII. Thus, we believe that stimulus differences do not explain the emergence of negative codes in barrel cortex. Rather, it reflects the adoption of multiple functions into single modules.

On a mechanistic level, one explanation for this observation could be that the fast spiking inhibitory interneurons in barrel cortex become suppressed probably through afferents from somatostatin-expressing GABAergic interneurons, allowing the excitatory network to be more activated. The contribution of excitatory and inhibitory neurons in the vibration discrimination task needs to be examined in future optogenetic and microstimulation studies. It should be noted that our current experimental approach is also limited by our inability to reconstruct the morphology and biochemical makeup (e.g. GABA, somatostatin, glutamate) of the neurons we study.

During the delay period only a negligible proportion of monkey primary somatosensory cortex neurons carried signals about S1 (Hernández et al., 2000). Differently from the primate SI, 30% of neurons in barrel cortex kept the trace of previous stimulus for up to half a second. In addition, at the end of the delay period (after 2 s), still a significant percentage of neurons (15%) carried stimulus signals in their firing rate. We also found that the memory of the first stimulus, S1, was re-encoded in a few units just prior to the second stimulus. Our findings are in agreement with other human and non-human primate studies suggesting the involvement of primary sensory cortex in short term storage of graded sensory information (Zhou and Fuster, 1996, 2000; Super et al., 2001, Harris et al., 2001a). Harris and colleagues investigated the role of human primary somatosensory cortex in a tactile working memory task by manipulating the topographic locations of stimuli and by disrupting SI activity. Performance of human subjects was significantly disrupted when a pulse of transcranial magnetic stimulation (TMS) was delivered to the contralateral SI early in the retention interval (300 or 600 msec after the conclusion of the first stimulus). TMS did not affect tactile working memory if delivered later in the delay (Harris et al., 2001b, Harris et al., 2002). Our results provide additional evidence consistent with a role for early sensory areas in parametric working memory.

In mPFC, 26% of neurons showed a modulation in firing rate (increased or decreased) in relation to vibration standard deviation, both during the online presentation of S1 and at early delay. Prior to S2 only 10% of units in this area represented a graded trace of S1. When computing conditional information measures, to quantify the purely stimulus-related information in the firing rate of these neurons, we still found 20% of neurons that carried a stimulus signal in different parts of delay.

In primate recordings from dorsolateral prefrontal cortex, Romo et al. found that 39% of neurons encoded the flutter frequency during the representation of the first stimulus and this percentage remained the same during early parts of the delay period, similar to our findings in rat prelimbic region of medial prefrontal cortex. In the middle of delay this percentage decreased to 17% following by a marked rise at the end of delay period, when 40% of neurons encoded the memory of the preceding vibration (Romo et al., 1999). We did not observe this late rise in our data, i.e. the percentage of memory encoding neurons decayed towards the delay end. Another discrepancy is the smaller percentage of memory neurons in the rat PL in comparison to the proportion observed in the dlPFC of monkey. Whether this is due to real functional distinction between these regions or because of the methodological differences in the electrophysiological approaches, needs to be assessed in similar experimental conditions. In the data presented here, we used fixed microelectrode arrays; therefore we did not move the electrodes searching for task-responsive neurons. Our method of non-selection of task-related neurons provides a fair representation of the region explored.

There is debate about the nature of the prefrontal cortex in non-primate species. Uulings et al. (2003) compared the structural and functional characteristics of the prefrontal cortex of nonhuman primates and rats. They argue that rats have a functionally divided prefrontal cortex that includes not only features of the medial and orbital areas in primates, but also some features of the primate dorsolateral prefrontal cortex. Preuss (1995) on the other hand claims that the medial frontal cortex consists of cortex homologous to primate premotor and anterior cingulate cortex and it lacks homologues of the dorsolateral prefrontal areas of primates. Based on this idea, he concludes that rats probably do not provide useful models of human dorsolateral frontal lobe function and dysfunction, although they might prove valuable for understanding other regions of frontal cortex.

In this study, we have found neurons in the prelimbic area of medial prefrontal cortex of rats that keep a graded representation of the stimulus during a subsequent delay period. These results together with previous lesion studies of this region indicating a deficit in delayed response tasks is more in favour of the idea that

PL in rats is involved in working memory, a higher cognitive function observed mainly in primate dlPFC. Further optogenetical manipulations could elucidate the causal role of this area in working memory.

Novel Information measures

The information analysis method proposed here establishes a general framework for quantifying task parameter signals in neuronal responses in the context of delayed comparison tasks. These tasks usually involve several stages including stimulus encoding, working memory and decision making. It usually happens that in some part of the stimulus set, stimulus and decision are correlated, e.g. first or second stimulus - *not* necessarily the relation between the two stimuli - leads to a unique decision. In this case existence of information about one parameter leads to spurious information about the other correlated one. This is particularly important when one attributes the presence of stimulus signal during the delay period to sensory working memory. One possible confound is that if subjects make their decision after receiving the first stimulus (which might be possible for some extreme pairs), the apparent stimulus signal observed could be explained not by the stimulus itself but rather by the future action associated with that stimulus. When using correlation analysis, investigators tend to remove parts of the stimulus span to remove those correlations. Instead, the conditional information method presented here resolves this problem by disentangling the different task related parameters while including all the stimulus space presented during the task.

Using this method we were also able to quantify the decision signal in the neuronal responses. We found that barrel cortex might participate in making the comparison. A small but significant proportion of neurons carried information about animal decision soon after S2 presentation. This percentage increased at post stimulus delay and reached 40% before the go cue was sounded, when the animal was still in the nose poke and needed to postpone his action. This results together with working memory signals in barrel cortex, indicates overlapping functions of rat barrel cortex and secondary somatosensory cortex in primates (Romo et al., 2002).

Medial PFC units also represented animal choice, but later in the trial in comparison to barrel cortex. Decision signals started to build up in this area after the termination of S2 and was present in 20% of neurons before the go cue. The mPFC of rats, like the prefrontal cortex of primates (Fuster, 1988 and Romo et al., 1999), appears to be directly involved in higher order cognitive functioning, including decision making and working memory.

Decoding

We used decoding approaches to decode stimulus and action signal in the population activity of barrel cortex and mPFC neurons (Quiroga & Panzeri, 2009). For this purpose, we implemented a regularized linear discriminant analysis (Friedman, 1988) whish was more data robust. In behavioral experiments with large stimulus space and few limited number of trials standard LDA could lead to overfitting and misclassification of new data. The RDA decoder comprising jointly recorded neuronal clusters in barrel cortex and PFC outperformed individual clusters and the standard LDA. We found that the stimulus and animal's decision could be extracted from population activity simply by linearly weighting the responses of different neuronal clusters. This was particularly remarkable given that recorded populations were not selected on the basis of a strong stimulus or decision-dependent response. Thus, the population signal was present even in epochs of trial where the single clusters were not informative. The functional significance of a linearly decodable population signal is that downstream neurons receiving input from a set of neurons in barrel cortex (or prefrontal cortex) could extract stimulus/decision signal on single trials through simple linear combination of these inputs.

Long-distance network communication

We finally examined neuronal oscillations to find out how the sensory information is transferred across the working memory network in rats brain. Coherent oscillations have been observed between parietal and frontal cortices during the decision-making period of a vibration delayed comparison task in primates (Nácher et al., 2013). We took a new measure of phase synchronization called WPLI which is robust against volume conduction and is more sensitive to detecting changes in phase synchronization (Vinck et al. 2011). We found that LFP signals recorded from barrel cortex and mPFC were mostly coherent at the theta range, at the beginning of the two stimuli and interestingly during the pre-stimulus delay period as the rat awaited, or anticipated, the first stimulus. High degrees of coherence in the pre-stimulus period might underlie the preparatory and expectation mechanisms. Our data reveal entrainment of BC by PFC during the epochs of high coherence (i.e. PFC leading BC by $\pi/2$), suggesting that top-down, not stimulus-evoked, modulations affect the phase synchronization between the two areas and facilitate the optimal transfer of information.

Conclusions

Until a few years ago, many neuroscientists attributed a wide range of perceptual functions to primates but not to rodents. As discussed in our earlier work (Fassihi et al., 2014) capacities of rats might have been overlooked because training regimes were not effectively adapted to their natural deportment. As a consequence, neural mechanisms of certain cognitive functions could only be addressed in human neuroimaging or monkey electrophysiological studies. With improving behavioral methodologies, rodents have been found to express surprising abilities. For instance, rats spontaneously recognize views of an object that differ by angle, size, and position (Tafazoli et al., 2012; Zoccolan et al.; 2009); such generalization is a hallmark of true visual perception and was once believed to belong only to primates. With regard to more abstract computations, rodents weigh sensory evidence (Kepecs et al., 2008), assess reward statistics (Karlsson et al., 2012), integrate multimodal sensory inputs (Raposo et al., 2012), accumulate evidence for optimal decision-making (Brunton et al., 2013), express certainty in the outcome of their choices (Mainen & Kepecs, 2009; Lavan et al., 2011), generalize rules (Murphy et al., 2008), and even integrate evidence to plan volitional or self-initiated actions (Murakami et al., 2014). In sum, mice and rats are becoming increasingly important for the study of perception (Carandini & Churchland, 2013). From our effort, parametric working memory joined other cognitive functions within the repertoire of rodent capacities (Fassihi et al., 2014) and we assessed its neuronal correlates in the present study. Recent advances in rat optogenetic manipulations (Musall et al., 2014), gives us the opportunity to switch on or off specific cell types during the task with high temporal and spatial precision in future studies. This will allow us to examine the causal role of different brain areas and contribution of cell types in various stages of a sensory working memory task.

Bibliography

Adibi, M., & Arabzadeh, E. (2011). A comparison of neuronal and behavioral detection and discrimination performances in rat whisker system. Journal of neurophysiology, 105(1), 356-365.

Akrami, A., Fassihi, A., Esmaeili, V., & Diamond, M. E. (2013). Tactile working memory in rat and human: Prior competes with recent evidence. Cosyne, Salt Lake City, USA

Anourova, I., Rämä, P., Alho, K., Koivusalo, S., Kahnari, J., & Carlson, S. (1999). Selective interference reveals dissociation between auditory memory for location and pitch. Neuroreport, 10(17), 3543-3547.

Arabzadeh, E., Panzeri, S., & Diamond, M. E. (2004). Whisker vibration information carried by rat barrel cortex neurons. The Journal of neuroscience, 24(26), 6011-6020.

Arabzadeh, E., von Heimendahl, M., & Diamond, M. (2009). Vibrissal texture decoding. Scholarpedia, 4(4), 6640.

Armstrong-James, M., & Fox, K. (1987). Spatiotemporal convergence and divergence in the rat S1 "barrel" cortex. Journal of Comparative Neurology, 263(2), 265-281.

Arnal, L. H., & Giraud, A. L. (2012). Cortical oscillations and sensory predictions. Trends in cognitive sciences, 16(7), 390-398.

Baeg, E. H., Kim, Y. B., Huh, K., Mook-Jung, I., Kim, H. T., & Jung, M. W. (2003). Dynamics of population code for working memory in the prefrontal cortex. Neuron, 40(1), 177-188.

Barbas, H. (1995). Anatomic basis of cognitive-emotional interactions in the primate prefrontal cortex. Neuroscience & Biobehavioral Reviews, 19(3), 499-510.

Barbas, H. (2000). Connections underlying the synthesis of cognition, memory, and emotion in primate prefrontal cortices. Brain research bulletin, 52(5), 319-330.

Barkat, S., Le Berre, E., Coureaud, G., Sicard, G., & Thomas-Danguin, T. (2012). Perceptual blending in odor mixtures depends on the nature of odorants and human olfactory expertise. Chemical senses, 37(2), 159-166.

Batschelet, E., Batschelet, E., Batschelet, E., & Batschelet, E. (1981). Circular statistics in biology (Vol. 371). London: Academic Press.

Battaglia, D., Witt, A., Wolf, F., & Geisel, T. (2012). Dynamic effective connectivity of inter-areal brain circuits. PLoS computational biology, 8(3), e1002438.

Batuev, A. S., Kursina, N. P., & Shutov, A. P. (1990). Unit activity of the medial wall of the frontal cortex during delayed performance in rats. Behavioural brain research, 41(2), 95-102.

Bean, B. P. (2007). The action potential in mammalian central neurons. Nature Reviews Neuroscience, 8(6), 451-465.

Benchenane, K., Peyrache, A., Khamassi, M., Tierney, P. L., Gioanni, Y., Battaglia, F. P., & Wiener, S. I. (2010). Coherent theta oscillations and reorganization of spike timing in the hippocampal-prefrontal network upon learning. Neuron, 66(6), 921-936.

Berendse, H. W., & Groenewegen, H. J. (1991). Restricted cortical termination fields of the midline and intralaminar thalamic nuclei in the rat. Neuroscience, 42(1), 73-102.

Berendse, H. W., Graaf, Y. G. D., & Groenewegen, H. J. (1992). Topographical organization and relationship with ventral striatal compartments of prefrontal corticostriatal projections in the rat. Journal of Comparative Neurology, 316(3), 314-347.

Berens, P. (2009). CircStat: a MATLAB toolbox for circular statistics. J Stat Softw, 31(10), 1-21.

Bisley, J. W., & Pasternak, T. (2000). The multiple roles of visual cortical areas MT/MST in remembering the direction of visual motion. Cerebral Cortex, 10(11), 1053-1065.

Bisley, J. W., Zaksas, D., & Pasternak, T. (2001). Microstimulation of cortical area MT affects performance on a visual working memory task. Journal of Neurophysiology, 85(1), 187-196.

Bisley, J. W., Zaksas, D., Droll, J. A., & Pasternak, T. (2004). Activity of neurons in cortical area MT during a memory for motion task. Journal of neurophysiology, 91(1), 286-300.

Blake, R., Cepeda, N. J., & Hiris, E. (1997). Memory for visual motion. Journal of Experimental Psychology: Human Perception and Performance, 23(2), 353.

Bohn, I., Giertler, C., & Hauber, W. (2003). NMDA receptors in the rat orbital prefrontal cortex are involved in guidance of instrumental behaviour under reversal conditions. Cerebral Cortex, 13(9), 968-976.

Bollinger, J., Rubens, M. T., Zanto, T. P., & Gazzaley, A. (2010). Expectation-driven changes in cortical functional connectivity influence working memory and long-term memory performance. The Journal of Neuroscience, 30(43), 14399-14410.

Bosman, C. A., Schoffelen, J. M., Brunet, N., Oostenveld, R., Bastos, A. M., Womelsdorf, T., ... & Fries, P. (2012). Attentional stimulus selection through selective synchronization between monkey visual areas. Neuron, 75(5), 875-888.

Brecht, M. (2007). Barrel cortex and whisker-mediated behaviors. Current opinion in neurobiology, 17(4), 408-416.

Brecht, M., Preilowski, B., & Merzenich, M. M. (1997). Functional architecture of the mystacial vibrissae. Behavioural brain research, 84(1), 81-97.

Brito, G. N., & Brito, L. S. (1990). Septohippocampal system and the prelimbic sector of frontal cortex: a neuropsychological battery analysis in the rat. Behavioural brain research, 36(1), 127-146.

Bruno, R. M., & Simons, D. J. (2002). Feedforward mechanisms of excitatory and inhibitory cortical receptive fields. The Journal of neuroscience, 22(24), 10966-10975.

Brunton, B. W., Botvinick, M. M., & Brody, C. D. (2013). Rats and humans can optimally accumulate evidence for decision-making. Science, 340(6128), 95-98.

Burchell, T. R., Faulkner, H. J., & Whittington, M. A. (1998). Gamma frequency oscillations gate temporally coded afferent inputs in the rat hippocampal slice. Neuroscience letters, 255(3), 151-154.

Burns, S. M., & Michael Wyss, J. (1985). The involvement of the anterior cingulate cortex in blood pressure control. Brain research, 340(1), 71-77.

Burton, H., & Sinclair, R. J. (2000). Attending to and remembering tactile stimuli: a review of brain imaging data and single-neuron responses. Journal of Clinical Neurophysiology, 17(6), 575-591.

Buschman, T. J., & Miller, E. K. (2007). Top-down versus bottom-up control of attention in the prefrontal and posterior parietal cortices. science, 315(5820), 1860-1862.

Buschman, T. J., & Miller, E. K. (2009). Serial, covert shifts of attention during visual search are reflected by the frontal eye fields and correlated with population oscillations. Neuron, 63(3), 386-396.

Canolty, R. T., & Knight, R. T. (2010). The functional role of cross-frequency coupling. Trends in cognitive sciences, 14(11), 506-515.

Carandini, M., & Churchland, A. K. (2013). Probing perceptual decisions in rodents. Nature neuroscience, 16(7), 824-831.

Carruthers, P. (2013). Evolution of working memory. Proceedings of the National Academy of Sciences, 110(Supplement 2), 10371-10378.

Cechetto, D. F., & Chen, S. J. (1990). Subcortical sites mediating sympathetic responses from insular cortex in rats. Am J Physiol, 258(1 Pt 2), R245-R255.

Cechetto, D. F., & Saper, C. B. (1990). Role of the cerebral cortex in autonomic function. Central regulation of autonomic functions, 208-223.

Champod, A. S., & Petrides, M. (2007). Dissociable roles of the posterior parietal and the prefrontal cortex in manipulation and monitoring processes. Proceedings of the National Academy of Sciences, 104(37), 14837-14842.

Chelazzi, L., Duncan, J., Miller, E. K., & Desimone, R. (1998). Responses of neurons in inferior temporal cortex during memory-guided visual search. Journal of Neurophysiology, 80(6), 2918-2940.

Clarke, S., Adriani, M., & Bellmann, A. (1998). Distinct short-term memory systems for sound content and sound localization. Neuroreport, 9(15), 3433-3437.

Clément, S., Demany, L., & Semal, C. (1999). Memory for pitch versus memory for loudness. The Journal of the Acoustical Society of America, 106(5), 2805-2811.

Condé, F., Audinat, E., Maire-Lepoivre, E., & Crépel, F. (1990). Afferent connections of the medial frontal cortex of the rat. A study using retrograde transport of fluorescent dyes. I. Thalamic afferents. Brain research bulletin, 24(3), 341-354.

Constantinidis, C. H. R. I. S. T. O. S., & Steinmetz, M. A. (1996). Neuronal activity in posterior parietal area 7a during the delay periods of a spatial memory task. Journal of Neurophysiology, 76(2), 1352-1355.

Curtis, C. E., Rao, V. Y., & D'Esposito, M. (2004). Maintenance of spatial and motor codes during oculomotor delayed response tasks. The Journal of neuroscience, 24(16), 3944-3952.

Curtis, J. C., & Kleinfeld, D. (2009). Phase-to-rate transformations encode touch in cortical neurons of a scanning sensorimotor system. Nature neuroscience, 12(4), 492-501.

Deco, G., & Thiele, A. (2009). Attention–oscillations and neuropharmacology. European journal of neuroscience, 30(3), 347-354.

Delatour, B., & Gisquest-Verrier, P. (1999). Lesions of the prelimbic–infralimbic cortices in rats do not disrupt response selection processes but induce delay-dependent deficits: evidence for a role in working memory?. Behavioral neuroscience, 113(5), 941.

Delatour, B., & Gisquet-Verrier, P. (1996). Prelimbic cortex specific lesions disrupt delayed-variable response tasks in the rat. Behavioral neuroscience, 110(6), 1282.

Delatour, B., & Gisquet-Verrier, P. (2000). Functional role of rat prelimbic-infralimbic cortices in spatial memory: evidence for their involvement in attention and behavioural flexibility. Behavioural brain research, 109(1), 113-128.

D'Esposito, M., Detre, J. A., Alsop, D. C., Shin, R. K., Atlas, S., & Grossman, M. (1995). The neural basis of the central executive system of working memory. Nature, 378(6554), 279-281.

D'Esposito, M., Postle, B. R., & Rypma, B. (2000). Prefrontal cortical contributions to working memory: evidence from event-related fMRI studies. Experimental Brain Research, 133(1), 3-11.

D'Esposito, M., Postle, B. R., Ballard, D., & Lease, J. (1999). Maintenance versus manipulation of information held in working memory: an event-related fMRI study. Brain and cognition, 41(1), 66-86.

Deutsch, D. (1972). Mapping of interactions in the pitch memory store. Science, 175(4025), 1020-1022.

Deutsch, D. (1973). Interference in memory between tones adjacent in the musical scale. Journal of Experimental Psychology, 100(2), 228.

Diamond, M. E. (2010). Texture sensation through the fingertips and the whiskers. Current opinion in neurobiology, 20(3), 319-327.

Diamond, M. E., & Arabzadeh, E. (2013). Whisker sensory system–from receptor to decision. Progress in neurobiology, 103, 28-40.

Diamond, M. E., Armstrong-James, M., & Ebner, F. F. (1993). Experience-dependent plasticity in adult rat barrel cortex. Proceedings of the National Academy of Sciences, 90(5), 2082-2086.

Diamond, M. E., von Heimendahl, M., & Arabzadeh, E. (2008). Whisker-mediated texture discrimination. PLoS biology, 6(8), e220.

Diamond, M. E., von Heimendahl, M., Knutsen, P. M., Kleinfeld, D., & Ahissar, E. (2008). 'Where'and'what'in the whisker sensorimotor system. Nature Reviews Neuroscience, 9(8), 601-612.

Duda, R. O., Hart, P. E., & Stork, D. G. (2012). Pattern classification. John Wiley & Sons.

Dudchenko, P. A. (2004). An overview of the tasks used to test working memory in rodents. Neuroscience & Biobehavioral Reviews, 28(7), 699-709.

Eden, C. G., Lamme, V. A. F., & Uylings, H. B. M. (1992). Heterotopic cortical afferents to the medial prefrontal cortex in the rat. A combined retrograde and anterograde tracer study. European Journal of Neuroscience, 4(1), 77-97.

Eichenbaum, H., & Cohen, N. J. (2001). From conditioning to conscious recollection: Memory systems of the brain. Oxford University Press.

Engel, A. K., Fries, P., & Singer, W. (2001). Dynamic predictions: oscillations and synchrony in top–down processing. Nature Reviews Neuroscience, 2(10), 704-716.

Engel, A. K., König, P., Kreiter, A. K., & Singer, W. (1991). Interhemispheric synchronization of oscillatory neuronal responses in cat visual cortex. Science, 252(5010), 1177-1179.

Ennaceur, A. (2010). One-trial object recognition in rats and mice: methodological and theoretical issues. Behavioural brain research, 215(2), 244-254.

Erlich, J. C., Bialek, M., & Brody, C. D. (2011). A cortical substrate for memory-guided orienting in the rat. Neuron, 72(2), 330-343.

Fassihi, A., (2012). Perception of tactile vibration and a putative neuronal code. Doctoral dissertation, SISSA, Trieste, Italy.

Fassihi, A., Akrami, A., Esmaeili, V., & Diamond, M. E. (2014). Tactile perception and working memory in rats and humans. Proceedings of the National Academy of Sciences, 111(6), 2331-2336.

Fell, J., & Axmacher, N. (2011). The role of phase synchronization in memory processes. Nature Reviews Neuroscience, 12(2), 105-118.

Fiebach, C. J., Rissman, J., & D'Esposito, M. (2006). Modulation of inferotemporal cortex activation during verbal working memory maintenance. Neuron, 51(2), 251-261.

Fisher, R. (1936). Linear discriminant analysis. Ann. Eugenics, 7, 179.

Floresco, S. B., Seamans, J. K., & Phillips, A. G. (1997). Selective roles for hippocampal, prefrontal cortical, and ventral striatal circuits in radial-arm maze tasks with or without a delay. The Journal of neuroscience, 17(5), 1880-1890.

Friedman, J. H. (1989). Regularized discriminant analysis. Journal of the American statistical association, 84(405), 165-175.

Fries, P. (2005). A mechanism for cognitive dynamics: neuronal communication through neuronal coherence. Trends in cognitive sciences, 9(10), 474-480.

Fuster, J. M. (1973). Unit activity in prefrontal cortex during delayed-response performance: neuronal correlates of transient memory. Journal of Neurophysiology.

Fuster, J. M. (1988). Prefrontal cortex (pp. 107-109). Birkhäuser Boston.

Fuster, J. M., & Alexander, G. E. (1971). Neuron activity related to short-term memory. Science, 173(3997), 652-654.

Fuster, J. M., & Jervey, J. P. (1982). Neuronal firing in the inferotemporal cortex of the monkey in a visual memory task. The Journal of Neuroscience, 2(3), 361-375.

Ganguly, K., & Kleinfeld, D. (2004). Goal-directed whisking increases phase-locking between vibrissa movement and electrical activity in primary sensory cortex in rat. Proceedings of the National Academy of Sciences of the United States of America, 101(33), 12348-12353.

Goldman-Rakic, P. S. (1994). The issue of memory in the study of prefrontal function. In Motor and cognitive functions of the prefrontal cortex (pp. 112-121). Springer Berlin Heidelberg.

Gottlieb, Y., Vaadia, E., & Abeles, M. (1989). Single unit activity in the auditory cortex of a monkey performing a short term memory task. Experimental Brain Research, 74(1), 139-148.

Gregoriou, G. G., Gotts, S. J., Zhou, H., & Desimone, R. (2009). High-frequency, long-range coupling between prefrontal and visual cortex during attention. science, 324(5931), 1207-1210.

Grobe, C., & Spector, A. (2006). Rats can learn a "Delayed Match/Delayed Non-Match to Sample" task using only taste stimuli. FASEB J, 20(4), A381.

Groenewegen, H. J., & Uylings, H. (2000). The prefrontal cortex and the integration of sensory, limbic and autonomic information. Progress in brain research, 126, 3-28.

Guo, Y., Hastie, T., & Tibshirani, R. (2006). Regularized linear discriminant analysis and its application in microarrays. Biostatistics, 8(1), 86-100.

Hardy, S. G. P., & Holmes, D. E. (1988). Prefrontal stimulus-produced hypotension in rat. Experimental brain research, 73(2), 249-255.

Harris, J. A., Harris, I. M., & Diamond, M. E. (2001). The topography of tactile working memory. The Journal of Neuroscience, 21(20), 8262-8269.

Harris, J. A., Harris, I. M., & Diamond, M. E. (2001). The topography of tactile learning in humans. The Journal of Neuroscience, 21(3), 1056-1061.

Harris, J. A., Miniussi, C., Harris, I. M., & Diamond, M. E. (2002). Transient storage of a tactile memory trace in primary somatosensory cortex. The Journal of neuroscience, 22(19), 8720-8725.

Harris, J. A., Petersen, R. S. and Diamond, M. E. (1999) Distribution of tactile learning and its neural basis. Proc Natl Acad Sci U S A 96, 7587-7591.

Harris, J. A., Petersen, R. S., & Diamond, M. E. (2001). The cortical distribution of sensory memories. Neuron, 30(2), 315-318.

Harvey, M., Bermejo, R. and Zeigler, H. (2001) Discriminative whisking in the head-fixed rat: optoelectronic monitoring during tactile detection and discrimination tasks. Somatosensory & motor research 18, 211.

Heidbreder, C. A., & Groenewegen, H. J. (2003). The medial prefrontal cortex in the rat: evidence for a dorso-ventral distinction based upon functional and anatomical characteristics. Neuroscience & Biobehavioral Reviews, 27(6), 555-579.

Hernández, A., Nácher, V., Luna, R., Zainos, A., Lemus, L., Alvarez, M., ... & Romo, R. (2010). Decoding a perceptual decision process across cortex. Neuron, 66(2), 300-314.

Hernández, A., Salinas, E., Garcıa, R., & Romo, R. (1997). Discrimination in the sense of flutter: new psychophysical measurements in monkeys. The Journal of neuroscience, 17(16), 6391-6400.

Hernández, A., Zainos, A., & Romo, R. (2000). Neuronal correlates of sensory discrimination in the somatosensory cortex. Proceedings of the National Academy of Sciences, 97(11), 6191-6196.

Hernández, A., Zainos, A., & Romo, R. (2002). Temporal evolution of a decision-making process in medial premotor cortex. Neuron, 33(6), 959-972.

Honig WK. (1978). Studies of working memory in the pigeon In: W.K. Honig, Editors, Cognitive processes in animal behaviour.

Hoover, W. B., & Vertes, R. P. (2007). Anatomical analysis of afferent projections to the medial prefrontal cortex in the rat. Brain Structure and Function, 212(2), 149-179.

Hurley-Gius, K. M., & Neafsey, E. J. (1986). The medial frontal cortex and gastric motility: microstimulation results and their possible significance for the overall pattern of organization of rat frontal and parietal cortex. Brain research, 365(2), 241-248.

Jadhav, S. P., Kemere, C., German, P. W., & Frank, L. M. (2012). Awake hippocampal sharp-wave ripples support spatial memory. Science, 336(6087), 1454-1458.

Jasmin, L., Granato, A., & Ohara, P. T. (2004). Rostral agranular insular cortex and pain areas of the central nervous system: A tract-tracing study in the rat. Journal of Comparative Neurology, 468(3), 425-440.

Jenks, R. A., Vaziri, A., Boloori, A. R. and Stanley, G. B. (2010) Self-motion and the shaping of sensory signals. J Neurophysiol 103, 2195-2207.

Jensen, K. F., & Killackey, H. P. (1987). Terminal arbors of axons projecting to the somatosensory cortex of the adult rat. I. The normal morphology of specific thalamocortical afferents. The Journal of neuroscience, 7(11), 3529-3543.

Jensen, O., Bonnefond, M., & VanRullen, R. (2012). An oscillatory mechanism for prioritizing salient unattended stimuli. Trends in cognitive sciences, 16(4), 200-206.

Joelving, F. C., Compte, A., & Constantinidis, C. (2007). Temporal properties of posterior parietal neuron discharges during working memory and passive viewing. Journal of neurophysiology, 97(3), 2254-2266.

Jones, E. G., & Diamond, I. T. (Eds.). (1995). The Barrel Cortex of Rodents: Volume 11: The Barrel Cortex of Rodents (Vol. 11). Springer.

Kaas, J. H., Merzenich, M. M., & Killackey, H. P. (1983). The reorganization of somatosensory cortex following peripheral nerve damage in adult and developing mammals. Annual review of neuroscience, 6(1), 325-356.

Kahana, M. J., & Sekuler, R. (2002). Recognizing spatial patterns: A noisy exemplar approach. Vision research, 42(18), 2177-2192.

Karlsson, M. P., Tervo, D. G., & Karpova, A. Y. (2012). Network resets in medial prefrontal cortex mark the onset of behavioral uncertainty. Science, 338(6103), 135-139.

Kepecs, A., Uchida, N., Zariwala, H. A., & Mainen, Z. F. (2008). Neural correlates, computation and behavioural impact of decision confidence. Nature, 455(7210), 227-231.

Knutsen, P. M., Pietr, M. and Ahissar, E. (2006) Haptic object localization in the vibrissal system: behavior and performance. J Neurosci 26, 8451-8464.

Koch, K. W., & Fuster, J. M. (1989). Unit activity in monkey parietal cortex related to haptic perception and temporary memory. Experimental Brain Research, 76(2), 292-306.

Kojima, S., & Goldman-Rakic, P. S. (1982). Delay-related activity of prefrontal neurons in rhesus monkeys performing delayed response. Brain research, 248(1), 43-50.

Kolb, B. (1984). Functions of the frontal cortex of the rat: a comparative review. Brain Research Reviews, 8(1), 65-98.

Kopell, N., Ermentrout, G. B., Whittington, M. A., & Traub, R. D. (2000). Gamma rhythms and beta rhythms have different synchronization properties. Proceedings of the National Academy of Sciences, 97(4), 1867-1872.

Lak, A., Arabzadeh, E. and Diamond, M. E. (2008) Enhanced response of neurons in rat somatosensory cortex to stimuli containing temporal noise. Cereb Cortex 18, 1085-1093.

Lak, A., Arabzadeh, E., Harris, J. A., & Diamond, M. E. (2010). Correlated physiological and perceptual effects of noise in a tactile stimulus. Proceedings of the National Academy of Sciences, 107(17), 7981-7986.

Lalonde, J., & Chaudhuri, A. (2002). Task-dependent transfer of perceptual to memory representations during delayed spatial frequency discrimination. Vision research, 42(14), 1759-1769.

Lavan, D., McDonald, J. S., Westbrook, R. F., & Arabzadeh, E. (2011). Behavioural correlate of choice confidence in a discrete trial paradigm. PloS one, 6(10), e26863.

Lee, B., & Harris, J. (1996). Contrast transfer characteristics of visual short-term memory. Vision research, 36(14), 2159-2166.

Loewy, A. D. (1991). Forebrain nuclei involved in autonomic control. Progress in brain research, 87, 253-268.

Lottem, E., & Azouz, R. (2011). A unifying framework underlying mechanotransduction in the somatosensory system. The Journal of Neuroscience, 31(23), 8520-8532.

Lu, Z. L., Williamson, S. J., & Kaufman, L. (1992). Behavioral lifetime of human auditory sensory memory predicted by physiological measures. SCIENCE-NEW YORK THEN WASHINGTON-, 258, 1668-1668.

Magnussen, S. (2000). Low-level memory processes in vision. Trends in neurosciences, 23(6), 247-251.

Magnussen, S., & Greenlee, M. W. (1992). Retention and disruption of motion information in visual short-term memory. Journal of Experimental Psychology: Learning, Memory, and Cognition, 18(1), 151.

Magnussen, S., Greenlee, M. W., & Thomas, J. P. (1996). Parrel processing in visual short-term memory. Journal of Experimental Psychology: Human Perception and Performance, 22(1), 202.

Magnussen, S., Greenlee, M. W., Asplund, R., & Dyrnes, S. (1991). Stimulus-specific mechanisms of visual short-term memory. Vision research, 31(7), 1213-1219.

Magnussen, S., Idås, E., & Myhre, S. H. (1998). Representation of orientation and spatial frequency in perception and memory: a choice reaction-time analysis. Journal of Experimental Psychology: Human perception and performance, 24(3), 707.

Magri, C., Whittingstall, K., Singh, V., Logothetis, N. K., & Panzeri, S. (2009). A toolbox for the fast information analysis of multiple-site LFP, EEG and spike train recordings. BMC neuroscience, 10(1), 81.

Mainen, Z. F., & Kepecs, A. (2009). Neural representation of behavioral outcomes in the orbitofrontal cortex. Current opinion in neurobiology, 19(1), 84-91.

Maravall, M., Petersen, R. S., Fairhall, A. L., Arabzadeh, E. and Diamond, M. E. (2007) Shifts in coding properties and maintenance of information transmission during adaptation in barrel cortex. PLoS Biol 5, e19.

Maris, E., & Oostenveld, R. (2007). Nonparametric statistical testing of EEG-and MEG-data. Journal of neuroscience methods, 164(1), 177-190.

McIntosh, A. R., Sekuler, A. B., Penpeci, C., Rajah, M. N., Grady, C. L., Sekuler, R., & Bennett, P. J. (1999). Recruitment of unique neural systems to support visual memory in normal aging. Current Biology, 9(21), 1275-S2.

Miller, E. K., Erickson, C. A., & Desimone, R. (1996). Neural mechanisms of visual working memory in prefrontal cortex of the macaque. The Journal of Neuroscience, 16(16), 5154-5167.

Miller, E. K., Li, L., & Desimone, R. (1993). Activity of neurons in anterior inferior temporal cortex during a short-term memory task. The Journal of neuroscience, 13(4), 1460-1478.

Mitchinson, B., Arabzadeh, E., Diamond, M. E. and Prescott, T. J. (2008) Spike-timing in primary sensory neurons: a model of somatosensory transduction in the rat. Biol Cybern 98, 185-194.

Mitchinson, B., Gurney, K. N., Redgrave, P., Melhuish, C., Pipe, A. G., Pearson, M., Gilhespy, I. and Prescott, T. J. (2004) Empirically inspired simulated electro-mechanical model of the rat mystacial follicle-sinus complex. Proc Biol Sci 271, 2509-2516.

Miyashita, Y., & Chang, H. S. (1988). Neuronal correlate of pictorial short-term memory in the primate temporal cortex. Nature, 331(6151), 68-70.

Montani, F., Ince, R. A., Senatore, R., Arabzadeh, E., Diamond, M. E. and Panzeri, S. (2009) The impact of high-order interactions on the rate of synchronous discharge and information transmission in somatosensory cortex. Philos Transact A Math Phys Eng Sci 367, 3297-3310.

Morris, R. (1984). Developments of a water-maze procedure for studying spatial learning in the rat. Journal of neuroscience methods, 11(1), 47-60.

Mountcastle, V. B., Steinmetz, M. A., & Romo, R. (1990). Frequency discrimination in the sense of flutter: psychophysical measurements correlated with postcentral events in behaving monkeys. The Journal of Neuroscience, 10(9), 3032-3044.

Murakami, M., Vicente, M. I., Costa, G. M., & Mainen, Z. F. (2014). Neural antecedents of self-initiated actions in secondary motor cortex. Nature neuroscience.

Murphy, R. A., Mondragón, E., & Murphy, V. A. (2008). Rule learning by rats. Science, 319(5871), 1849-1851.

Musall, S., von der Behrens, W., Mayrhofer, J. M., Weber, B., Helmchen, F., & Haiss, F. (2014). Tactile frequency discrimination is enhanced by circumventing neocortical adaptation. Nature neuroscience.

Nácher, V., Ledberg, A., Deco, G., & Romo, R. (2013). Coherent delta-band oscillations between cortical areas correlate with decision making. Proceedings of the National Academy of Sciences, 110(37), 15085-15090.

Neafsey, E. J., Hurley-Gius, K. M., & Arvanitis, D. (1986). The topographical organization of neurons in the rat medial frontal, insular and olfactory cortex projecting to the solitary nucleus, olfactory bulb, periaqueductal gray and superior colliculus. Brain research, 377(2), 261-270.

Neafsey, E. J., Terreberry, R. R., Hurley, K. M., Ruit, K. G., & Frysztak, R. J. (1993). Anterior cingulate cortex in rodents: connections, visceral control functions, and implications for emotion. In Neurobiology of cingulate cortex and limbic thalamus (pp. 206-223). Birkhäuser Boston.

Neafsey, E. J., Terreberry, R. R., Hurley, K. M., Ruit, K. G., & Frysztak, R. J. (1993). Anterior cingulate cortex in rodents: connections, visceral control functions, and implications for emotion. In Neurobiology of cingulate cortex and limbic thalamus (pp. 206-223). Birkhäuser Boston.

Nelder, J. A., & Baker, R. J. (1972). Generalized linear models. John Wiley & Sons, Inc..

Nolte, G., Bai, O., Wheaton, L., Mari, Z., Vorbach, S., & Hallett, M. (2004). Identifying true brain interaction from EEG data using the imaginary part of coherency. Clinical Neurophysiology, 115(10), 2292-2307.

Öngür, D., & Price, J. L. (2000). The organization of networks within the orbital and medial prefrontal cortex of rats, monkeys and humans. Cerebral cortex, 10(3), 206-219.

Optican, L. M., Gawne, T. J., Richmond, B. J., & Joseph, P. J. (1991). Unbiased measures of transmitted information and channel capacity from multivariate neuronal data. Biological cybernetics, 65(5), 305-310.

Orlov, A. A., Kurzina, N. P., & Shutov, A. P. (1988). Activity of medial wall neurons in frontal cortex of rat brain during delayed response reactions. Neuroscience and behavioral physiology, 18(1), 31-37.

Otto, T., & Eichenbaum, H. (1992). Complementary roles of the orbital prefrontal cortex and the perirhinal-entorhinal cortices in an odor-guided delayed-nonmatching-to-sample task. Behavioral neuroscience, 106(5), 762.

Panzeri, S., & Schultz, S. R. (2001). A unified approach to the study of temporal, correlational, and rate coding. Neural Computation, 13(6), 1311-1349.

Panzeri, S., Petersen, R. S., Schultz, S. R., Lebedev, M., & Diamond, M. E. (2001). The role of spike timing in the coding of stimulus location in rat somatosensory cortex. Neuron, 29(3), 769-777.

Passingham, R. E., Bengtsson, S. L., & Lau, H. C. (2010). Medial frontal cortex: from self-generated action to reflection on one's own performance. Trends in cognitive sciences, 14(1), 16-21.

Paxinos, G. (1999). Chemoarchitectonic atlas of the rat forebrain.

Peña, T., Pitts, R. C., & Galizio, M. (2006). IDENTITY MATCHING-TO-SAMPLE WITH OLFACTORY STIMULI IN RATS. Journal of the experimental analysis of behavior, 85(2), 203-221.

Perry, C., & Felsen, G. (2012). Rats can make relative perceptual judgments about sequential stimuli. Animal cognition, 15(4), 473-481.

Pesaran, B., Nelson, M. J., & Andersen, R. A. (2008). Free choice activates a decision circuit between frontal and parietal cortex. Nature, 453(7193), 406-409.

Petersen, C. C. (2007). The functional organization of the barrel cortex. Neuron, 56(2), 339-355.

Petersen, R. S., Panzeri, S., & Diamond, M. E. (2001). Population coding of stimulus location in rat somatosensory cortex. Neuron, 32(3), 503-514.

Petrides, M. (1995). Impairments on nonspatial self-ordered and externally ordered working memory tasks after lesions of the mid-dorsal part of the lateral frontal cortex in the monkey. The Journal of Neuroscience, 15(1), 359-375.

PIERROT-DESEILLIGNY, C. H., Müri, R. M., Nyffeler, T., & Milea, D. (2005). The role of the human dorsolateral prefrontal cortex in ocular motor behavior. Annals of the New York Academy of Sciences, 1039(1), 239-251.

Pontecorvo, M. J., Sahgal, A., & Steckler, T. (1996). Further developments in the measurement of working memory in rodents. Cognitive brain research, 3(3), 205-213.

Pratt, W. E., & Mizumori, S. J. (2001). Neurons in rat medial prefrontal cortex show anticipatory rate changes to predictable differential rewards in a spatial memory task. Behavioural brain research, 123(2), 165-183.

Prescott, T. J., Diamond, M. E. and Wing, A. M. (2011) Active touch sensing: An introduction to the theme issue. Philosophical Transactions of the Royal Society B: Biological Sciences 366, 2989-2995.

Preuss, T. (1995). Do rats have prefrontal cortex? The Rose-Woolsey-Akert program reconsidered. Cognitive Neuroscience, Journal of, 7(1), 1-24.

Quiroga, R. Q., & Panzeri, S. (2009). Extracting information from neuronal populations: information theory and decoding approaches. Nature Reviews Neuroscience, 10(3), 173-185.

Quiroga, R. Q., Reddy, L., Koch, C., & Fried, I. (2007). Decoding visual inputs from multiple neurons in the human temporal lobe. Journal of neurophysiology, 98(4), 1997-2007.

Ragozzino, M. E., Adams, S., & Kesner, R. P. (1998). Differential involvement of the dorsal anterior cingulate and prelimbic–infralimbic areas of the rodent prefrontal cortex in spatial working memory. Behavioral neuroscience, 112(2), 293.

Raposo, D., Sheppard, J. P., Schrater, P. R., & Churchland, A. K. (2012). Multisensory decision-making in rats and humans. The Journal of Neuroscience, 32(11), 3726-3735.

Ray, J. P., & Price, J. L. (1992). The organization of the thalamocortical connections of the mediodorsal thalamic nucleus in the rat, related to the ventral forebrain–prefrontal cortex topography. Journal of Comparative Neurology, 323(2), 167-197.

Reep, R. L., Goodwin, G. S., & Corwin, J. V. (1990). Topographic organization in the corticocortical connections of medial agranular cortex in rats. Journal of Comparative Neurology, 294(2), 262-280.

Regan, D. (1985). Storage of spatial-frequency information and spatial-frequency discrimination. JOSA A, 2(4), 619-621.

Ringach, D., & Shapley, R. (2004). Reverse correlation in neurophysiology. Cognitive Science, 28(2), 147-166.

Roelfsema, P. R., Engel, A. K., Konig, P., & Singer, W. (1997). Visuomotor integration is associated with zero time-lag synchronization among cortical areas. Nature, 385, 157-161.

Romanski, L. M., Bates, J. F., & Goldman-Rakic, P. S. (1999). Auditory belt and parabelt projections to the prefrontal cortex in the rhesus monkey. Journal of Comparative Neurology, 403(2), 141-157.

Romo R, Brody CD, Hernández A & Lemus L (1999) Neuronal correlates of parametric working memory in the prefrontal cortex Nature 399.

Romo, R., & Salinas, E. (2001). Touch and go: decision-making mechanisms in somatosensation. Annual review of neuroscience, 24(1), 107-137.

Romo, R., & Salinas, E. (2003). Flutter discrimination: neural codes, perception, memory and decision making. Nature Reviews Neuroscience, 4(3), 203-218.

Romo, R., Hernández, A., Zainos, A., Lemus, L., & Brody, C. D. (2002). Neuronal correlates of decision-making in secondary somatosensory cortex. Nature neuroscience, 5(11), 1217-1225.

Safaai, H., von Heimendahl, M., Sorando, J. M., Diamond, M. E., & Maravall, M. (2013). Coordinated population activity underlying texture discrimination in rat barrel cortex. The Journal of Neuroscience, 33(13), 5843-5855.

Salazar, R. F., Dotson, N. M., Bressler, S. L., & Gray, C. M. (2012). Content-specific fronto-parietal synchronization during visual working memory. Science, 338(6110), 1097-1100.

Sams, M., Hari, R., Rif, J., & Knuutila, J. (1993). The human auditory sensory memory trace persists about 10 sec: neuromagnetic evidence. Cognitive Neuroscience, Journal of, 5(3), 363-370.

Schoenbaum, G., Setlow, B., & Ramus, S. J. (2003). A systems approach to orbitofrontal cortex function: recordings in rat orbitofrontal cortex reveal interactions with different learning systems. Behavioural brain research, 146(1), 19-29.

Seamans, J. K., Floresco, S. B., & Phillips, A. G. (1995). Functional differences between the prelimbic and anterior cingulate regions of the rat prefrontal cortex. Behavioral neuroscience, 109(6), 1063.

Seamans, J. K., Lapish, C. C., & Durstewitz, D. (2008). Comparing the prefrontal cortex of rats and primates: insights from electrophysiology. Neurotoxicity research, 14(2-3), 249-262.

Siapas, A. G., Lubenov, E. V., & Wilson, M. A. (2005). Prefrontal phase locking to hippocampal theta oscillations. Neuron, 46(1), 141-151.

Siegel, M., Donner, T. H., & Engel, A. K. (2012). Spectral fingerprints of large-scale neuronal interactions. Nature Reviews Neuroscience, 13(2), 121-134.

Simons, D. J. (1978). Response properties of vibrissa units in rat SI somatosensory neocortex. J Neurophysiol, 41(3), 798-820.

Sinclair, R. J., & Burton, H. (1996). Discrimination of vibrotactile frequencies in a delayed pair comparison task. Perception & psychophysics, 58(5), 680-692.

Stam, C. J., Nolte, G., & Daffertshofer, A. (2007). Phase lag index: assessment of functional connectivity from multi channel EEG and MEG with diminished bias from common sources. Human brain mapping, 28(11), 1178-1193.

Sullivan, E. V., & Turvey, M. T. (1972). Short-term retention of tactile stimulation. The Quarterly journal of experimental psychology, 24(3), 253-261.

Summerfield, C., & Egner, T. (2009). Expectation (and attention) in visual cognition. Trends in cognitive sciences, 13(9), 403-409.

Super, H., Spekreijse, H., & Lamme, V. A. (2001). A neural correlate of working memory in the monkey primary visual cortex. Science, 293(5527), 120-124.

Tafazoli, S., Di Filippo, A., & Zoccolan, D. (2012). Transformation-tolerant object recognition in rats revealed by visual priming. The Journal of Neuroscience, 32(1), 21-34.

Terreberry, R. R., & Neafsey, E. J. (1983). Rat medial frontal cortex: a visceral motor region with a direct projection to the solitary nucleus. Brain Research, 278(1), 245-249.

Thierry, A. M., Jay, T. M., Pirot, S., Mantz, J., Godbout, R., & Glowinski, J. (1994). Influence of afferent systems on the activity of the rat prefrontal cortex: Electrophysiological and pharmacological characterization. In Motor and Cognitive Functions of the Prefrontal Cortex (pp. 35-50). Springer Berlin Heidelberg.

Tiesinga, P. H., Fellous, J. M., José, J. V., & Sejnowski, T. J. (2001). Computational model of carbachol-induced delta, theta, and gamma oscillations in the hippocampus. Hippocampus, 11(3), 251-274.

Treves, A., & Panzeri, S. (1995). The upward bias in measures of information derived from limited data samples. Neural Computation, 7(2), 399-407.

Uylings, H. B. M., De Bruin, C. V. E. J., Corner, M. A., & Feenstra, M. G. P. (1990). Prefrontal cortical control of the autonomic nervous system: anatomical and physiological observations. The Prefrontal Cortex: Its Structure, Function, and Pathology: Proceedings of the 16th International Summer School of Brain Research, Held at the Royal Tropical Institute and the Royal Netherlands Academy of Sciences Amsterdam, the Netherlands, from 28 August to 1 September 1989, 85, 147.

Uylings, H., Groenewegen, H. J., & Kolb, B. (2003). Do rats have a prefrontal cortex?. Behavioural brain research, 146(1), 3-17.

Uylings, H., Van Eden, C., & De Bruin, J. F. M. & Pennartz, C., eds.(2000) Progress in brain research, vol. 126: Cognition, emotion and autonomic responses: The integrative role of the prefrontal cortex and limbic structures.

Varela, F., Lachaux, J. P., Rodriguez, E., & Martinerie, J. (2001). The brainweb: phase synchronization and large-scale integration. Nature reviews neuroscience, 2(4), 229-239.

Verberne AJ, Lewis SJ, Worland PJ, Beart PM, Jarrott B, Christie MJ, Louis WJ. (1987) Medial prefrontal cortical lesions modulate baroreflex sensitivity in the rat. Brain Res 426:243–249

VERBERNE, A. J., & OWENS, N. C. (1998). Cortical Modulation of theCardiovascular System. Progress in neurobiology, 54(2), 149-168.

Vertes, R. P. (2006). Interactions among the medial prefrontal cortex, hippocampus and midline thalamus in emotional and cognitive processing in the rat. Neuroscience, 142(1), 1-20.

Vertes, R. P., Hoover, W. B., Do Valle, A. C., Sherman, A., & Rodriguez, J. J. (2006). Efferent projections of reuniens and rhomboid nuclei of the thalamus in the rat. Journal of Comparative Neurology, 499(5), 768-796.

Vincent, S. (1912) The functions of the vibrissae in the behavior of the white rat. University of Chicago.

Vinck, M., Lima, B., Womelsdorf, T., Oostenveld, R., Singer, W., Neuenschwander, S., & Fries, P. (2010). Gamma-phase shifting in awake monkey visual cortex. The Journal of Neuroscience, 30(4), 1250-1257.

Vinck, M., Oostenveld, R., van Wingerden, M., Battaglia, F., & Pennartz, C. (2011). An improved index of phase-synchronization for electrophysiological data in the presence of volume-conduction, noise and sample-size bias. Neuroimage, 55(4), 1548-1565.

Vogels, R., & Orban, G. A. (1986). Decision processes in visual discrimination of line orientation. Journal of Experimental Psychology: Human Perception and Performance, 12(2), 115.

Volgushev, M., Chistiakova, M., & Singer, W. (1998). Modification of discharge patterns of neocortical neurons by induced oscillations of the membrane potential. Neuroscience, 83(1), 15-25.

von Heimendahl, M., Itskov, P. M., Arabzadeh, E. and Diamond, M. E. (2007) Neuronal activity in rat barrel cortex underlying texture discrimination. PLoS Biol 5, e305.

Von Stein, A., & Sarnthein, J. (2000). Different frequencies for different scales of cortical integration: from local gamma to long range alpha/theta synchronization. International Journal of Psychophysiology, 38(3), 301-313.

Wang, M., Yang, Y., Wang, C. J., Gamo, N. J., Jin, L. E., Mazer, J. A., ... & Arnsten, A. F. (2013). NMDA receptors subserve persistent neuronal firing during working memory in dorsolateral prefrontal cortex. Neuron, 77(4), 736-749.

Welker, C. and Woolsey, T. A. (1974). Structure of layer IV in the somatosensory neocortex of the rat: description and comparison with the mouse. J Comp Neurol 158, 437-453.

Westerhaus, M. J., & Loewy, A. D. (2001). Central representation of the sympathetic nervous system in the cerebral cortex. Brain Research, 903(1), 117-127.

Womelsdorf, T., & Fries, P. (2007). The role of neuronal synchronization in selective attention. Current opinion in neurobiology, 17(2), 154-160.

Woolsey, T. A., & Van der Loos, H. (1970). The structural organization of layer IV in the somatosensory region (SI) of mouse cerebral cortex: the description of a cortical field composed of discrete cytoarchitectonic units. Brain research, 17(2), 205-242.

Zaksas, D., Bisley, J. W., & Pasternak, T. (2001). Motion information is spatially localized in a visual working-memory task. Journal of neurophysiology, 86(2), 912-921.

Zatorre, R. J., Evans, A. C., & Meyer, E. (1994). Neural mechanisms underlying melodic perception and memory for pitch. The Journal of Neuroscience, 14(4), 1908-1919.

Zhang, Z., & Oppenheimer, S. M. (1997). Characterization, distribution and lateralization of baroreceptor-related neurons in the rat insular cortex. Brain research, 760(1), 243-250.

Zhou, Y. D., & Fuster, J. M. (1996). Mnemonic neuronal activity in somatosensory cortex. Proceedings of the National Academy of Sciences, 93(19), 10533-10537.

Zhou, Y. D., & Fuster, J. M. (2000). Visuo-tactile cross-modal associations in cortical somatosensory cells. Proceedings of the National Academy of Sciences, 97(17), 9777-9782.

Zhou, Y. D., Ardestani, A., & Fuster, J. M. (2007). Distributed and associative working memory. Cerebral Cortex, 17(suppl 1), i77-i87.

Zoccolan, D., Oertelt, N., DiCarlo, J. J., & Cox, D. D. (2009). A rodent model for the study of invariant visual object recognition. Proceedings of the National Academy of Sciences, 106(21), 8748-8753.

Appendix 2. Behavioral Paper (PNAS)

"Tactile perception and working memory in rats and humans"

Fassihi, A., Akrami, A., Esmaeili, V., & Diamond, M. E.

Proceedings of the National Academy of Sciences, (2014), 111(6), 2331-2336.

Tactile perception and working memory in rats and humans

Arash Fassihi[1], Athena Akrami[1,2], Vahid Esmaeili, and Mathew E. Diamond[3]

Tactile Perception and Learning Laboratory, International School for Advanced Studies (SISSA), 34136 Trieste, Italy

Edited* by Ranulfo Romo, Universidad Nacional Autonóma de México, Mexico D.F., Mexico, and approved December 5, 2013 (received for review August 9, 2013)

Primates can store sensory stimulus parameters in working memory for subsequent manipulation, but until now, there has been no demonstration of this capacity in rodents. Here we report tactile working memory in rats. Each stimulus is a vibration, generated as a series of velocity values sampled from a normal distribution. To perform the task, the rat positions its whiskers to receive two such stimuli, "base" and "comparison," separated by a variable delay. It then judges which stimulus had greater velocity SD. In analogous experiments, humans compare two vibratory stimuli on the fingertip. We demonstrate that the ability of rats to hold base stimulus information (for up to 8 s) and their acuity in assessing stimulus differences overlap the performance demonstrated by humans. This experiment highlights the ability of rats to perceive the statistical structure of vibrations and reveals their previously unknown capacity to store sensory information in working memory.

psychophysics | somatosensory | decision making | delayed comparison | vibrissa

Advances in understanding the neuronal mechanisms of cognition often occur when investigators examine in simpler mammals a behavioral capacity known to be part of the primate repertoire. An example is the perception of space, where the inquiry into the fundamental neuronal mechanisms in rats (1–4) has informed research in humans (5, 6).

Working memory (WM), the storage and manipulation of information across a limited time interval, has been explored in humans and monkeys in many experimental paradigms (7). However, "remarkably, given its central importance in human life, there has been very little comparative investigation of WM abilities across species" (ref. 8, p. 10371). In rats, WM has been examined in the framework of match- or nonmatch-to-sample tasks that involve the comparison of stimuli that differ by their quality and identity (9, 10); WM has also been examined in navigation tasks that involve the storage of multimodal sensory inputs (e.g., combined visual cues and path integration) (11, 12).

In contrast, the experiment reported here is a delayed comparison between stimuli that reside within a single, defined sensory domain and differ only by the value of one parameter, the velocity SD of the vibration. Rats compare two vibrations delivered sequentially to their whiskers, whereas humans compare two vibrations on the fingertip. This task requires several operations: (*i*) encoding the first stimulus and extracting the relevant parameter; (*ii*) storing the parameter value in memory; (*iii*) encoding the second stimulus and extracting the relevant parameter; (*iv*) comparing the second parameter value to the memory of the first; and (*v*) from the outcome of the comparison, applying the decision rule. The task was designed to open the way to the study of how neuronal circuits in the rat encode and store stimulus parameters.

Results

Experimental Design. The main chamber of the behavioral apparatus (Fig. 1) was a Plexiglas compartment. The rat received whisker stimulation by extending its head from the main chamber into the stimulus delivery port.

Stimuli were irregular "noisy" vibrations, consisting of changes in the plate position in the rostral/caudal direction. The sequence of velocity values was taken from a normal distribution with 0 mean, and SD denoted by σ. Velocity distributions and time series for two example stimuli are illustrated in Fig. 2*A*.

Fig. 2*B* shows the task structure. When the rat positioned its snout in the nose poke, the trial began with the prestimulus delay. At the conclusion of the delay, the base stimulus was presented, characterized by σ_{base}. After the interstimulus delay, the comparison stimulus was presented, characterized by $\sigma_{comparison}$. The rat had to remain in the nose poke for the entire trial, including the poststimulus delay. When the "go" cue sounded, the rat withdrew and selected the left or right spout according to the relative values of $\sigma_{comparison}$ and σ_{base}. An advantage of the delayed comparison paradigm is that it allows a more accurate estimate of acuity. Thresholds in discriminating stimulus difference are lower in tasks where subjects compare two sequential stimuli than in tasks where they compare single stimuli to reference memory (13, 14).

As for any discrimination task, difficulty increased as the stimulus difference decreased. Difficulty depended on the difference between σ_{base} and $\sigma_{comparison}$, quantified by the SD index (SDI):

$$SDI = \frac{\sigma_{comparison} - \sigma_{base}}{\sigma_{base} + \sigma_{comparison}}. \quad [1]$$

On a typical trial, a well-trained rat (Fig. 2*C*) placed its snout in the stimulus delivery port to initiate the trial and receive stimuli

Significance

Many higher cognitive functions involve working memory (WM), the storage and manipulation of information across limited time intervals. Comparing the WM capacity of different species is a key step toward understanding the underlying brain mechanisms. This study uncovers previously unknown sensory WM abilities in rats. They received two vibratory stimuli on their whiskers, separated by a variable delay, and had to compare vibration features. In analogous experiments, human subjects compared two stimuli applied to the fingertip. The acuity shown by rats in judging stimulus differences and their WM proficiency (across delays of 8 s, the longest tested) overlapped those of humans. Sensory WM now joins other cognitive functions within the rodent repertoire, setting the stage for exploration of its neuronal coding.

Author contributions: A.F., A.A., and M.E.D. designed research; A.F. and A.A. performed research; A.F., A.A., V.E., and M.E.D. analyzed data; and A.F., A.A., and M.E.D. wrote the paper.

The authors declare no conflict of interest.

*This Direct Submission article had a prearranged editor.

[1]A.F. and A.A. contributed equally to this work.

[2]Present address: Department of Molecular Biology, Princeton University, Howard Hughes Medical Institute, Princeton, NJ 08544-1014.

[3]To whom correspondence should be addressed. E-mail: diamond@sissa.it.

This article contains supporting information online at www.pnas.org/lookup/suppl/doi:10.1073/pnas.1315171111/-/DCSupplemental.

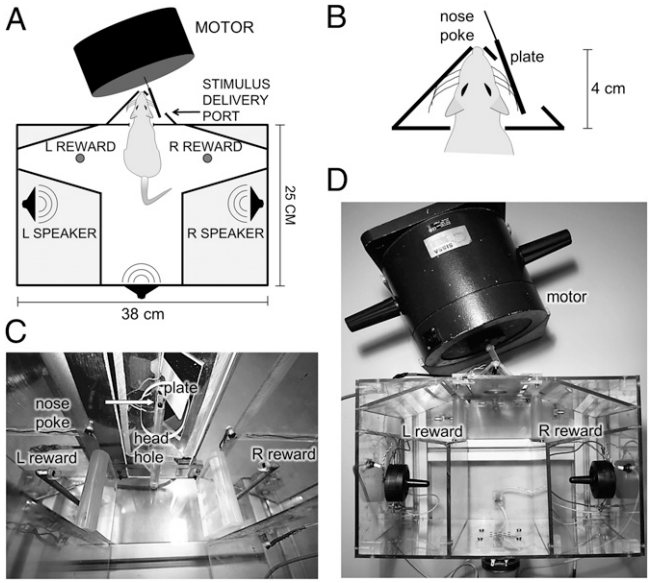

Fig. 1. Apparatus for rats. (*A*) Dark boundaries represent Plexiglas walls. The rat is sketched with snout extended into the stimulus delivery port. Left (L) and right (R) reward ports are indicated. (*B*) Magnified sketch of the stimulus delivery port. The rat extended through the head hole and placed its whiskers in contact with the plate. The plate's surface is approximately vertical and is seen as a line segment from above. (*C*) Photograph from within the apparatus. Reward spouts are visible laterally. In front, the head hole opens to the stimulus delivery port, which houses the vibrator plate. Arrow points to nose poke hole. (*D*) Photograph of the apparatus from above. The configuration mirrors the sketch in *A*.

(Fig. 2*C*, *Left*, and Movie S1); it withdrew from the nose poke after the go cue (Fig. 2*C*, *Center*) and turned to one of the two reward ports (Fig. 2*C*, *Right*). Fig. S1 confirms that rats remained in the nose poke to attend to both stimuli and the go cue, excluding the possibility that they adhered to some stereotyped timing routine (15). In well-trained rats, the self-generated motion known as "whisking" was suppressed throughout the trial (Movie S2), indicating that the sensorimotor system entered a "receptive sensing" mode of operation (16, 17).

Experiments with human subjects (Fig. 2*D*) used corresponding stimuli delivered to the index finger (see *SI Text* for details).

Stimulus Generalization Matrix. The first result involves training rats to generalize the comparison rule across the entire stimulus dimension (see *SI Text* and Table S1 for details). If the base stimulus were fixed across all trials and only the comparison stimulus shifted, the rat might solve the task by ignoring the base stimulus and applying a constant threshold to the comparison stimulus. Likewise, if the comparison stimulus were fixed across all trials, the rat might simply apply a constant threshold to the base stimulus. To avoid such shortcut strategies, we used the stimulus generalization matrix (SGM). The SGM, adapted from Romo and coworkers (13, 18), consisted of stimuli spanning a wide range of σ values (Fig. 3). Neither the base stimulus nor the comparison stimulus, taken alone, contained sufficient information to solve the task, so the rat was required to execute a direct comparison between the two stimuli on every trial. Fig. S2 shows that during training, rats learned to weigh both stimuli.

In the final stage of training (*SI Text*), rats proceeded to an SGM with 10–14 [σ_{base}, $\sigma_{comparison}$] stimulus pairs (Fig. 3*A*, *Left*). The σ values were evenly distributed in a logarithmic scale. The diagonal line represents $\sigma_{base} = \sigma_{comparison}$; all stimulus pairs on one side of the diagonal were associated with the same action.

When rats showed stable performance across sessions, they were assigned to (*i*) a protocol to test tactile working memory proficiency or (*ii*) a protocol to measure acuity in judging σ differences. The working memory protocol (Fig. 3*A*, *Right*) involved a fixed SDI (absolute value of 0.35) with systematic modulation of the delay between base and comparison stimuli. The values of delay were taken from the set 0.2, 2, 4, 6, and 8 s;

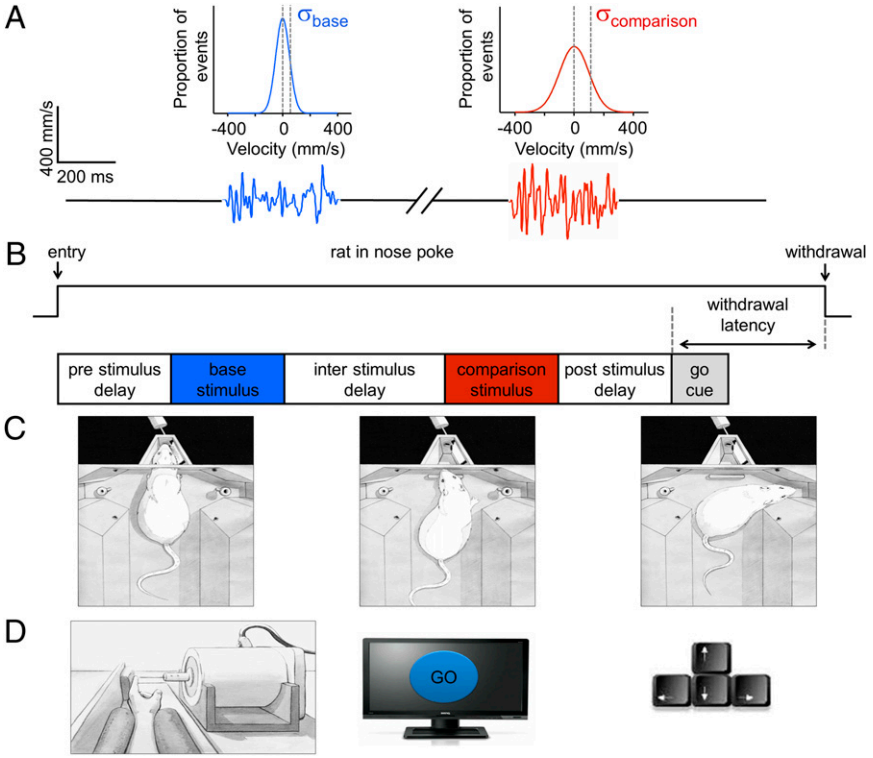

Fig. 2. Structure of a single trial. (*A*) Stimuli were composed of a series of velocity values where the sampling probability of a given velocity value was given by a normal distribution with mean = 0 and SD = σ. Example base and comparison stimuli are illustrated, resulting from the sampling of the distribution shown above each stimulus, with σ = 55 mm/s (blue) and σ = 110 mm/s (red) and duration 400 ms. (*B*) Upper trace indicates at far left the time of entry of the rat in the nose poke and at far right the time of withdrawal. Below, key events of the trial are given. Withdrawal latency was measured as elapsed time between the onset of the go cue and withdrawal from the nose poke. (*C*) Sketches depicting one trial. (*Left*) The rat places its snout in the stimulus delivery port to initiate the trial and receive stimuli. (*Center*) Upon hearing the go cue, the rat withdraws. (*Right*) The rat selects the right reward port. (*D*) Human participants performed the same discrimination task as rats, holding their fingertip in contact with the tip of a rod attached to the motor (*Left*). After the base and comparison stimuli were delivered, a go cue appeared on the monitor (*Center*), and the subject responded by pressing left or right arrow keys on a standard keyboard (*Right*).

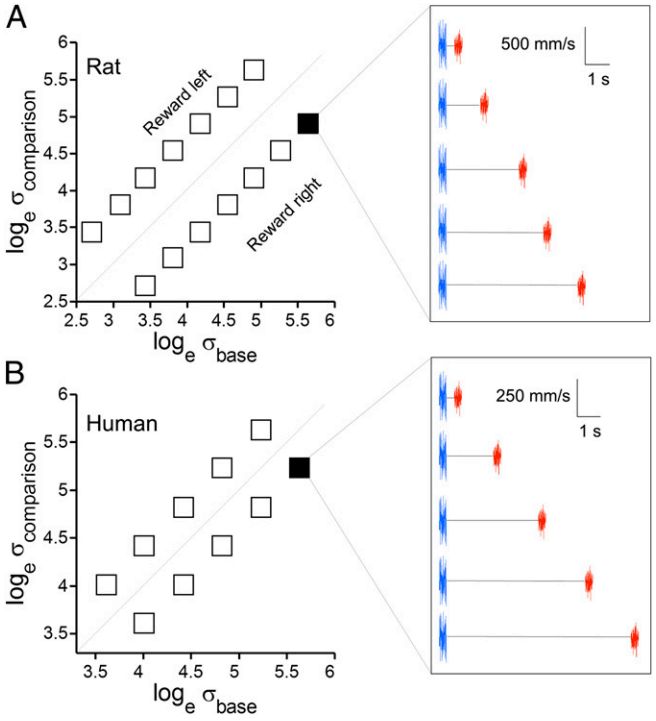

Fig. 3. Stimulus generalization matrix. (*A*) Stimulus set for rats. The [σ_{base}, $\sigma_{comparison}$] pair for each trial was selected randomly from among those represented by the boxes. Base stimulus values are distributed along the abscissa, and comparison stimulus values are distributed along the ordinate; note logarithmic scales. Diagonal line separates $\sigma_{comparison} > \sigma_{base}$ (reward left) from $\sigma_{comparison} < \sigma_{base}$ (reward right) stimulus pairs. (*Right*) For one stimulus pair, varying interstimulus delay intervals are illustrated. (*B*) Stimulus set for humans. As in *A*, for one stimulus pair, varying interstimulus delay intervals are illustrated.

trials with different delays were randomly interleaved. For humans, the SGM and working memory protocol are illustrated in Fig. 3*B*. Typically, the SGM included 10 stimulus pairs and SDI of 0.25. Delays were 0.5, 3, 6, 9, and 12 s, randomly interleaved.

Performance. Four rats participated in the working memory protocol. Fig. 4*A* shows mean performance for each stimulus pair, averaged across rats and across delay durations. Performance was good for all pairs except [2.8, 3.4]; a potential explanation is given in *Discussion*.

Fig. 4*B* illustrates the same data but now sorted by the interstimulus delay, with all stimulus pairs merged. Rats achieved just above 70% correct and did not present any decrement with interstimulus delay up to 8 s. Data from 19 human subjects, under analogous experimental conditions, are shown in Figs. 4 *C* and *D*. It is possible that faced with more difficult stimulus comparisons, both rats and humans would show a performance decrease in relation to the duration of the delay interval, as found in other tasks (19).

The sensory acuity protocol entailed the fine-grain modulation of trial difficulty within a session. In one group of stimulus pairs, σ_{base} was fixed, whereas $\sigma_{comparison}$ varied, yielding a graded set of SDI values. In a second group, $\sigma_{comparison}$ was fixed, whereas σ_{base} varied, yielding another graded set of SDI values. Both stimuli had a duration of 400 ms; interstimulus interval was 800 ms. To ensure that subjects did not shift to a strategy of merely applying a threshold to the base or comparison stimulus, at least 30% of trials adhered to the SGM stimulus set. Rats and humans performed well on SGM trials, implying that they solved the trials in the acuity test using the intended stimulus comparison strategy.

Seven rats participated in the tactile acuity protocol. On the fixed σ_{base} stimulus set (Fig. 5*A*, vertically arranged stimulus pairs) they performed well, showing accuracy close to or above 70% when the SDI absolute value was equal to or greater than 0.1. On the fixed $\sigma_{comparison}$ stimulus set (Fig. 5*A*, horizontally arranged stimulus pairs), performance was slightly lower. Data from 29 human subjects are shown in Fig. 5*B*. Like the rats, the humans performed worse on the variable-base stimulus set, a stimulus configuration known to be more difficult in monkeys as well (20).

To quantify the effect of comparison difficulty on accuracy, for the vertically arranged stimulus pairs of Fig. 5 *A* and *B* we computed the percent of trials, averaged across sessions, in which each subject judged $\sigma_{comparison} > \sigma_{base}$ as a function of SDI. We fit the resulting data with a four-parameter logistic function (*SI Text*) to generate psychometric curves. If performance were perfect, subjects would report $\sigma_{comparison} > \sigma_{base}$ on 0% of trials with negative SDI and on 100% of trials with positive SDI; this would give rise to a step function, going from 0% to 100% at SDI = 0. Because performance is never perfect, psychometric curves assume a sigmoid (S-shape) function. Fig. 5*C* shows the psychometric curves for seven rats (gray traces) and their average (orange). Fig. 5*D* shows psychometric curves for 29 humans (average in green). Humans on average exhibited a steeper psychometric function and lower error rates on easy stimulus comparisons.

To directly compare rats and humans, for each subject's curve we calculated the maximum slope (*SI Text*); we also calculated the subject's accuracy over all pairs. Fig. 5*E* illustrates both values together as a scatter plot. The two performance measures are correlated, as expected. Although the average performance (circled points) of humans is better than that of rats, there is

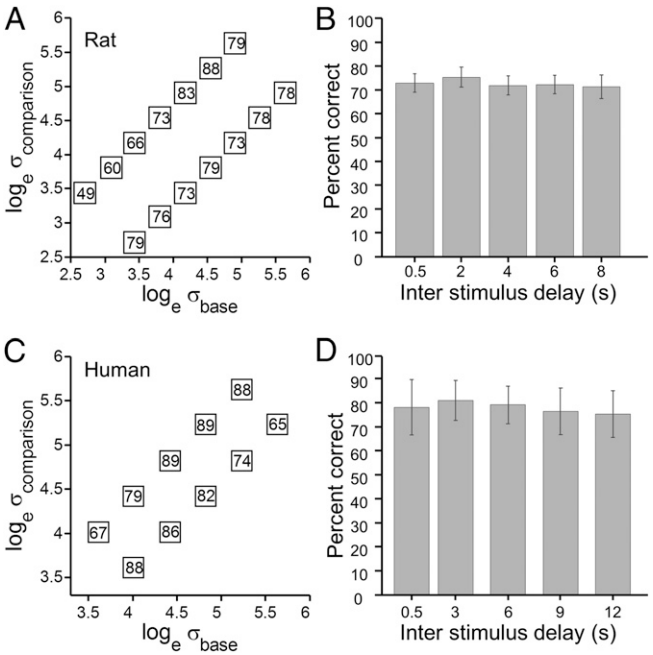

Fig. 4. Working memory performance. (*A*) For rats, stimuli had duration of 400 ms, and SDI was held constant at 0.35; interstimulus delay varied randomly from 0.5 s to 8 s. Data from four rats are separated by [σ_{base}, $\sigma_{comparison}$] pair but averaged across rats and over different delay durations. (*B*) Performance, averaged across rats and across all stimuli, as a function of delay duration. (*C*) For humans, stimuli had duration of 400 ms, and SDI was held constant at 0.25; the interstimulus delay varied randomly from 0.5 s to 12 s. Data from 19 subjects are shown. (*D*) Performance, averaged across subjects and across all stimuli, as a function of delay duration.

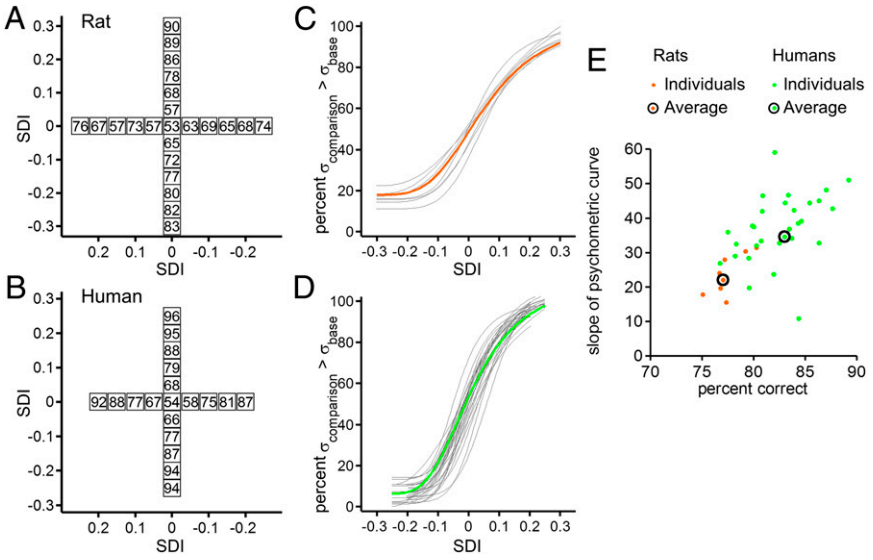

Fig. 5. Tactile acuity. (*A*) Data averaged across seven rats. To generate the vertical set of stimulus pairs, σ_{base} was fixed (80 mm/s), whereas $\sigma_{comparison}$ varied in small steps. To generate the horizontal set of stimulus pairs, σ_{base} varied in small steps, whereas $\sigma_{comparison}$ was fixed (80 mm/s). Both stimulus sets were embedded within the full SGM. (*B*) Analogous data from 29 humans. (*C*) Individual psychometric curves for seven rats; orange trace is the average. (*D*) Individual psychometric curves for 29 humans; green trace is the average. (*E*) Two measures of performance are plotted for individual rats (orange) and humans (green). Average values are indicated by black circles.

overlap between the rat cloud and the human cloud. We conclude that although a typical human is better than a typical rat, nevertheless, a well-performing rat is better than a poorly performing human and approaches the average human performance.

Statistical Evidence for Delayed Comparison. The final step in demonstrating sensory working memory in rats is to prove that they attended to and stored the base stimulus. To do so, we applied statistical tests to assess to what extent their choices depended on the value of σ_{base}. We computed the percent of trials judged as $\sigma_{comparison} > \sigma_{base}$ for each value of $\sigma_{comparison}$. Each value of $\sigma_{comparison}$ could be preceded by one of two values of σ_{base}. The results, averaged across rats, are given in the boxes in Fig. 6*A*. If the values in the paired boxes along a gray iso-$\sigma_{comparison}$ band were equal, we would conclude that choice was unaffected by the value of σ_{base}. Instead, the large differences (right side of the gray bands) indicate that choices depended on σ_{base}.

By a resampling procedure, we obtained Z-scores to estimate whether the apparent dependence of rats' choices on σ_{base} could be explained by chance (*SI Text*). In Fig. 6*A*, *Right*, the Z-scores of individual rats are shown as black points; they commonly exceeded 10 SDs, where a value of 2 may be considered significant. Fig. 6*B* reports the same analysis carried out on data from humans.

We set up statistical tests using the algorithm described above to prove that rats and humans attended not only to the base stimulus but also to the comparison stimulus. Results are given in *SI Text* and Fig. S3.

To summarize, Fig. 6 demonstrates that rats and humans encoded the base stimulus and therefore executed the task as a true delayed comparison. One apparent species difference is that Z-scores were more dispersed in the rats, suggesting more pronounced individual differences.

Discussion

Although there can be no doubt that rodents store short-term memories, it was unclear before now what form of information they could hold in working memory. Rodents express spatial working memory, but navigation tasks do not constrain the modality or entity of stored information; choices could even be held in memory through body posture and other nonneuronal mechanisms (8, 21). Can rodents perform parametric working memory; that is, can they store a stimulus not according to its identity or quality (22) but only by its position along the scale of a single sensory dimension? One earlier study showed that rats could compare two sequential odorant mixtures (23). However, because shifts in the proportion of odorants in a mixture lead to qualitatively different odor percepts (24), it is not clear that the odor mixtures are sensed as steps in a single parameter or else as discrete percepts.

Delayed comparison tasks have been an effective means for studying working memory for over 30 y (25). The present report demonstrates that the performance of rats in a tactile delayed comparison task resembles, to a first approximation, that of humans (Fig. 5). Our study is notable for its parallels to studies of tactile delayed comparison in monkeys by Romo and Salinas (26). In common with our task, the monkey receives two vibrations separated by a variable delay; it then makes a choice according to the difference between the vibrations (26, 27). There are several distinctions in experimental design. In our task, rather than applying stimuli to the fingertip, we selected the whisker sensory system due to its behavioral importance in rats (16, 17, 28–34). Another distinction is the structure of the vibration. Although the studies in monkeys typically use regular, periodic skin deflections in the form of either a sinusoid or a pulse train (35), we opted for a stochastic stimulus composed of filtered noise (36). The choice was motivated by several factors. First, in pilot studies, rats attended to noisy stimuli better than to periodic stimuli and were more likely await the go cue before withdrawing. Second, noisy vibrissal stimuli evoke a more robust cortical response (37, 38), an advantage for future neurophysiological studies. Third, the structure of the noise stimulus is well suited to reverse correlation methods (39) and will provide rich data for studying the kinematic features extracted by sensory neurons (40, 41).

We implemented unique strategies to uncover rats' perceptual capacities. We trained them to remain immobile in the nose poke for variable times, as short as 100 ms and as long as 5 s (stage 3 of training; *SI Text*). At this point, we were able to introduce two whisker stimuli on each trial with the rat constrained to receive both stimuli (stage 4). We could then allow the rat to discover the rule that related the tactile stimuli to the reward location (stages 4 and 5). Moreover, with the rat immobile for extended periods, we could vary the interstimulus delay duration to study working memory proficiency (stages 6 and 7).

In addition, we introduced the SGM (Fig. 3) to ensure that subjects attended to both the base and comparison stimuli. Neither stimulus, taken alone, contained sufficient information to solve the task. Thus, the simpler strategy of ignoring one stimulus and attending to the other would lead to performance close to chance (13).

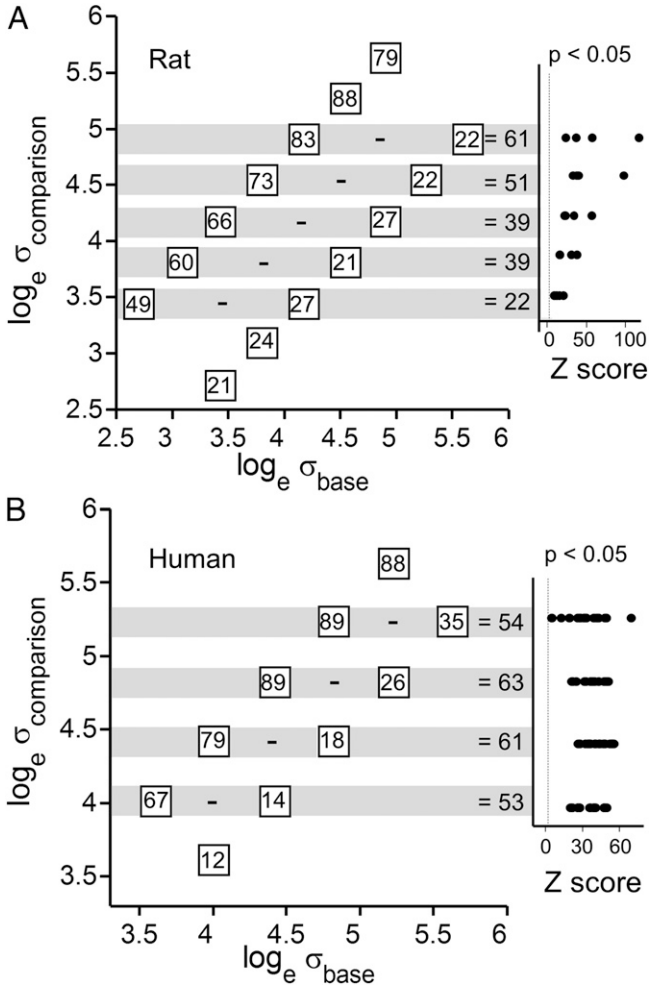

Fig. 6. Statistical analysis of effect of σ_{base}. (*A*) Values in the boxes give the percent of trials in which rats, on average, judged $\sigma_{comparison} > \sigma_{base}$. The difference between paired boxes in a gray band represents the dependence of choice on whether $\sigma_{comparison}$ was preceded by smaller or larger σ_{base}. (*Right*) The statistical significance (see *Statistical Evidence for Delayed Comparison*) of the choice for all single rats is given as a Z-score. (*B*) Same analysis carried out on data from humans.

Performance in rats faltered for the stimulus pairs [2.8, 3.4] and [3.2, 3.8], where σ_{base} assumed low values (Fig. 4*A*). Poor performance might be explained by "contraction bias," which posits that during the interstimulus delay, the neuronal representation of σ_{base} drifts toward the expected value, or "prior," of all base stimuli presented in recent history (42, 43).[†] By this account, on low-σ_{base} trials, the representation of σ_{base} shifted in the upward direction, toward the mean σ_{base} of the complete SGM. As a consequence, $\sigma_{comparison}$, whose value was greater than that of σ_{base}, was matched against a memory of σ_{base} that had grown during the delay. The outcome was a reduction in likelihood that $\sigma_{comparison}$ was correctly judged to be greater than σ_{base}.

For human subjects (Fig. 4*C*), performance also was poor (67% correct) for the stimulus pair where σ_{base} assumed its lowest value. This finding of contraction bias suggests that there may be shared mechanisms for working memory across rats and humans. However, one species difference emerged: human subjects—but not rats—showed a contraction bias (65%) for the stimulus pair with highest σ_{base} value, [5.6, 5.2]. At present, we have no explanation for the symmetric high/low contraction bias in humans versus the asymmetric bias in rats.

Until a few years ago, many neuroscientists attributed a wide range of perceptual functions to primates but not to rodents. The capacities of rats might have been overlooked because training regimes were not effectively adapted to their natural deportment. With improving behavioral methodologies, rodents have been found to express surprising abilities. For instance, rats spontaneously recognize views of an object that differ by angle, size, and position (44, 45); such generalization is a hallmark of true visual perception and was once believed to belong only to primates. With regard to more abstract computations, rodents weigh sensory evidence (46), assess reward statistics (47), integrate multimodal sensory inputs (48), accumulate evidence for optimal decision-making (49), express certainty in the outcome of their choices (50), and even generalize rules (51). In sum, mice and rats are becoming increasingly important for the study of perception (52). From the present effort, parametric working memory joins other cognitive functions within the repertoire of rodent capacities. In humans and primates, parametric working memory has been associated with a network of prefrontal and parietal cortical regions (7, 18, 25, 53–55); the analogous networks have yet to be systematically explored in rodents.

Materials and Methods

Subjects. Eleven male Wistar rats (Harlan Laboratories) were housed individually or with one cage mate and kept on a 14/10 light/dark cycle. They were examined weekly by a veterinarian. At the start of the experiment they were 6–8 wk old and weighed 225–250 g; they gained weight steadily throughout the study. Protocols conformed to international norms and were approved by the Italian Health Ministry and the Ethics Committee of the International School for Advanced Studies.

Forty-four human subjects (16 males and 28 females, ages 22–35) were tested. Protocols conformed to international norms and were approved by the Ethics Committee of the International School for Advanced Studies. Subjects signed informed consent.

Materials and Instrumentation. The animal apparatus (Fig. 1) consisted of a Plexiglas compartment measuring 25 × 25 × 38 cm (height × width × length). In the front wall, a 3.8 cm (width) by 5 cm (height) head hole opened to the stimulus delivery port. Within the stimulus delivery port a 0.85-cm-diameter nose poke was centered in front; the nose poke contained an optic sensor illuminated by an infrared photo beam to detect the rat's snout. Above the nose poke, a blue LED was fixed. LED illumination signaled to the rat that the next trial may begin.

A shaker motor (type 4808; Bruel and Kjaer), with 12.7 mm peak-to-peak displacement, was used to generate stimuli. The motor was placed on its flank to produce motion in the horizontal dimension (Fig. 1). A 20 × 30 mm plate was attached to the diaphragm of the shaker. Once trained, the rat received the stimulus by placing its whiskers on the plate. Double-sided adhesive was fixed to the plate to keep the whiskers in contact and thus to follow the motor's motion.

Both rat and human experiments were controlled using LabVIEW software (National Instruments).

Generation of Vibrations and Their Statistical Structure. We generated the velocity time series as follows. First, we constructed in LabVIEW a unitless normal distribution centered at 0 and sampled it 10,000 times per s; then, we applied a Butterworth filter with 150 Hz cutoff to yield low-pass filtered noise. This time series was amplified (type 2719; Bruel and Kjaer) and transmitted as voltage values to the motor. Thus, the velocity distribution delivered to the whiskers had SD proportional to the SD of the original unitless normal distribution. The velocity time series for a given trial was taken randomly from among 50 seeds.

Because the motor was constructed to keep acceleration constant across a frequency range from 5 Hz to 10 KHz, it follows that if peak-to-peak input voltage was held constant, displacement diminished as frequency increased. Due to this built-in displacement clamp, a theoretical derivation of motion was complex: motion must be assessed empirically. We tested the motor before installing it in the apparatus by fixing a position transducer (LD 310-25; OMEGA Engineering) to a rod extending from the diaphragm and then

[†]Akrami A, Fassihi A, Esmaeili V, Diamond ME (2013) Tactile working memory in rat and human: Prior competes with recent evidence. *Cosyne Abstracts 2013 Salt Lake City USA.*

executing the entire stimulus library while recording 1,000 frames per s video clips (Optronis CamRecord 450). We computed plate motion with a custom-made video tracking script in MATLAB (MathWorks) and used the tracked video to calibrate the transducer. Finally, we compared tracked videos of plate motion under the two conditions—position transducer attached and removed—and confirmed that the transducer did not measurably affect motion. At this point, we could install the motor in the behavioral apparatus with full knowledge of its output. The position transducer provided an online signal to check the operation of the motor. Descriptions of the stimulus are based on the true measured output of the motor.

The same stimuli used in rats were delivered to the subject's fingertip except that the range of velocity distribution width was limited to a maximum of 270 mm/s. Subjects viewed a computer monitor and wore headphones that presented acoustic noise and eliminated ambient sounds. They received feedback (correct/incorrect) on each trial through the monitor.

Exclusion of Nontactile Signals. Test sessions on rats were run under dim ambient or red light that did not allow visualization of the stimulator motion. No potential olfactory or gustatory cues about the vibrations were available. However, the motor generated acoustic signals (easily heard by humans), and precautions were taken to ensure that rats did not use such signals to judge the stimuli, as described in *SI Text* and Figs. S4 and S5.

ACKNOWLEDGMENTS. The authors thank Armin Lak for participation in pilot experiments, Fabrizio Manzino and Marco Gigante for technical contributions, and Francesca Pulecchi for animal care and training. Marco Gigante made the drawings in Fig. 2. This work was supported by the Human Frontier Science Program (Project RG0041/2009-C), European Research Council Advanced Grant Construction of Perception from Touch Signals (CONCEPT) (Project 294498), European Union Future and Emerging Technologies (FET) Grant Choreographing Neural Networks: Coupling Activity Dynamics Across Biomimetic Brain Interfaces with Neuromorphic VLSI (CORONET) (Project 269459), and the Compagnia San Paolo.

1. O'Keefe J, Dostrovsky J (1971) The hippocampus as a spatial map. Preliminary evidence from unit activity in the freely-moving rat. *Brain Res* 34(1):171–175.
2. Moser EI, Kropff E, Moser M-B (2008) Place cells, grid cells, and the brain's spatial representation system. *Annu Rev Neurosci* 31:69–89.
3. McNamara RK, Skelton RW (1993) The neuropharmacological and neurochemical basis of place learning in the Morris water maze. *Brain Res Brain Res Rev* 18(1):33–49.
4. Itskov PM, Vinnik E, Diamond ME (2011) Hippocampal representation of touch-guided behavior in rats: Persistent and independent traces of stimulus and reward location. *PLoS ONE* 6(1):e16462.
5. Burgess N, Maguire EA, O'Keefe J (2002) The human hippocampus and spatial and episodic memory. *Neuron* 35(4):625–641.
6. Doeller CF, Barry C, Burgess N (2010) Evidence for grid cells in a human memory network. *Nature* 463(7281):657–661.
7. Pasternak T, Greenlee MW (2005) Working memory in primate sensory systems. *Nat Rev Neurosci* 6(2):97–107.
8. Carruthers P (2013) Evolution of working memory. *Proc Natl Acad Sci USA* 110(Suppl 2): 10371–10378.
9. Grobe C, Spector A (2006) Rats can learn a "Delayed Match/Delayed Non-Match to Sample" task using only taste stimuli. *FASEB J* 20(4):A381 (abstr).
10. Peña T, Pitts RC, Galizio M (2006) Identity matching-to-sample with olfactory stimuli in rats. *J Exp Anal Behav* 85(2):203–221.
11. Jadhav SP, Kemere C, German PW, Frank LM (2012) Awake hippocampal sharp-wave ripples support spatial memory. *Science* 336(6087):1454–1458.
12. Morris RG (1984) Developments of a water maze procedure for studying spatial learning in the rat. *J Neurosci Methods* 11(1):47–60.
13. Hernández A, Salinas E, García R, Romo R (1997) Discrimination in the sense of flutter: New psychophysical measurements in monkeys. *J Neurosci* 17(16):6391–6400.
14. Nahum M, Daikhin L, Lubin Y, Cohen Y, Ahissar M (2010) From comparison to classification: A cortical tool for boosting perception. *J Neurosci* 30(3):1128–1136.
15. Ölveczky BP (2011) Motoring ahead with rodents. *Curr Opin Neurobiol* 21(4):571–578.
16. Diamond ME, Arabzadeh E (2013) Whisker sensory system - from receptor to decision. *Prog Neurobiol* 103:28–40.
17. Prescott TJ, Diamond ME, Wing AM (2011) Active touch sensing. *Philos Trans R Soc Lond B Biol Sci* 366(1581):2989–2995.
18. Romo R, Brody CD, Hernández A, Lemus L (1999) Neuronal correlates of parametric working memory in the prefrontal cortex. *Nature* 399(6735):470–473.
19. Müller U, von Cramon DY, Pollmann S (1998) D1- versus D2-receptor modulation of visuospatial working memory in humans. *J Neurosci* 18(7):2720–2728.
20. Hernández A, et al. (2010) Decoding a perceptual decision process across cortex. *Neuron* 66(2):300–314.
21. Dudchenko PA (2004) An overview of the tasks used to test working memory in rodents. *Neurosci Biobehav Rev* 28(7):699–709.
22. Ennaceur A (2010) One-trial object recognition in rats and mice: Methodological and theoretical issues. *Behav Brain Res* 215(2):244–254.
23. Perry C, Felsen G (2012) Rats can make relative perceptual judgments about sequential stimuli. *Anim Cogn* 15(4):473–481.
24. Barkat S, Le Berre E, Coureaud G, Sicard G, Thomas-Danguin T (2012) Perceptual blending in odor mixtures depends on the nature of odorants and human olfactory expertise. *Chem Senses* 37(2):159–166.
25. Kojima S, Goldman-Rakic PS (1982) Delay-related activity of prefrontal neurons in rhesus monkeys performing delayed response. *Brain Res* 248(1):43–49.
26. Romo R, Salinas E (2003) Flutter discrimination: Neural codes, perception, memory and decision making. *Nat Rev Neurosci* 4(3):203–218.
27. Mountcastle VB, Steinmetz MA, Romo R (1990) Frequency discrimination in the sense of flutter: Psychophysical measurements correlated with postcentral events in behaving monkeys. *J Neurosci* 10(9):3032–3044.
28. Diamond ME, von Heimendahl M, Knutsen PM, Kleinfeld D, Ahissar E (2008) 'Where' and 'what' in the whisker sensorimotor system. *Nat Rev Neurosci* 9(8):601–612.
29. Diamond ME (2010) Texture sensation through the fingertips and the whiskers. *Curr Opin Neurobiol* 20(3):319–327.
30. Diamond ME, von Heimendahl M, Arabzadeh E (2008) Whisker-mediated texture discrimination. *PLoS Biol* 6(8):e220.
31. Brecht M (2007) Barrel cortex and whisker-mediated behaviors. *Curr Opin Neurobiol* 17(4):408–416.
32. Petersen CC (2007) The functional organization of the barrel cortex. *Neuron* 56(2): 339–355.
33. Adibi M, Arabzadeh E (2011) A comparison of neuronal and behavioral detection and discrimination performances in rat whisker system. *J Neurophysiol* 105(1):356–365.
34. Harris JA, Petersen RS, Diamond ME (1999) Distribution of tactile learning and its neural basis. *Proc Natl Acad Sci USA* 96(13):7587–7591.
35. Hernández A, Zainos A, Romo R (2000) Neuronal correlates of sensory discrimination in the somatosensory cortex. *Proc Natl Acad Sci USA* 97(11):6191–6196.
36. Maravall M, Petersen RS, Fairhall AL, Arabzadeh E, Diamond ME (2007) Shifts in coding properties and maintenance of information transmission during adaptation in barrel cortex. *PLoS Biol* 5(2):e19.
37. Lak A, Arabzadeh E, Diamond ME (2008) Enhanced response of neurons in rat somatosensory cortex to stimuli containing temporal noise. *Cereb Cortex* 18(5): 1085–1093.
38. Lak A, Arabzadeh E, Harris JA, Diamond ME (2010) Correlated physiological and perceptual effects of noise in a tactile stimulus. *Proc Natl Acad Sci USA* 107(17): 7981–7986.
39. Ringach D, Shapley R (2004) Reverse correlation in neurophysiology. *Cogn Sci* 28(2): 147–166.
40. Arabzadeh E, Panzeri S, Diamond ME (2004) Whisker vibration information carried by rat barrel cortex neurons. *J Neurosci* 24(26):6011–6020.
41. Lottem E, Azouz R (2011) A unifying framework underlying mechanotransduction in the somatosensory system. *J Neurosci* 31(23):8520–8532.
42. Ashourian P, Loewenstein Y (2011) Bayesian inference underlies the contraction bias in delayed comparison tasks. *PLoS ONE* 6(5):e19551.
43. Hollingworth HL (1910) The central tendency of judgment. *The Journal of Philosophy. J Philos Psychol Sci Methods* 7(17):461–469.
44. Tafazoli S, Di Filippo A, Zoccolan D (2012) Transformation-tolerant object recognition in rats revealed by visual priming. *J Neurosci* 32(1):21–34.
45. Zoccolan D, Oertelt N, DiCarlo JJ, Cox DD (2009) A rodent model for the study of invariant visual object recognition. *Proc Natl Acad Sci USA* 106(21):8748–8753.
46. Kepecs A, Uchida N, Zariwala HA, Mainen ZF (2008) Neural correlates, computation and behavioural impact of decision confidence. *Nature* 455(7210):227–231.
47. Karlsson MP, Tervo DG, Karpova AY (2012) Network resets in medial prefrontal cortex mark the onset of behavioral uncertainty. *Science* 338(6103):135–139.
48. Raposo D, Sheppard JP, Schrater PR, Churchland AK (2012) Multisensory decision-making in rats and humans. *J Neurosci* 32(11):3726–3735.
49. Brunton BW, Botvinick MM, Brody CD (2013) Rats and humans can optimally accumulate evidence for decision-making. *Science* 340(6128):95–98.
50. Lavan D, McDonald JS, Westbrook RF, Arabzadeh E (2011) Behavioural correlate of choice confidence in a discrete trial paradigm. *PLoS ONE* 6(10):e26863.
51. Murphy RA, Mondragón E, Murphy VA (2008) Rule learning by rats. *Science* 319(5871):1849–1851.
52. Carandini M, Churchland AK (2013) Probing perceptual decisions in rodents. *Nat Neurosci* 16(7):824–831.
53. Smith EE, Jonides J (1999) Storage and executive processes in the frontal lobes. *Science* 283(5408):1657–1661.
54. Miller EK, Cohen JD (2001) An integrative theory of prefrontal cortex function. *Annu Rev Neurosci* 24(1):167–202.
55. McNab F, Klingberg T (2008) Prefrontal cortex and basal ganglia control access to working memory. *Nat Neurosci* 11(1):103–107.

Supporting Information

Fassihi et al. 10.1073/pnas.1315171111

This section provides details concerning the apparatus, the training protocol, and the monitoring of animal performance.

Apparatus for Rats

The main chamber of the apparatus (Fig. 1) was illuminated by dark red LEDs and by ambient lighting whose intensity could be modulated according to the stage of training. Two video systems monitored the rat's actions. First, mounted 40 cm above the apparatus floor, a webcam (HD Webcam C310; Logitech) collected images of the entire apparatus at 30 frames per s. Second, mounted above the stimulus delivery port, a high-speed video camera (CamRecord 450; Optronis) equipped with a macro zoom (LMZ45T3 18–108 mm lens; Kowa Company) collected images of the snout, whiskers, and stimulus plate at 500 frames per s.

The chamber contained left and right reward spouts mounted on 8-cm–high pedestals. Each spout housed a custom-made infrared LED-based contact sensor. An AVR32 board (National Instruments) acquired all sensor signals and controlled the liquid syringe pump (NE-500 programmable OEM; New Era Pump Systems) for reward delivery. Three audio speakers were positioned just outside the walls of the apparatus. The central one, located at the back of the apparatus, delivered the go cue. The two lateral speakers were positioned near the two reward spouts to present a "reward delivery cue" as a reinforcer of the release of juice.

Exclusion of Nontactile Signals

We took numerous steps to be certain that rats used tactile rather than acoustic signals to judge the stimuli. We recorded sounds (LAN-XI type 3052; Bruel and Kjaer) during playback of the complete vibration library and examined the frequency spectrum (Fig. S4). The highest acoustic frequencies generated by the motor were below 500 Hz so that albino rats, which possess the higher-frequency hearing characteristic of mammals (1–3), would be expected to be insensitive to such sounds.

As a further test, in numerous sessions with well-trained rats we detached the motor from the plate assembly. Auditory cues remained but with no accompanying whisker motion; the performance of rats dropped to the chance level (Fig. S5). As a final control, we left the motor attached to the plate but removed the adhesive surface from the plate so that the whiskers slipped along it and no longer followed the motor. Again, auditory cues remained but with reduced whisker motion, and performance dropped to about 60%. The behavioral tests were limited to strings of about 10–20 trials because the absence of whisker stimulation might confuse the rats. In no case did we clip off the whiskers as a test because this would lead to general disorientation and would not be a specific test of whisker use in the task.

Apparatus for Humans

Human subjects viewed a computer monitor and wore headphones that presented acoustic noise and eliminated ambient sounds. They rested their left arm on a firm cushion and placed the left index finger in contact with the tip of a probe driven by a motor (Fig. 2*D*). To start a trial, the subject pressed the keyboard up arrow with the right hand. This triggered presentation of the base and comparison stimuli. After a poststimulus delay, a blue panel illuminated on the monitor, and the subject pressed the left or right arrow on the keyboard, signifying selection of the base or comparison stimulus, respectively.

In pilot experiments the stimulus scale used for rats was perceived by humans as intense; this is because stimulus energy was delivered directly to the skin at a normal angle (unlike the case in rats where stimuli were tangential to the skin surface and the interposed whisker shaft absorbed much energy). For this reason, we imposed an upper bound of SD equal to 270 mm/s.

Training of Rats

Good performance of the working memory and acuity task was the outcome of a seven-stage training routine. Typical duration of training was 2–3 mo but varied according to the experiment's intended data set and individual differences in rate of learning.

Stage 1: Handling. For half an hour each day, the investigator held and petted the rat and fed it by hand. This stage lasted for 10 d. After every session of handling and, later, after training sessions in the apparatus, the subject was placed in a large enriched play arena (Imac, Tezze di Arzignano, Italy) with other rats. From this stage onward, a water restriction schedule was implemented, whereby the rat collected rewards in the apparatus and was given ad libitum access to water for 1 h after each session.

Stage 2: Training to Nose Poke and to Collect Rewards. The goal of stage 2 was for the rat to explore the apparatus and to learn that three zones were crucial to obtaining rewards: the nose poke in the stimulus delivery port and the left and right spouts (Fig. 1). Specifically, the aim was to teach the rat a simple sequence of actions and events: (*i*) position snout in nose poke, (*ii*) attend the go cue, and (*iii*) withdraw and move toward the baited reward spout.

The arena was provided with visible ambient lighting. To start the first session, the rat was placed in the apparatus and allowed about 1/2 h of free exploration. Both spouts released a reward (pear juice diluted in water 1:3) whenever the rat licked them. Simultaneously with the reward, a speaker placed just outside the chamber emitted a train of five clicks.

Later in the first session, the investigator began to draw the rat into the nose poke in the stimulus delivery port by offering it, just external to the hole, a handheld dropper containing diluted juice. The whisker stimulation plate was present but immobile. The entry of the rat's snout into the nose poke was detected by an optic sensor; this event immediately triggered a 200-ms 5-KHz acoustic go cue. The go cue signaled the enabling of one reward spout. At the conclusion of the go cue, a click train was initiated at the speaker lateral to one of the reward spouts. Because this click train had the same pitch as the reward delivery cue and its purpose was to draw the rat toward the baited spout, we refer to it as the "reward target cue." Once triggered, the reward target cue remained active until the rat reached the designated spout. As the rat licked for a reward of 0.1 mL of diluted pear juice, the reward delivery cue was emitted. The rat quickly learned to place its snout in the nose poke to trigger the go cue and the reward target cue; at this point it was no longer necessary for the investigator to manually guide it with the dropper.

A blue LED positioned within the stimulus delivery port served as an additional cue to draw the rat's attention to the nose poke and then to give the rat feedback on correct positioning. In this and all successive stages, the LED was illuminated until the rat entered the nose poke and was turned off when the rat interrupted the nose poke LED sensor. As soon as the rat collected the reward, the LED was again illuminated, signaling that the rat may return to the nose poke to start the next trial.

Stage 2 lasted for two to three sessions and was terminated when the rat showed at least 100 repetitions per session of a

stereotyped behavior consisting of nose poke entry followed by withdrawal to either the left or right spout to retrieve a reward.

Stage 3: Training to Wait for the Go Cue. In stage 2, entry into the nose poke immediately triggered the go cue. In stage 3, we introduced a delay before initiation of the go cue, with the objective of prolonging the period spent in the stimulus delivery port. In addition to the nose poke sensor, high-speed video of the stimulus delivery port was now acquired, and a custom algorithm was operated online to measure head movement. The rat needed to occupy the nose poke and maintain head movement below a user-set threshold for a specified waiting period. If the rat left the nose poke before the go cue sounded (early withdrawal), no reward was made available. Provided that early withdrawal did not occur, the go cue was followed by the reward target cue at either the left or right speaker (chosen randomly for that trial), and the corresponding spout was baited.

In the first session the waiting period was just 10–100 ms. In the next sessions, according to the rat's ability to remain immobile, the maximum period was gradually increased while maintaining trials with shorter periods (e.g., interspersed waiting periods of 100, 200, 300, and 400 ms). Finally, waiting periods of up to 5 s were presented. In parallel with the increase in the waiting period, the threshold for an acceptable level of head movement was steadily reduced.

The arena lighting level was reduced so that by the end of stage 3, the rat worked at full speed under dim red light. Like in stage 2, the whisker stimulation plate remained immobile. This stage lasted for two to three sessions, with 200–400 trials per session, and terminated when the rat registered an early withdrawal on fewer than 10% of the 5-s delay trials.

Stage 4: Introduction of Tactile Stimuli. The goal of stage 4 was for the rat to learn to receive whisker stimuli and to become aware of the relationship between stimulus features and the reward location. Now, when the rat entered the nose poke, the go cue was not sounded until completion of two sequential whisker vibrations, denoted base and comparison (Fig. 2*B*). As before, no reward was made available if the rat left the nose poke before the go cue sounded. After the go cue, the reward target cue was sounded adjacent to the baited spout. The side of the reward depended on a rule associated with the velocity distributions, σ_{base} and $\sigma_{comparison}$, of the two whisker vibrations. For instance, the rule for one subject might be as follows: when $\sigma_{base} > \sigma_{comparison}$, the reward is at the left spout, and when $\sigma_{base} < \sigma_{comparison}$, the reward is at the right spout. The rule was assigned randomly to each rat and was fixed for the remainder of the study.

In this stage, the difference between σ_{base} and $\sigma_{comparison}$ [as quantified by the SD index (SDI)] was 0.4. The range of velocity SDs was 128–300 mm/s. Other task parameters were varied. Stimulus duration was varied from 50 to 500 ms. The interstimulus delay also was varied, in 100-ms steps, from 200 ms to 3 s. Stimulus parameters and other experimental variables are given in Table S1. The objective of such variations was for the rat to learn that stimulus features, as well as the time course of the trial, were changeable. The rat's acceptance of trial-to-trial unpredictability was crucial for the later implementation of the stimulus generalization matrix (SGM).

In this stage, the rat did not receive the reward at the side deemed incorrect on that trial; however, when its first choice was wrong, it was allowed to continue to the opposite (correct) spout, where the reward was dispensed. By this error remediation protocol, the rat began to uncover the relationship between stimulus features and reward location. Although we did not score the performance of the rats, there was evidence that they began to attend to the vibratory whisker stimulation: by examining video recordings of the whiskers, we found that by the end of stage 4 the rat began to hold its whiskers immobile on the vibrating plate, presumably to optimize the collection of signals. Whisker position in one trial is illustrated in Movie S2.

This stage lasted for 10–20 sessions, with 200–300 trials per session, and terminated when the rat registered an early withdrawal on fewer than 10% of trials.

Stage 5: Implementation of the Stimulus Comparison Rule. This stage differed from the preceding one in the following ways. First, the reward target cue was omitted. This means that the rat could identify the correct reward spout only through the tactile stimulus comparison rule rather than by following the acoustic signal. The reward delivery cue was still used to reinforce correct choices. Second, error remediation was no longer allowed. If the rat's first choice was incorrect, it could not find a reward by checking the opposite (correct) spout. This increased the error cost. Third, an error led to a 5-s timeout. During the timeout, the blue LED above the stimulus delivery port remained off, and the rat could not initiate a new trial. The timeout further increased the error cost.

As the rat gained competence, the SDI was decreased progressively from an absolute value of 0.4 to 0.35 (Table S1).

In this stage we quantified accuracy according to the rat's first choice on each trial. It is important to note that because the number of stimulus pairs in this stage was limited, rats may start to use alternative strategies to do the task, rather than the intended comparison rule (*Stimulus Generalization Matrix* in *Results*). To avoid that, the next stage of training was introduced as soon as performance rose above chance.

Stage 6: Tolerance to Variation in Parameters. In this stage the stimulus comparison rule (stages 4–5) was stabilized through the execution of many hundreds of trials. Beyond that, the goal of stage 6 was for the rat to continue to learn that stimulus features, as well as the time course of the trial, were changeable. Rodents are known to have a tendency to form stereotyped, inflexible patterns (1). Stage 6 was crucial in maintaining the rat's elasticity and thus minimizing its likelihood of developing superstitious timing routines. Moreover, the rat's learned tolerance to variation allowed us to run future test sessions with all experiment parameters randomized from trial to trial. Among the varied parameters were the σ value of the vibrations, vibration durations, and interstimulus interval (Table S1).

By varying the σ value of the vibrations, we required the rat to generalize the stimulus comparison rule. Stimulus pairs were selected pseudorandomly across trials. The purpose of generalizing the rule was described in *Stimulus Generalization Matrix*.

Our long-term goal is to exploit this behavioral task to study the neuronal basis of tactile sensation, working memory, decision making, and action selection. To accomplish these aims, it is necessary that the structure of each trial allows the cognitive operations to be at least partially separated in time. At the conclusion of the comparison stimulus, all possible sensory data have been collected. We inserted a poststimulus delay between the comparison stimulus and the go cue (Fig. 2*B*) to allow us to examine the motor program of the rat following the integration and comparison of sensory signals. To be certain that the rat attends to both stimuli and the go cue before acting, we made stimulus duration and poststimulus delay variable.

Fig. S1 illustrates the timing of the rat's withdrawal in one session. Each trial is represented by one point. The *x* axis plots the poststimulus delay, defined as the time from the end of the comparison stimulus until the onset of the go cue (see Fig. 2*B* for time line). The *y* axis plots the sum of the poststimulus delay and the withdrawal latency, where latency is defined as the time from the go cue onset until the instant in which the rat's snout left the nose poke sensor. Aside from a small number of early withdrawals, all trials lie about 200–400 ms above the diagonal line. From these data, we draw two conclusions. First, the rat attended

the conclusion of the comparison vibration, independently of the duration of the two vibrations and the delay between them; otherwise, many early withdrawals would have occurred. Second, the time of withdrawal was bound to the time of the go cue. If the time of withdrawal were bound to the conclusion of the comparison stimulus rather than the go cue, the points would have been distributed in the horizontal, not diagonal, direction.

When performance was above 80% averaged across all conditions for three consecutive sessions, the rat was ready for the next stage. This usually required 10–15 sessions.

Stage 7: Finalization of the Vibration Comparison Task. In stage 7, the rat was presented with new combinations of stimulus pairs until it reached the final form of the SGM, which was composed of 10–14 stimulus pairs; this SGM configuration is illustrated in Fig. 3*A*. Stage 7 usually required 20–30 sessions. When performance was above 80% in the basic SGM for three consecutive sessions, the rat proceeded to the testing stage, with findings described in *Results*. Fig. S2 shows the improvement of performance in four rats across stages 6 and 7.

Analysis of Learning in Delayed Comparison. To chart rats' learning, we carried out an analysis to weigh the contributions of σ_{base} and $\sigma_{comparison}$ to the animal's choice, as follows. From the data originating in a single training session, for each [σ_{base}, $\sigma_{comparison}$] stimulus pair, we fit the animal's choice with a logistic regression using a generalized linear model. This model posits a linear combination of $\sigma_{comparison}$ and σ_{base} which is mapped nonlinearly onto the animal choice (i.e., percent of trials in which the subject judged $\sigma_{base} > \sigma_{comparison}$) through a link function as follows:

$$\text{percent of trials judged } \sigma_{comparison} > \sigma_{base} = \frac{1}{1+e^{-\left(c+w_1\left(\log \sigma_{base}\right)+w_2\left(\log \sigma_{comparison}\right)\right)}},$$

where w_1 is the σ_{base} regressor, w_2 is the $\sigma_{comparison}$ regressor, and c is the baseline regressor that captures the overall (stimulus-independent) bias of the subject in calling $\sigma_{base} > \sigma_{comparison}$ (for instance, a bias against turning right, the side associated with the judgment $\sigma_{base} > \sigma_{comparison}$).

The coefficients w_1, w_2, and c were derived to most closely reproduce the observed performance in that session by an iteratively reweighted least squares algorithm. The w_1 and w_2 regressors quantify the strength of the relationship between σ_{base} and $\sigma_{comparison}$, respectively, and the animal's choice. If the regressors are plotted in Cartesian coordinates, the critical issue becomes the direction of the vectors formed by w_1 and w_2. An ideal performer—one who precisely encodes the base stimulus, holds it in the memory, precisely encodes the comparison stimulus, and then accurately judges the difference between σ_{base} and $\sigma_{comparison}$—would yield $w_1 = -w_2$, corresponding to the dashed line.

Data from four rats are illustrated in Fig. S2. Any possible bias c is independent of stimulus weighting and would not affect angle. Each vector of form (w_1, w_2) derives from one training session. Sessions from stage 6 are plotted in red; sessions from stage 7 are plotted in blue. It is evident that from stage 6 to stage 7 the vectors became more closely aligned to the dashed line, indicating that rats learned to give nearly equal weight to the values of σ_{base} and $\sigma_{comparison}$. To quantify the changes in vector direction, we carried out a circular version of the Watson–Williams test on the distribution of angles. For rats 2, 3, and 4, there was from stage 6 to stage 7 a significant shift ($P < 0.002$) of vector direction toward the angle $w_1 = -w_2$. For rat 1, the single-session vectors (w_1, w_2) by stage 6 were already distributed, on average, symmetrically around $w_1 = -w_2$. In this rat, the evolution from stage 6 to stage 7 consisted of a significant decrease in angular dispersion, indicating that the rat became more consistent in attributing equal weight to σ_{base} and $\sigma_{comparison}$.

Psychometric Curves. In the tactile acuity protocol (Fig. 5), we computed the proportion of trials in which subjects reported $\sigma_{comparison} > \sigma_{base}$. We fit the data with a four-parameter logistic function using the maximum likelihood method in MATLAB, as follows:

$$\text{Percent judged } \sigma_{comparison} > \sigma_{base} = \frac{\text{Min} - \text{Max}}{1+\left(\frac{\text{SDI}}{\text{IF}}\right)^{\text{Slopefactor}}} + \text{Max},$$

where the four parameters are as follows: Min is the lower asymptote determined by the number of alternative choices (two in our task), Max is the upper asymptote, IF is the inflection point along the SDI axis, and Slopefactor is the maximum slope of the curve. The slope is calculated by taking the derivative of the curve and setting SDI = IF:

$$\text{Slope} = \text{Slopefactor}\frac{(\text{Max} - \text{Min})}{4\text{IF}}.$$

Statistical Test for Delayed Comparison Performance. A given value of $\sigma_{comparison}$ could be preceded by either a smaller or a larger value of σ_{base}. For these two cases, the rat correctly judged $\sigma_{comparison} > \sigma_{base}$ or $\sigma_{comparison} < \sigma_{base}$, respectively, on some percent of trials. In Fig. 6*A*, the frequency of the choice $\sigma_{comparison} > \sigma_{base}$ is plotted in the boxes. Gray shading links trials with one value of $\sigma_{comparison}$ preceded by one of two values of σ_{base}. If performance were perfect, values on the left side would be 100, and those on the right would be 0. The difference between the frequency of these two choices, averaged across animals, is given on the right edge of the gray bars (values are 61, 51, 39, 39, and 22). If rats attended to $\sigma_{comparison}$ but ignored σ_{base}, the difference values would be close to 0. To test the significance of the observed values, for each rat and each fixed $\sigma_{comparison}$ value, we computed the choice difference for 500 trials selected pseudorandomly from that rat's data set and then repeated the resampling 1,000 times. This generated a new bootstrap distribution of differences. Next we compared this resampled difference distribution to a difference distribution obtained after randomly shuffling the σ_{base} and $\sigma_{comparison}$ labels on each trial. The shuffled distribution simulated the expected choices of rats if those choices were not determined by comparing σ values. The distance between the mean of the resampled difference (obtained from real observations) and the mean of the simulated, shuffled distribution, divided by the SD of the distributions, gave a Z-score. On the right side of Fig. 6*A*, the Z scores are aligned by $\sigma_{comparison}$ value, with each rat plotted as a point. Conventionally, Z scores > 2 are considered significant (dashed line), and in this analysis, Z scores were found to be much higher. Thus, for most $\sigma_{comparison}$ values, the effect on rats' actions of σ_{base} exceeded 10 SDs and was thus strongly significant. The statistical procedure was repeated on data from human subjects in Fig. 6*B*.

Similarly, a given value of σ_{base} could be followed by either a larger or smaller value of $\sigma_{comparison}$. For these two cases, the rat correctly judged $\sigma_{comparison} > \sigma_{base}$ or $\sigma_{comparison} < \sigma_{base}$, respectively, on some percent of trials. In Fig. S3*A*, the frequency of the choice $\sigma_{comparison} > \sigma_{base}$ is plotted in the boxes. Gray shading links trials with one value of σ_{base} followed by two values of $\sigma_{comparison}$. If performance were perfect, values at the bottom end of each gray bar would be 0, and those at the upper end would be 100. The difference between the frequency of these two choices, averaged across animals, is given at the top of the gray

bars (values are 45, 49, 56, 67, and 52). If rats attended to σ_{base} but ignored $\sigma_{comparison}$, the difference values would be close to 0. The significance test was equivalent to that applied in Fig. 6. At the top of Fig. S3*A*, the Z-scores are aligned by the σ_{base} value, with each rat plotted as a point. For most σ_{base} values, the effect on rats' actions of $\sigma_{comparison}$ exceeded 10 SDs and was thus strongly significant. The statistical procedure was repeated on data from human subjects in Fig. S3*B*.

1. Ölveczky BP (2011) Motoring ahead with rodents. *Curr Opin Neurobiol* 21(4):571–578.
2. Kelly JB, Masterton B (1977) Auditory sensitivity of the albino rat. *J Comp Physiol Psychol* 91(4):930–936.
3. Masterton B, Diamond IT (1973) Hearing—Central neural mechanisms. *Handbook of Perception* (Academic, New York), Vol 3, pp 407–448.

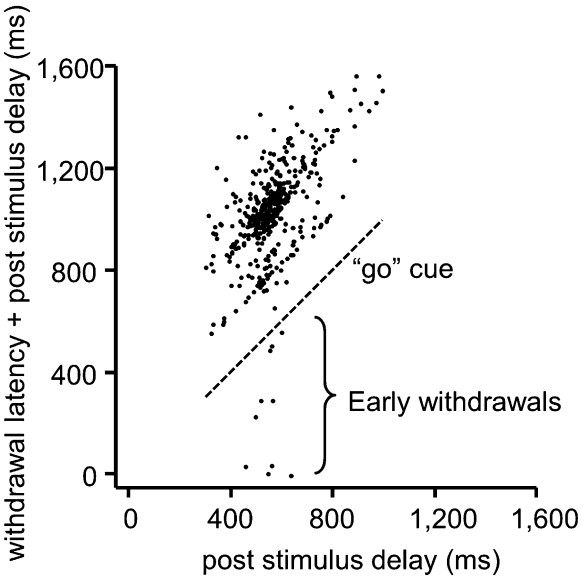

Fig. S1. Withdrawal from nose poke is triggered by the go cue. Data from one session are illustrated. The *x* axis plots the poststimulus delay, defined as the time from the end of the comparison stimulus until the onset of the go cue. The *y* axis plots the sum of the poststimulus delay and the withdrawal latency, where latency is defined as the time from the go cue onset until the instant in which the rat leaves the nose poke sensor. The plot shows that the time of withdrawal was bound to the time of the go cue.

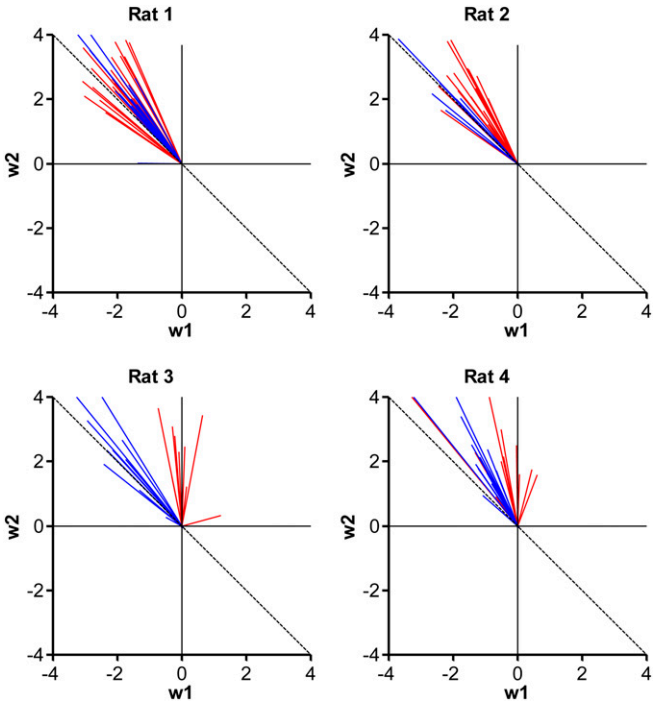

Fig. S2. Rats learned to perceive and compare the two stimuli. The analysis method is described in *SI Text*. Here data from four rats are illustrated. Any possible bias *c* is independent of stimulus weighting and is not illustrated in this analysis. Each vector of form (w_1, w_2) derives from one training session. Sessions from stage 6 are plotted in red; sessions from stage 7 are plotted in blue. It is evident that from stage 6 to stage 7 the vectors became more closely aligned to the dashed line, indicating that rats learned to give nearly equal weight to the values of σ_{base} and $\sigma_{comparison}$. To quantify the changes in vector direction, we carried out a circular version of the Watson–Williams test on the distribution of angles. For rats 2, 3, and 4, there was from stage 6 to stage 7 a significant shift ($P < 0.002$) of vector direction toward the angle $w_1 = -w_2$. For rat 1, the single-session vectors (w_1, w_2) by stage 6 were already distributed, on average, symmetrically around $w_1 = -w_2$. In this rat, the evolution from stage 6 to stage 7 consisted of a significant decrease in angular dispersion, indicating that the rat became more consistent in attributing equal weight to σ_{base} and $\sigma_{comparison}$.

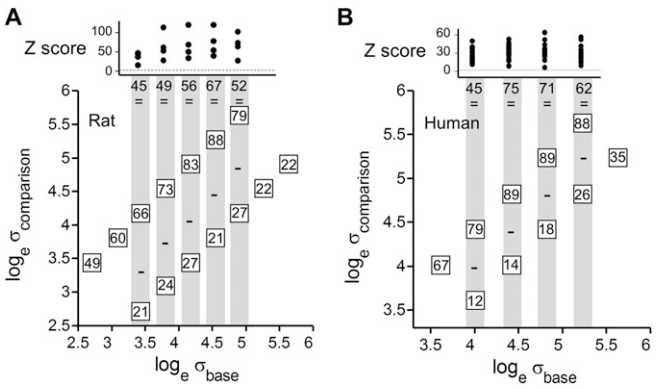

Fig. S3. Statistical analysis of effect of $\sigma_{comparison}$. (*A*) Values in the boxes give the percent of trials in which rats judged $\sigma_{comparison} > \sigma_{base}$. The difference between paired boxes in a gray band represents the dependence of choice on whether σ_{base} was followed by smaller or larger $\sigma_{comparison}$. The statistical significance of the choice for all single rats is given as a Z-score at the top. (*B*) Same analysis carried out on data from humans.

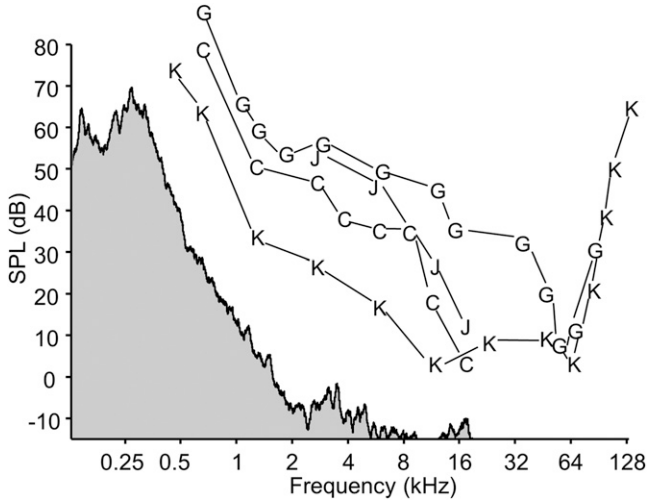

Fig. S4. Sound cues were below rats' acoustic sensitivity. Recordings in the apparatus (gray plot) show that the vibratory stimuli emitted sound in a frequency range that is not perceived by rats. The plots in the higher-frequency range indicate the sensitivity of albino rats, adapted from (2). This analysis is consistent with behavioral evidence that performance dropped to chance level when whiskers were not moved by the plate.

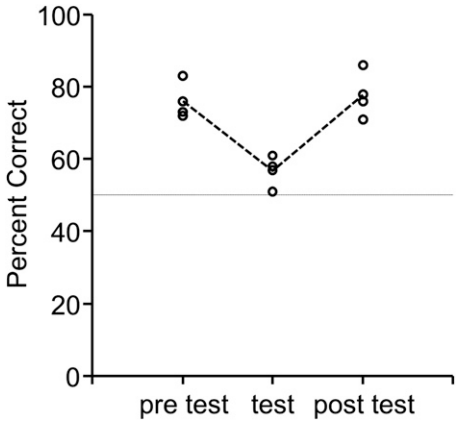

Fig. S5. Task execution depended on motion of the plate. We tested whether rats could use the acoustic cues associated with actuation of the motor without actual movement of the whiskers. To do so, with well-trained rats we divided four sessions into three blocks: (*i*) pretest, trials executed before detaching the motor from the plate; (*ii*) test, trials executed with the rod/plate assembly still present in the stimulus delivery port but detached from the motor; and (*iii*) posttest, trials executed after reattaching the rod/plate assembly to the motor. With the rod/plate assembly detached, the sound of the motor remained. Each block consisted of approximately 20 trials. Mean performance per block is illustrated, and it is evident that accuracy dropped to chance level when the rod/plate assembly was detached. From this we conclude that rats could not achieve good performance using acoustic cues.

Table S1. Experimental conditions in stages 4, 5, and 6

Parameter	Stage 4: introduction of tactile stimuli	Stage 5: implementation of the stimulus comparison rule	Stage 6: tolerance to variation in parameters
Prestimulus delay, ms	300	300	200–500
Base stimulus duration, ms	50–500	50–500	50–600
Comparison stimulus duration, ms	50–500	50–500	50–600
Interstimulus delay, ms	200–3,000	2,000–3,000	500–5,000
Poststimulus delay, ms	100	300	300–800
Velocity SD, mm/s	128–300	50–300	23–420
Reward target cue	Yes	No	No
Error remediation allowed	Yes	No	No
5-s time-out after error	No	Yes	Yes
SDI	−0.4–0.4	−0.35–0.35	−0.35–0.35

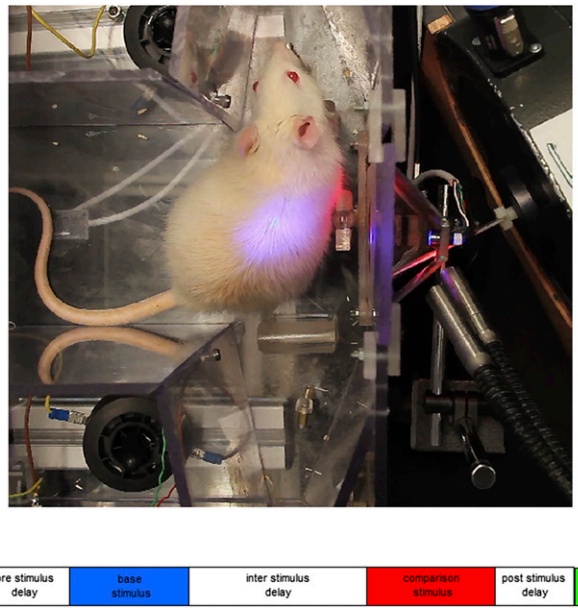

Movie S1. Performance of the tactile working memory task. A well-trained rat is shown on a single trial. The rat places its snout in the nose poke and, after a prestimulus delay, receives two vibrations, separated by a delay. On presentation of the go cue the rat turns to the left reward spout. Visible lighting was used to augment video quality; however, normally, the behavior was carried out in the dark. Acoustic noise signals originating in the motor were readily perceived by human observers but not by the rats.

Movie S1

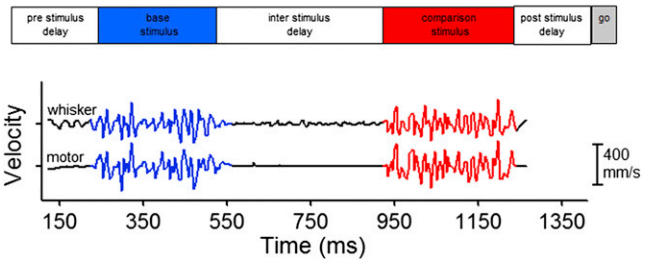

Movie S2. Motor and whisker motion are tracked across one trial. High-speed video reveals the transmission of motor motion to the whiskers. At the outset, the plate and the whisker of interest are indicated as green bars. Both bars are tracked throughout the duration of the trial by custom-made tracking programs. The whisker closely follows the plate during both the base stimulus (blue trace) and comparison stimulus (red trace). Self-generated whisking was suppressed.

Movie S2